Error Correction, the Basal Ganglia, and the Cerebellum

Ph.D. Dissertation

Maurice Smith

Table of Contents

Table of Figures

Chapter 1 – Introduction

Basal Ganglia Function – The Action Selection Theory

The basal ganglia have long been suspected to play an important role in motor control, but characterization of this role has been difficult. The prevailing view is that the basal ganglia are involved in the selection and inhibition of motor programs. The characterization of basal ganglia motor function as that of action selection is mainly derived from observations of the main symptoms of the two most common diseases affecting this brain region, Parkinson's disease and Huntington's Disease.

Parkinson's disease is the most common disease of the basal ganglia. Degeneration of the nigrostriatal tract occurs in Parkinson's disease, resulting in abnormally low levels of dopamine and subsequent dysfunction of neurons and neural pathways in the striatum that require this neurotransmitter. Neurons in the substantia nigra and locus coeruleus also degenerate. Parkinson's disease most often begins late in life, and is characterized by a severe, progressive motor dysfunction. The primary symptoms of this dysfunction are difficulty with movement initiation, slowing of voluntary movement, and the occurrence of an involuntary resting tremor. The impairment in movement initiation seen in Parkinson's disease is profound. Many patients find the task of getting up from a chair difficult or impossible without assistance although they easily possess the necessary muscle strength, and a 'freezing' phenomenon is also common in many patients: while walking these individuals can come to a stop and be unable to get themselves moving again. This difficulty with movement initiation

evident in Parkinson's disease may correspond to insufficient activation of appropriate motor programs.

In contrast, the hallmark symptom of Huntington's disease is chorea, the occurrence of occasional but uncontrollable complex, multi-joint, irregular and arrhythmic involuntary movements. It is widely believed that the chorea seen in Huntington's disease (HD) may result from the lack sufficient of inhibition of inappropriate motor programs. In a nutshell, the action selection theory of basal ganglia function holds that Parkinson's disease results in insufficient basal ganglia output leading to inadequate ability to select and initiate motor actions while Huntington's disease results in excessive basal ganglia output leading to the inability to prevent the occurrence of inappropriate motor actions. The action selection theory is also supported by neurophysiologic evidence. Neurons in the putamen and caudate nuclei within the basal ganglia are organized in a hierarchical fashion, receive a very large number of inputs (up to 10,000), and inhibit surrounding neurons when they are electrically excited. This architecture appears compatible with action selection as a function. The hierarchical layout may represent pruning or fine tuning of an action decision, the large input space may represent the information upon which an action decision is made, and the reciprocal surround inhibition may promote the emergence of a single dominant action selection from multiple competing actions.

Huntington's Disease Background

Huntington's disease (HD) is an autosomal dominant inherited neurologic disorder caused by a trinucleotide repeat expansion in the IT-15 gene on the short arm of chromosome 4[1]. Individuals lacking the Huntington's disease mutation generally possess

alleles for this gene which contain 19 to 24 repeats of a cytosine-adenine-guanine (CAG) trinucleotide, but the CAG triplet is repeated 37 or more times in one of the alleles of patients with Huntington's disease. When HD is maternally inherited, the mutation is generally quite stable, but with paternal transmission the trinucleotide repeat (TNR) expansion may increase by several repeats (cite). The length of the trinucleotide repeat correlates with age of clinically detectable disease onset and disease severity within Huntington's patients. Disease symptoms usually appear in the fourth or fifth decade of life, and then progress steadily during the succeeding 10-20 years[2], but a rare childhood-onset variant of HD also occurs and is associated with extremely large TNR lengths (>90) and a more rapid course. Motor dysfunction, cognitive decline, and psychiatric disturbances all characterize the manifestation of HD. Significant, progressive atrophy of the basal ganglia as a whole, and in particular, the caudate nucleus are evident in HD[3] and may even be detectable before clinical onset of disease[4].

The hallmark motor sign of HD is chorea: the occurrence of rapid, irregular, and arrhythmic complex involuntary movements. In fact, Huntington's disease is often referred to as Huntington's chorea. The severity of chorea progresses during the first 8-12 years of the disease but then levels off, and may even subside at late stages in the disease. Despite the fact that chorea is the most distinctive and well-known feature of HD, substantial impairment of voluntary movement also occurs, and it may be of greater functional importance in the lives of symptomatic patients[5]. Early in the disease course, rapidly alternating movements are slowed or disrupted. Patients become somewhat clumsy and may have trouble with fine motor tasks such as tying shoelaces, buttoning clothing, or performing needlework[2]. In the later stages of HD most voluntary

movements are markedly slow, and eventually, many patients deteriorate into a rigid state in which they are largely incapable of movement.

The existence of performance deficits on tests of behavioral function before the clinical onset of HD is controversial. To date, assessments of motor, cognitive, or psychiatric function in HD have revealed only subtle deficits in presymptomatic subject groups[6,7,8] (Siemers, 2k) if any[9,10,11]. Even when changes have been detected, they were not sufficiently specific to permit discrimination between mutation positive and mutation negative individuals, or even reliable identification of people with early stage manifest HD. In contrast, functional imaging of the basal ganglia reveals low glucose metabolism in about two thirds of asymptomatic at risk individuals[12,13,14,15] and basal ganglia volumes may be reduced years before clinical onset[4], suggesting that brain pathology may substantially lead manifestation of the behavioral dysfunction previously studied. Do behavioral correlates to the early brain pathology of HD exist? If so, understanding them may give substantial insights into the pathophysiology of the devastating motor symptoms of HD, and into function of brain structures damaged early in HD.

Sensorimotor Processing in Huntington's Disease

The characterization of basal ganglia function as that of primary action selection is at best incomplete as basal ganglia damage also affects the ability of individuals to integrate ongoing sensory information into their actions. Perhaps the simplest form of this appears in voluntary control of reflexive behaviors. When a perturbation displaces the hand, stretch-reflex mechanisms originating in the spinal cord provide a short-latency compensatory response, but a secondary, long-latency response is also observed. It is believed that this response involves a pathway that leads from the spinal cord to the

thalamus to the somatosensory cortex, to the motor cortex, and then back to the spinal cord (Marsden et al 1978, Rothwell 1990, Petersen 1998). Importantly, one function of the basal ganglia may be to modulate this pathway. In HD, short-latency stretch reflex responses generated in the spinal cord are normal, but long-latency responses generated through transcortical pathways are reduced or absent in some muscles (Noth et al. 1985, Thompson et al. 1988, Thilman et al. 1991). Intriguingly, when peripheral nerves are stimulated with electrical impulses, the resulting cortical responses as measured by evoked potentials from the somatosensory cortex are also reduced in HD[24,26], although the sensory afferent input up to the level of the thalamus has been found to be normal[26]. Additionally, electrical transmission in descending motor tracts has been demonstrated to be normal (Eisen et al, 1989), and conduction times within the cortex (Thompson et al, 1986; Homberg and Lange, 1990) as well as neural transmission in subcortical projection systems within the brainstem and mid-brain (Mann, 1989) are normal in HD. Taken together, this suggests that while the afferent system of the spinal cord may be relatively intact in HD, the systems that relay somatic information to the cortex are inappropriately modulated or gated.

While previous work had considered long-latency reflexes generally as a part of the system that allows maintenance of steady posture (e.g., in HD, see Fellows 1997), we thought that it might also play a fundamental role in control of voluntary movements. Despite the widespread clinical recognition of qualitative impairment in voluntary movement, and the lack of understanding about how these deficits arise from the known disease pathology, functional characterization of this dysfunction in movement control has not been well established. We hypothesized that careful study of the dynamics and

kinematics of voluntary movement trajectories could reveal substantial functional manifestations of the sensory processing deficits associated with HD. When subtle errors occur in the execution of simple reaching movements, the errors must first be detected among the large amount of sensory feedback to the brain. Successful detection should then result in the selection of the appropriate motor response and the modification of ongoing descending motor commands. Because of the large delays in sensory feedback, this is a difficult computational problem, but one that may be solved with a system that predicts sensory consequences of motor commands from current sensory information and knowledge of those motor commands[41]. Such a system can be referred to as a forward model of the motor system and physical dynamics. Because this computation is likely to provide a formidable challenge to the CNS and depends heavily on the appropriate processing of sensory information, we hypothesized that even small disturbances in the processing of sensory signals might have a substantial effect on the function of this predictive error feedback control system, and so even healthy asymptomatic individuals who carry the HD gene mutation might display identifiable manifestations of error correction dysfunction when only minimal deficits in sensory processing are present.

Cerebellar Disease

The cerebellum is believed to play an important role in the coordination of movement. Damage to the cerebellum does not abolish voluntary movement, but rather impairs its smoothness and precision. It is believed to assemble motor sequences, muscle synergies, and the appropriate time courses of motor activation into automatic motor actions for task performance. This characterization is similar to the control theory

concept of an inverse model[16]. An inverse model transforms desired system behavior (output) into the motor commands (control signals) that will accomplish this behavior.

Patients with cerebellar dysfunction often suffer from problems with gait and balance. Arm and eye movements can also be affected. Both ballistic and tracking movements of the eyes and arm can be impaired, suggesting a dysfunction in both feedforward and feedback control.

Substantial motor learning deficits have been demonstrated in patients with cerebellar dysfunction. Learning of new complex movement sequences is impaired by cerebellar damage[17,18] as is performance on simple tasks of visuospatial adaptation, but performance on these tasks can be strongly modulated by cognitive function. For example, adaptation to wearing prism glasses which horizontally shift a subject's visual field is impaired in cerebellar subjects[19,20]. Prism adaptation has been tested using pointing and throwing tasks in which a subject must reach a given target. Cerebellar patients perform poorly at these tasks. They adapt more slowly than people without cerebellar damage. However, the level of performance on these tasks is highly correlated to cognitive factors for cerebellar patients. A subject who repeatedly points too far to the left while wearing prism glasses may consciously decide to point more rightwardly. Patients who are demented perform much more poorly than cerebellar patients with normal cognitive ability, and so the magnitude of the cerebellar contribution to task performance is unclear. The size of the after effect – the reversal in performance error when the glasses are removed - seems to be the best indicator of motor (non-cognitive) learning in these tasks. The study of learning on motor tasks with a smaller cognitive contribution (or at least less opportunity for simple cognitive decisions to improve

performance) may be able to better characterize the cerebellum's role in motor control processes, although quantifying the cognitive contribution toward performance on any task is problematic.

Other learning deficits have been associated with cerebellar damage. Classical conditioning has been shown to be impaired by cerebellar damage, both in human patients (?), and in rabbits given cerebellar lesions (Thompson,1996), and cerebellar patients are impaired on a ball catching task in which they display poor adaptation to weight changes in the balls they catch (Thatch).

Development of Analytical Tools for Understanding the Dynamics of Movement Data

A great deal of the work studying motor learning or motor control measures only the performance on achievement of the final goal, without regard for the intermediate motor actions that contributed to this final outcome. Measuring complete motor output – all motor commands and muscular activation signals – is not currently possible, but measurement of the time course of the kinematics and dynamics of motion, may provide information on characteristics of the types of motor output changes that are and are not achieved when motor learning dysfunction is present.

The time courses of unconstrained or partially constrained movement trajectories make up a large but potentially rich data set. The potential richness of this data set inspires study, but its large dimensionality suggests the need for robust computational tools to help understand the data. Since only rudimentary computational tools are currently available, fruitful study has remained difficult. In short, movement trajectories

may contain substantial information about how the brain controls motor behavior that we are currently unable to interpret.

To make ideal use of this information one would like to know both the nature of all the physiologic motor control processes which underlie the movement set and the optimal way to transform the motion trajectories in order estimate the contribution of each of these on a movement by movement basis. Unfortunately, we currently know neither the nature of all the important physiologic motor control processes nor the optimal way to delineate the contribution of any of the motor control processes that we think are important on a movement-by-movement basis. The full solution to the sort of optimal computational signal processing problem stated above is a difficult, open-ended, and possibly intractable task. But tractable approaches do exist that may give insight into this problem and advance our understanding of the motor control process.

One approach is to hypothesize about the existence or importance of a particular process and design an experiment around this hypothesis. This is by far the most common approach to the study of motor control and its use has substantially increased our scientific understanding, but the generation of new hypotheses is challenging and this approach provides a relatively slow and costly mechanism for testing these hypotheses – perhaps encouraging the testing of hypotheses which are a priori more likely to be true by virtue of their similarity to hypotheses which have already been tested. Criticism of the problems with the experimental design approach is difficult however because so much of our current understanding stems from it. However this approach could be nicely complemented by the development of new computational approaches on large 'standard' sets of data. This methodology has recently met with some success. Thoroughman was

able to uncover the direction specific nature of the motor primitives used in learning a viscous force field**Error! Bookmark not defined.** by using a discrete direction-state dependent learning model to characterize data from motor learning experiments not specifically designed to uncover direction specific effects. In this thesis, computational methods were developed (1) to analyze the efficiency of motion based on principles of optimal control hypothesized to govern voluntary movement[29,30] and (2) to assess the integrity of error feedback control function by analyzing the trial-to-trial variability in the performance of movements in which errors were not externally induced. Specifically, error control function was gauged by relating the occurrence of subtle, self-generated early-movement errors to trial-by-trial changes in end-movement performance. It is the author's hope that the analytical methods developed here can be used or can be modified to be used in other motor control studies, and possibly inspire the development of new analytic methods for studying dynamic motion.

Motivation

The study of motor disorders (or any disease process) can allow the simultaneous pursuit of two lofty goals. First, such study may lead to better fundamental understanding of not only the disease process but also of normal function of the human body. Second, such study may lead directly to specific insights about the creation, improvement, or assessment of strategies for prevention, therapy, or rehabilitation of the disease. One in 10,000 Americans carry the HD gene mutation that will eventually manifest as the disease, and the neuroscience of motor behavior is still in its infancy.

Characterization of the functional deficits associated with a disease process is an important step toward understanding the mechanisms through which the disease

pathology manifests itself. Two control processes are hypothesized to play important roles in the execution of arm movements. Feedforward control is the generation and execution of motor commands based a priori on the desired action and an internal model of the system's response[21,22,23], while feedback control entails the 'mid-flight' correction of these commands based on errors detected during their execution. Quantitative analysis of voluntary movement trajectories in a control theory framework has the power to differentiate disturbance in these two control processes and to provide valuable insights into the nature of the motor dysfunction in Huntington's disease and cerebellar dysfunction.

There is some reason to believe that feedback control processes may be disturbed in HD, although control-process specific behavioral deficits have not yet been demonstrated early in the disease course. Previous reports have shown that cortical sensorimotor pathways are affected in patients with manifest HD. While short-loop reflexes that are mediated by spinal mechanisms are normal, long-loop reflexes, which involve the transfer of proprioceptive information through cortical pathways, are reduced or absent in HD[24,25]. Cortical responses to peripheral nerve stimulation, as measured by somatosensory evoked potentials (SEPs), are also reduced in HD[15,24,26,27], suggesting that diminished cortical sensory input is responsible for the long-loop reflex reduction[25]. Additionally, a strong correlation exists between SEP deterioration and striatal glucose metabolism early in the course of HD[15], hinting at a possible involvement of the striatum in the pathology of the SEPs and long-loop reflexes in HD. Since cortical sensorimotor pathways play a large role in mediating error correction during voluntary movement,

disruption of these pathways could lead to dysfunctional feedback control during movement.

Scope of This Work

The primary goal of this thesis was to gain a better understanding of the motor dysfunction in Huntington's disease and cerebellar dysfunction by studying the motor function associated with these disease processes in feedforward / feedback control systems framework. Another important aim was to develop both analytical techniques and experimental paradigms to further the study of voluntary movement in this framework.

A crucial aspect in the overall design of the studies presented here was that we concomitantly looked at patients who had been clinically diagnosed with Huntington's disease and individuals who carried the HD gene mutation but in whom disease symptoms had not yet become clinically manifest. The inclusion of presymptomatic subjects in our study allowed us to assess the earliest manifestations of disease. This provided two distinct advantages in relating our findings to basal ganglia function. (1) Early pathology, before clinical onset of disease, is believed to be restricted to the basal ganglia, but as HD progresses more global atrophy has been found, particularly in frontal cortex. Thus, changes in motor function found early in the disease course are likely to arise purely from basal ganglia dysfunction, whereas changes in later stages of disease may reflect dysfunction in other brain areas. (2) In stages of the disease when symptoms are strongly manifest, compensatory mechanisms are likely to begin to operate. Therefore changes in motor function during these stages of disease may reflect the effects of compensatory mechanisms as well as the primary motor disturbance. In contrast,

motor changes found when symptoms are subtle and clinically undetectable are more likely reflect the primary motor dysfunction. In short, presymptomatic subjects are likely to display a purer though more subtle motor disorder than patients later in the disease course, and studying presymptomatic and symptomatic HD patients alongside one another allows for the tracing of disease progression.

In chapter 2, error feedback control function is analyzed in patients with Huntington's disease, in asymptomatic subjects carrying the HD mutation, and patients with cerebellar dysfunction. The relationship between the occurrence of self-generated errors during movement as well as the effect of externally imposed error-producing perturbations on the quality of the error response is explored. Here we find that the response to both self-generated and externally-imposed errors is disturbed in both patient with Huntington's disease and asymptomatic gene carriers of the HD mutation. Cerebellar subjects, while not normal, display substantially less disturbance in their error responses than do HD subjects.

In chapter 3, reactions to externally imposed, random perturbations are investigated in more detail in patients with Huntington's disease and cerebellar dysfunction. The role of visual feedback, the time course of the perturbing force pulses, and the direction dependence of the error feedback control dysfunction are analyzed. Here we find that visual perception or misperception of error during motion did not account for the error feedback control disturbance seen in HD. Perturbations that occurred near the beginning or end of a movement produced similarly disturbed error responses and the disturbance in error feedback control was not specific to certain muscle groups In fact, neither the muscle groups involved in the primary motion nor the

perturbation response, nor the relationship between these muscle groups affected the degree of error feedback control dysfunction.

In chapter 4, the effects of Huntington's disease on visual reaction times are studied. In general, visual reaction times for arm movements are prolonged in patients with manifest HD, but not in asymptomatic gene carriers, suggesting that the processing of sensory information may not be as considerably disturbed if error correction is not involved.

In chapter 5, the motor leaning dysfunction occurring in Huntungton's disease and cerebellar dysfunction is investigated. Here we study motor learning on a task that is strongly dependent on feedforward control. Markedly impaired learning is detected in patients with cerebellar disease, while learning on this task appears normal in Huntington's disease.

Chapter 2 - Huntington's Disease Begins as a Dysfunction in Error Feedback Control

Introduction

Huntington's disease (HD) is an autosomal dominant inherited neurologic disorder caused by a trinucleotide repeat expansion in the IT15 gene on the short arm of chromosome 4[1]. Disease symptoms usually appear in the fourth or fifth decades of life, and then progress steadily during the succeeding 10-20 years[2]. Motor dysfunction, cognitive decline, and psychiatric disturbances characterize the manifestation of HD. Significant, progressive atrophy of the basal ganglia as a whole, and in particular, the caudate and putamen are evident in HD[3] and may even be detectable before clinical onset[4].

The hallmark motor sign of HD is chorea: the occurrence of rapid, irregular, and arrhythmic complex involuntary movements. In fact, Huntington's Disease is often referred to as Huntington's chorea. The severity of chorea progresses during the first 8-12 years of the disease but then levels off, and may even subside at late stages in the disease. Despite the fact that chorea is the most distinctive and well-known feature of HD, substantial impairment of voluntary movement also occurs, and it may be of greater functional importance in the lives of symptomatic patients[5]. Early in the disease course, rapidly alternating movements are slowed or disrupted. Patients become somewhat clumsy and may have trouble with fine motor tasks such as tying shoelaces, buttoning clothing, or performing needlework**2**. In the later stages of HD most voluntary

movements are markedly slow, and eventually, many patients deteriorate into a rigid state in which they are largely incapable of movement.

Characterizing the functional deficits associated with a disease process is an important step toward understanding the mechanisms through which the disease pathology manifests itself. Despite the widespread clinical recognition of qualitative impairment in voluntary movement, and the lack of understanding about how these deficits arise from the known disease pathology, functional characterization of this dysfunction in movement control has not been well established. Two control processes are hypothesized to play important roles in the execution of arm movements. Feedforward control is the generation and execution of motor commands based a priori on the desired action and an internal model of the system's response[21,22,23], while feedback control entails the 'mid-flight' correction of these commands based on errors detected during their execution. Quantitative analysis of voluntary movement trajectories in a control theory framework has the power to differentiate disturbance in these two control processes and to provide valuable insights into the nature of the motor dysfunction in HD in general. To this end, we used a high performance manipulandum[28] to record visually guided point to point reaching arm movements in patients with HD and presymptomatic individuals with the HD mutation.

Methods

Subjects

11 patients positive for the IT-15 mutation and symptomatic with Huntington's Disease, 16 mutation-positive presymptomatic subjects, 3 mutation-negative subjects who

had a parent with HD, and 12 other age-matched controls participated in the first experiment. 5 symptomatic and 9 presymptomatic HD subjects, 8 age-matched controls, and 6 subjects with cerebellar lesions participated in the second experiment. All subjects used their dominant hand, and all but one presymptomatic in the first experiment were right handed. The direct gene test for IT-15 mutation was conducted at the Johns Hopkins Huntington's Disease Project. The length of the CAG trinucleotide repeat was determined, and subjects with a CAG repeat length of at least 37 were called mutation-positive. Subjects with CAG repeat length less than 34 were called mutation-negative. All cerebellar subjects that we studied had been diagnosed clinically with cerebellar dysfunction, and all had lesions localized to the cerebellum on MRI. 4 patients had generalized cerebellar atrophy, and 2 had suffered strokes of the right posterior inferior cerebellar artery (PICA). One of these patients also had a left PICA and a right superior cerebellar artery stroke.

Task

Subjects made quick reaching movements to targets spaced 10cm away while grasping a lightweight two-joint manipulandum. The 1cm square targets and a small cursor indicating the subject's hand position were displayed on a computer monitor in front of the subject[21]. During the first experiment, the training took place in two sessions and within sessions it was subdivided into 100-movement sets. In the first session, subjects completed three sets of training. After a 3 to 4 hour break, they began the second session, which consisted of a single set. The robot arm remained passive for all movements in both sessions. During the second experiment the robot produced a 70 ms bell shaped force pulse on a minority of randomly pre-selected trials (with a probability of

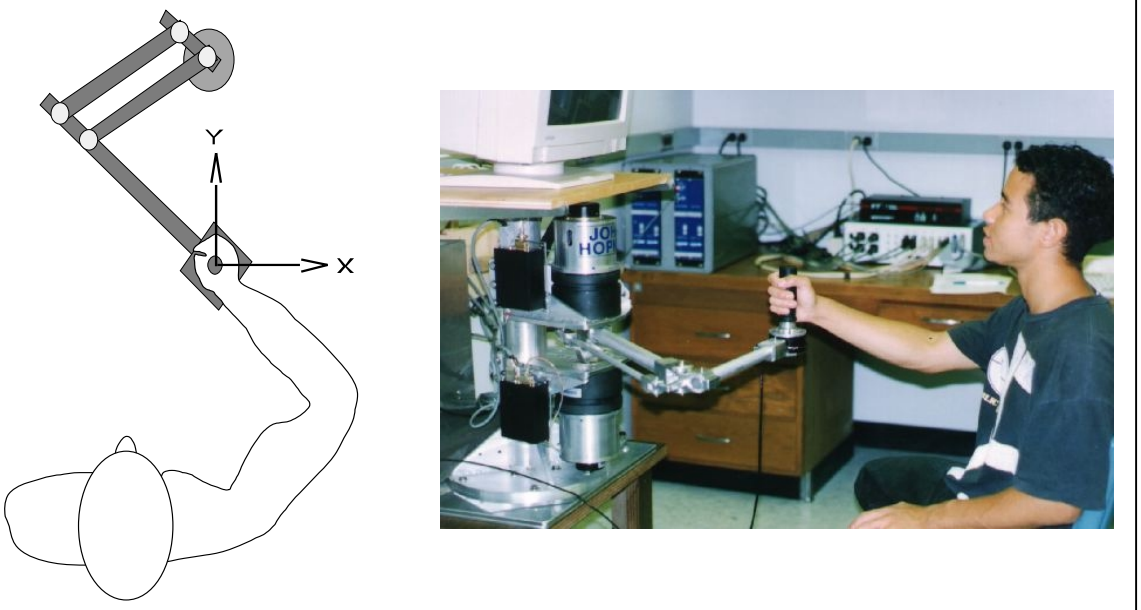

Figure 2.1: Diagram and photo of subject grasping manipulandum.

1 in 4). The force pulse could be in any one of 8 directions and of magnitude 6, 12, or 18N. One force pulse in each direction and of each magnitude was given for each direction of movement. During both experiments we used a sling suspended from the ceiling to support the subject's upper arm in the horizontal plane. This helped regularize the subjects' arm position and minimize the effort required to support the arm against gravity.

Analysis

Position and velocity of the joints of the robot arm were recorded at 100Hz from absolute and relative joint position encoders with resolution of $5.5*10^{-3}$ degrees and $8.0*10^{-4}$degrees, respectively. This produced estimates of hand position and velocity in Cartesian coordinates with accuracy greater than 0.1mm and 1.3mm/sec, respectively. We define the end of the movement as the end of the first time interval after movement onset when hand velocity always remained below a threshold of 0.03m/s for 200ms.

We characterized aiming direction by defining angular aiming error as the difference between the target direction and the direction of travel up to the peak speed point. Note that aiming error for a given movement can be positive or negative. Aiming bias for each subject was defined as the average of the magnitude of the aiming error in each target direction. Similarly, aiming variability for each subject was defined as the average of the standard deviation of aiming error in each target direction.

Jerk is defined as the rate of change of acceleration with respect to time. In order to minimize the effect of discretization noise on the differentiation of the velocity signal, jerk was estimated by applying a fourth order Savitsky-Golay filter on a 250ms window of velocity data. This filter is equivalent to taking the second derivative at the window's center of the continuous least squares best fit fourth order polynomial. This fourth order polynomial fit is a linear, low-pass, finite impulse response (non-recursive) filter with a cutoff frequency of 6.83Hz. Power spectra of mean subtracted velocity profiles of very fast 10cm reaching movements show that 99.9% of the power is below 6Hz.

The minimum total squared jerk (TSJ) required for a point-to-point movement is proportional to the fifth power of the movement speed and inversely proportional to the third power of movement excursion. Because of the strength of the relationship between these variables and TSJ, it is critical to appropriately normalize movement speed and excursion when comparing the amount of jerk between two movements. To account for the effect of speed and excursion on a movement's typical jerk, we normalized the TSJ measured for each movement by the average TSJ for movements made after practice by a large separate group of controls (n=35), at the appropriate speed and excursion. Similarly, we normalized the TSJ in the pre-peak and post-peak movement segments by

the average values of these quantities for control movements of the same peak speed and excursion, and we refer to these quantities as pre-peak jerk and post-peak jerk.

Since the trajectories of perturbed movements were often quite irregular, and the peak speed was often strongly influenced by the presence and direction of the perturbing force pulse, normalization of jerk by peak speed was no longer appropriate for these movements. Instead, we normalized the post-perturbation jerk for a given movement by the minimum possible jerk required to make the movement state transition displayed in that movement segment – determined by analytical solution of this optimization problem using the calculus of variations (Flash 1987). Similarly, we define post-perturbation path length as the path length between the point of perturbation offset and the end point of movement divided by the straight-line distance between these two points. We compare the values of these quantities for movements during which perturbations were given to the corresponding values for unperturbed movement. For unperturbed movements, we define the time point of "perturbation offset" as that time when perturbation offset would have occurred had a perturbation been given.

Results

Basic Properties of Point-To-Point Reaching in Huntington's Disease

Figure 2 displays the hand paths of the two most regular and the two least regular movements in each direction, for several subjects after 200 practice movements. The regularity of each movement was accessed by the correlation coefficient[21] between that movement's velocity profile and that of the subject's most typical movement in its direction. The movement in each direction with highest average correlation to all other

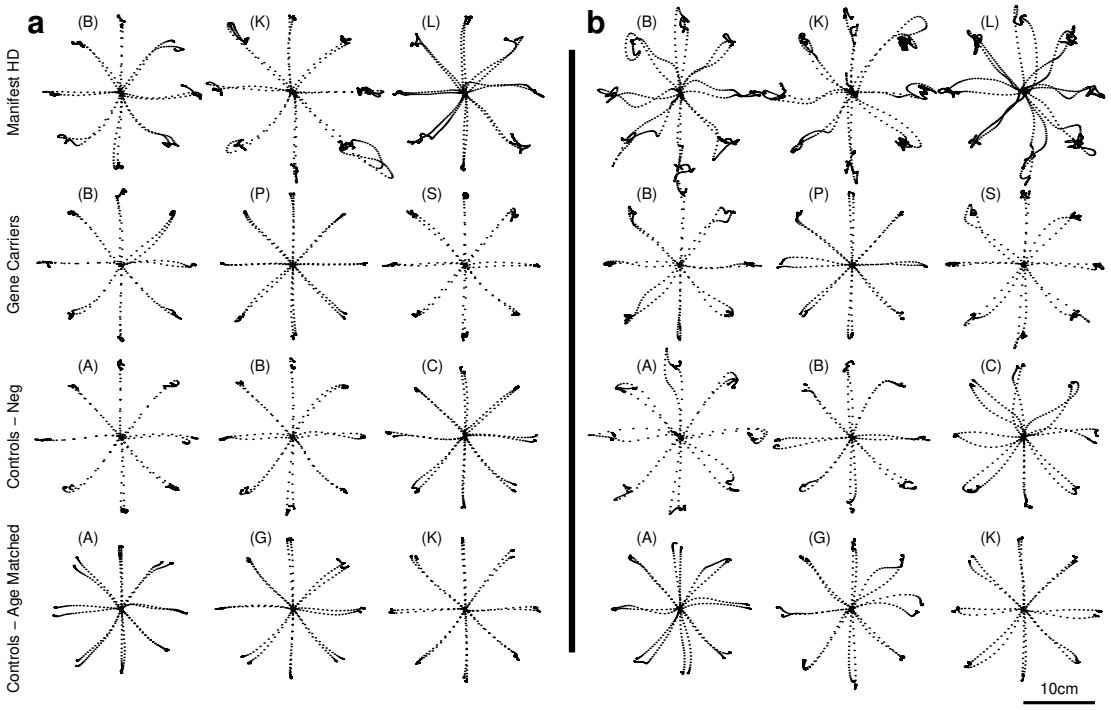

Figure 2.2: Hand paths from selected subjects after 200 practice trials (movements 201-300). **a,** The two most regular movements in each direction. **b,** The two least regular movements each direction. Movement regularity was determined by the correlation coefficient[21] of the velocity profile with the velocity profile of that subject's typical movement. The typical movement was defined as the movement in each direction with the highest average correlation to other movements. Hand paths are plotted from the center out relative to their starting positions. Points are spaced 30ms apart in time. The distance between consecutive points is proportional to the movement speed during that interval. Top row: subjects with manifest HD. Second row: asymptomatic gene-carriers. Third row: controls who have a parent with HD but who are mutation negative. Bottom row: controls age matched to the asymptomatic gene-carriers. The letter that labels each subject identifies him or her in figure 3.

movements was deemed most typical. The hand paths are plotted from the center out, so that each path plot begins at the center and moves outwardly. In each plot, points are spaced equally in time so that the distance between consecutive points in a plot is proportional to the speed during that part of the movement.

Some movements made by symptomatic HD subjects appear normal while others are markedly irregular. After practice, the range of movement quality is generally much larger in HD patients than controls. Specifically, many HD movements have large changes in direction, smooth or abrupt, before approaching the target, while almost all

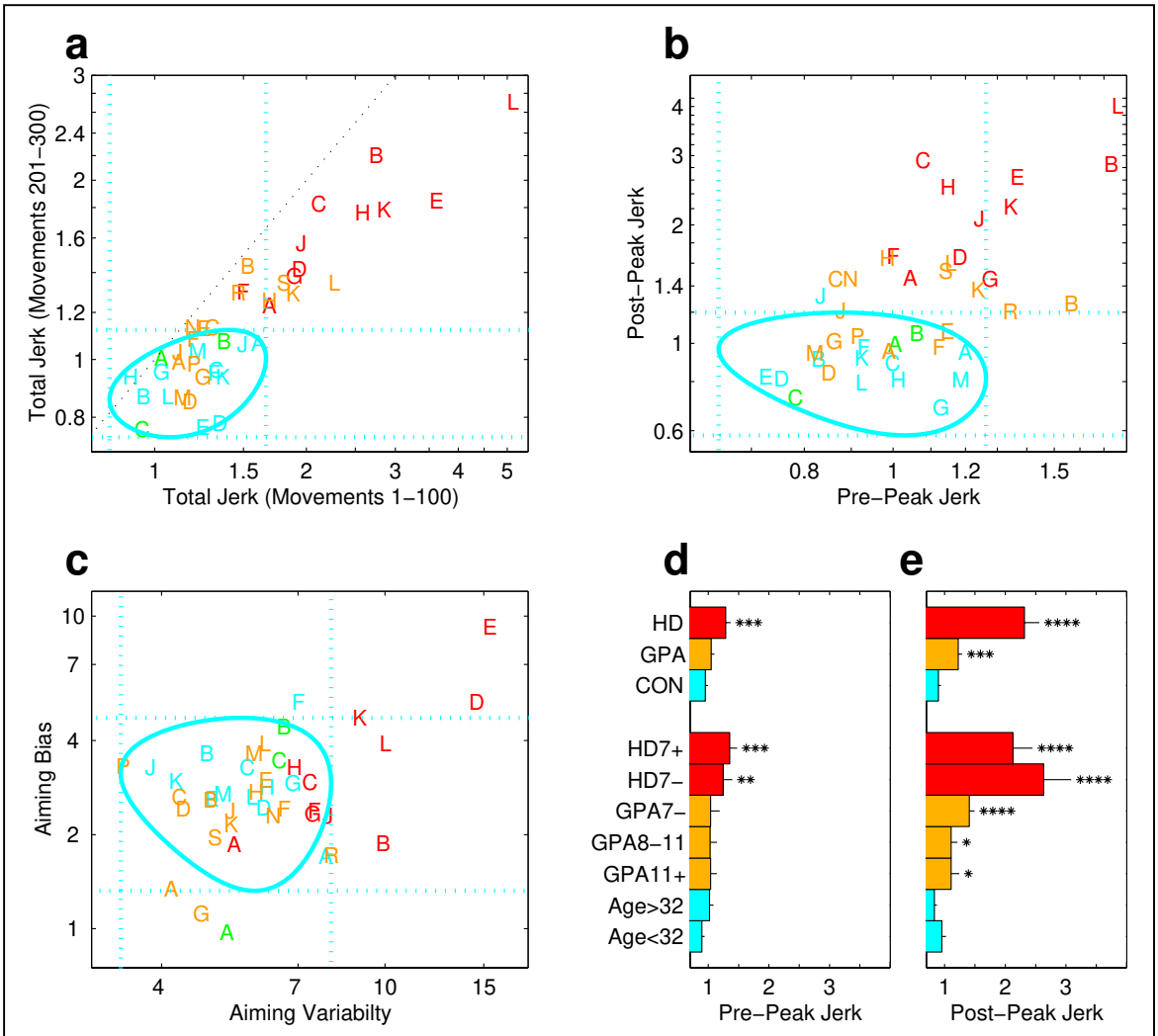

Figure 2.3: . Quantification of movement properties. Red: subjects with manifest HD. Orange: asymptomatic gene-carriers. Blue: age matched controls. Green: gene-negative individuals having a parent with HD. Note that a-c are plotted on a logarithmic scale for clarity. The blue dotted lines show the 95% confidence intervals for the control distribution (mean +/- 1.96 standard deviations). The black diagonal line in a represents the axis of equality (y=x). **a**, The mean of the normalized total squared jerk for all subjects in the first 100 movements and in movements 201-300. **b**, The mean of normalized jerk (in movements 201-300) before and after the peak in the movement speed. The pre-peak segment, which reflects movement initiation, appears much less disturbed in HD than post-peak segment, which reflects movement completion. **c**, Aiming bias and aiming variability. We refer to aiming as the direction of travel with respect to the initial target direction, during the pre-peak movement segment. Like pre-peak jerk, aiming reflects the quality of movement. **d,e**, Group-wise comparisons of normalized pre-peak and post-peak jerk, respectively. Asterisks indicate significantly worse performance than control subjects. * p<0.05. ** p<0.01. *** p<0.001. **** p<0.0001. HD7+: Subjects with manifest HD for more than 7 years. HD7-: Subjects with manifest HD for less than 7 years. GPA7-: Gene-carriers less than 7 years from predicted onset. GPA7-11: Gene-carriers 7 to 11 years from predicted onset. GPA11+: Gene-carriers more than 11 years from predicted onset. Age>32: control subjects more than 32 years old. Age<32: controls less than 32 years old.

.

movements fail to stop efficiently and smoothly near the target - note the wiggling and abrupt deceleration and acceleration near the target.

One way to characterize these irregularities is to quantify the smoothness of each movement. One widely held view in motor control theory is that the best movement is the smoothest possible movement that will accomplish the task. Smoothness can be defined as the lack of abrupt change, so a trajectory that minimizes abrupt changes in a variable will maximize its smoothness. Human reaching movements have been found to be of near maximal acceleration smoothness, quantified by minimal cumulative squared acceleration change[29], also referred to as minimum total squared jerk. Smooth reaching movement plans also produce maximal endpoint accuracy in the face of motor system variability[30].

Figure 3a shows that all HD patients tested made movements with higher than normal jerk. Several presymptomatic, mutation positive subjects also made movements with higher than normal jerk, but other asymptomatic subjects made movements whose average fell within the normal range. Notably, all HD subjects reduced their movement jerk with practice, although not nearly to control levels. The smoothness of movements increased over time even in subjects who were markedly more jerky than normal.

In order to compare the initiation and completion of movement, we split each movement in half at the peak in the speed profile. This is roughly the point at which movement toward the target switches from acceleration to deceleration. Comparison of the total squared jerk before and after the peak in the speed profile (figure 3b) reveals that while fewer than half of the HD patients have high jerk during both parts of the movement, all have greater than normal post-peak jerk. Only 2 of 16 presymptomatic

subjects have above normal pre-peak jerk, but 9 of 16 have higher than normal post-peak jerk. To assess disease progression in presymptomatic subjects, we used an estimate of disease onset age based on each subject's parental onset age and trinucleotide repeat length[4]. The amount of post-peak jerk correlated significantly (r=-0.62) with estimated time to disease onset for presymptomatic subjects while the pre-peak jerk did not (r=0.02). Post-peak jerk was above normal in 4 of 5 close to onset (<7 years) subjects and in 3 of 9 far from onset subjects. As groups, both HD patients and presymptomatic subjects had significantly higher than normal post-peak jerk ($p<10^{-6}$, $p<0.00012$) (see figure 3e). Moreover, AGC subjects who were close to predicted disease onset (< 7 years) had significantly higher jerk in the third set than far from onset (> 7 years) subjects ($p<0.0062$) who in turn had significantly higher jerk than controls ($p<0.013$).

Figure 3c shows that initial aiming is not dramatically disturbed in HD. Average directional aiming bias (see methods) is normal in 9 of 11 HD patients. Aiming variability is in the control range for a majority (6 of 11) of patients, although as a group, subjects with manifest HD display increased aiming variability. All presymptomatic subjects have normal aiming biases of 3-7 degrees and none have above normal aiming variability.

The comparisons of the pre-peak and post-peak movement segments suggest that HD movements often begin normally, but become jerky and irregular at some point during their course. Comparison of the average time course of raw squared jerk profiles between groups for movements in different speed ranges (figure 4), reveals a strikingly consistent pattern of HD behavior relative to controls. At each speed range, the HD average squared jerk profile closely matches the control profile during the beginning of

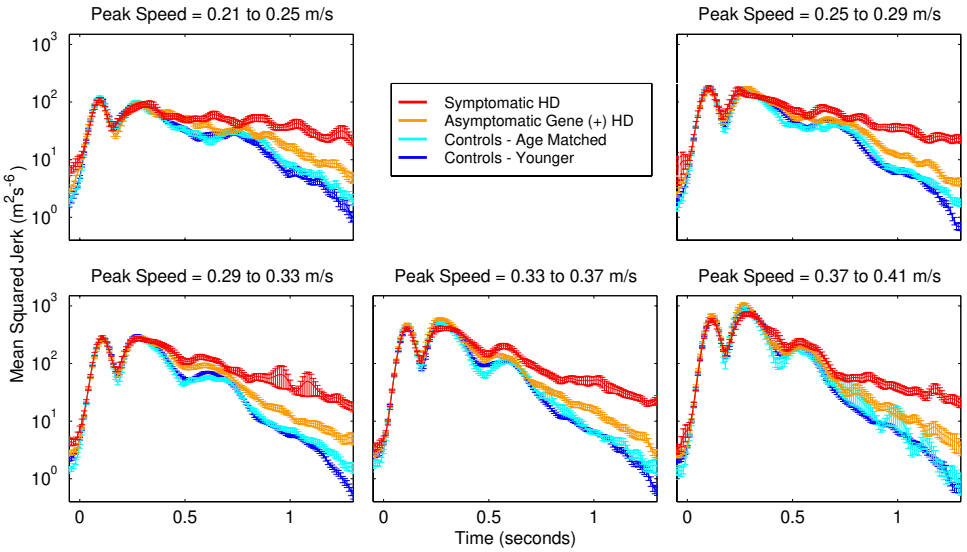

Figure 2.4: Squared jerk profiles for different movement speeds. Average raw squared jerk ± standard error is plotted on a logarithmic scale as function of time since movement onset for movements in each speed range, in different subject groups. For reference, the second peak in the squared jerk profile approximately corresponds to the peak in the speed profile. Note that at all speed ranges the separate groups have quite similar jerk profiles until 300ms, but HD subjects have very different profiles after this point.

movement, but begins to separate from it 200-300 msec after onset. Note that the end movement squared jerk is 10-30 times greater in HD's than controls.

Why might HD movements begin to become irregular 200-300ms into their course and not before? Corrective actions based on sensory information acquired during the movement begin to take place at about the time at which HD movements become irregular, so one possibility is that the system that generates these corrective actions is disturbed. Vision plays a substantial role in the planning, guidance and correction of arm movements[31], and visual feedback sensorimotor reaction delays are believed to be 200-300ms[32,33]. Movement corrections based on proprioceptive sense can also take place, and these corrections have delays of 100-200ms[33,34]. Thus, there appears to be a close correspondence between the estimated time of first corrective responses and the time

when HD movements become irregular, suggesting that a disturbed error correction process may lead to some of the irregularity in HD movements. Another possibility is that there is a disturbance in end-movement control independent of error handling. The time point at which HD movements become irregular also roughly corresponds to the switch between the accelerative and decelerative phases of movements. So there may simply be a disturbance in controlling the decelerative phase of movement independent of the error correction process.

Characterization of the Performance of Error Feedback Control Systems in Response to Self-Generated Errors

To distinguish between a disturbance in error feedback control and a disturbance in end-movement control independent of error feedback, we attempted to characterize the performance of the error feedback control system in HD. If the system that generates corrective actions during movements (the feedback controller) is affected in HD, then a strong relationship should exist between the error during the early stages of movement and the disturbance later. Error, the difference between desired system state and actual state at any point in time, is the primary input to a feedback controller. If the error during a movement is small, then large corrective actions are not necessary and dysfunction of the feedback control system should generally have only a minimal effect on the movement. However, if errors during a movement are large, substantial corrective actions are required, and dysfunction in the feedback controller may have a significant effect on the movement.

During our experiment, we can measure actual movements quite accurately. However, we have no reliable way of estimating the desired motion state within a single

movement. This makes direct estimate of error time course infeasible. If errors are symmetrically distributed, then the average movement profile should approximate the average motion plan. However, the plan may not be stationary throughout any set of movements. A subject might easily try to move a bit faster on one trial then slower on the next, and these trial-to-trial variations in the kinematic plan may be as large as the typical errors between plan and action. Although the desired motor action might change from one trial to the next, a few of its properties seem to be invariant. The velocity profiles of well-practiced point to point arm movements are symmetric and unimodal: a single large peak in the velocity profile exists and it generally occurs very close to the movement's midway point, regardless of the movement's amplitude, direction, or speed[35]. Therefore, the distance between the midway point and the position where the peak speed occurs can be used as an indicator of error early in the movement.

The relationship between error early in the movement and jerk late in the movement is shown in figure 5. The probability distributions of peak speed positions (PSPs) do not differ dramatically between groups (figure 5a,c,e,g,i) although presymptomatic subjects appear to have somewhat less variation in PSP than controls while symptomatic subjects have somewhat more. This implies that amount of error early in the movement is comparable between groups. However, the reaction to this error is very different between groups. Figure 5b,d,f,h,j show that the jerk that occurs after the hand reaches the PSP varies considerably with PSP in all subject groups. When the PSP is far from the midway point, indicating large error early in the movement, post-peak jerk is high. However, the sensitivity of post-peak jerk to PSP is much greater in presymptomatic subjects and HD patients than controls. Figure 5h shows that the

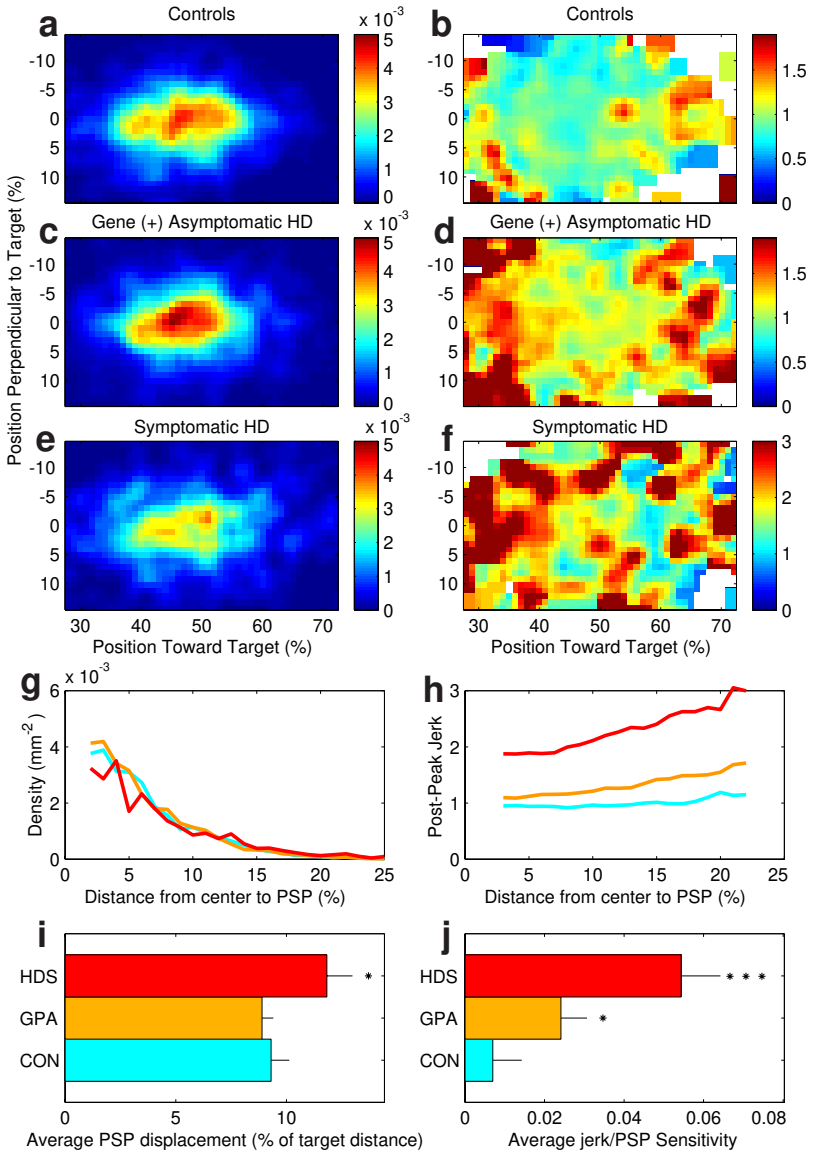

Figure 2.5: Errors that occur early in the movement, before the hand reaches its peak speed, predict jerk that occurs later. a,c,e, The two-dimensional probability densities of peak speed positions (PSPs), for each group during movements 301-400. This is the likelihood of the peak speed occurring at each position. The x-axes are in the target direction, and the y-axes are in the direction perpendicular to the target. PSPs are clustered near the movement midway point. **g,** Summary of **a,c,e**: the average probability density at a given displacement between the PSP and movement midway point (50%, 0%). Large values for the distance from midway point to peak speed position indicate large early-movement errors, which are uncommon. The similarity of these distributions indicates that there are not large differences in the pattern of error recorded from the three subject groups early in the movement. **b,d,f**, End-movement jerk as a function of peak speed position. When large early movement errors occur, as indicated by large PSP displacements (near the image boundaries), the post-peak jerk is increased for all groups, but the increase is greater for asymptomatic and symptomatic HD subjects than controls. White color on images indicates no data. **h**, Summary of **b,d,f**: the average end-movement jerk at a given displacement between the PSP and movement midway point. i, average PSP displacement for each group. j, sensitivity of end movement jerk to PSP, measured as the slope of the relationship between them. Asterisks indicate significantly worse performance than control subjects. * $p<0.05$. ** $p<0.01$. *** $p<0.001$.

disparity in mean post-peak jerk between controls and presymptomatic subjects is much greater at large PSP displacements than at small displacements. Subjects with manifest HD ($p=0.006$) and asymptomatic gene-positive subjects ($p=0.04$) display significantly higher sensitivity in the response of their end-movement jerk to early movement error than do controls, as measured by slope in this relationship. The sensitivity of post-peak jerk to PSP displacement indicates the degree to which end-movement smoothness depends on early-movement error. The increase in this sensitivity in HD subjects with and without clinically manifest symptoms suggests that an error dependent control process is disturbed early in the disease course and further deteriorates with disease progression.

Previous reports have shown that cortical sensorimotor pathways are affected in patients with manifest HD. While short-loop reflexes that are mediated by spinal mechanisms are normal, long-loop reflexes, which involve the transfer of proprioceptive information through cortical pathways, are reduced or absent in HD[24,25]. Cortical responses to peripheral nerve stimulation, as measured by somatosensory evoked potentials (SEPs), are also reduced in HD[24,15,26,27], suggesting that diminished cortical sensory input is responsible for the long-loop reflex reduction[25]. Additionally, a strong correlation exists between SEP deterioration and striatal glucose metabolism early in the course of HD[15], hinting at a possible involvement of the striatum in the pathology of the SEPs and long-loop reflexes in HD. Since cortical sensorimotor pathways play a large role in mediating error correction during voluntary movement, disruption of these pathways could lead to dysfunctional feedback control during movement.

Responses to Externally Applied Perturbations

Our analysis of the response to internal, self-generated errors suggested that error correction in general might be disturbed in HD. To test this hypothesis we studied the response of these individuals to externally imposed errors during voluntary movement by developing a task in which subjects make point to point movements but occasionally receive a short (70ms) well-controlled force pulse shortly after movement initiation. These pulses were delivered by our manipulandum and were applied randomly on a minority of trials, and could be in 8 different directions and of 3 different magnitudes: 6, 12, and 18 Newtons peak force. In addition to subjects with Huntington's disease, we were able to study the performance of individuals with cerebellar deficits on this task. Hand paths of two symptomatic HD subjects, one presymptomatic subject, one control, and three cerebellar subjects for movements perturbed with 12 and 18 Newton force pulses are shown in figure 6. These perturbations to movement are substantial: trajectories can be altered by up to 4 or 5cm (target distance is 10cm). Control subjects correct these perturbations relatively smoothly and monotonically, but several corrections made by HD subjects seem somewhat unstable. Extremely large successive overshoots are seen during certain HD movement corrections that never appear during the perturbed movements of controls. Not all HD movement corrections appear disturbed, but some are so dramatically disturbed that they bore little qualitative similarity to any movements that we recorded from controls. Some of the movements made by HD subjects become dramatically disturbed after a perturbation is applied. A few of the most greatly disturbed trajectories are highlighted in red. Note the highlighted trajectory towards 10:30 for HD subject 1. Here the movement begins in the correct direction but is perturbed to the left.

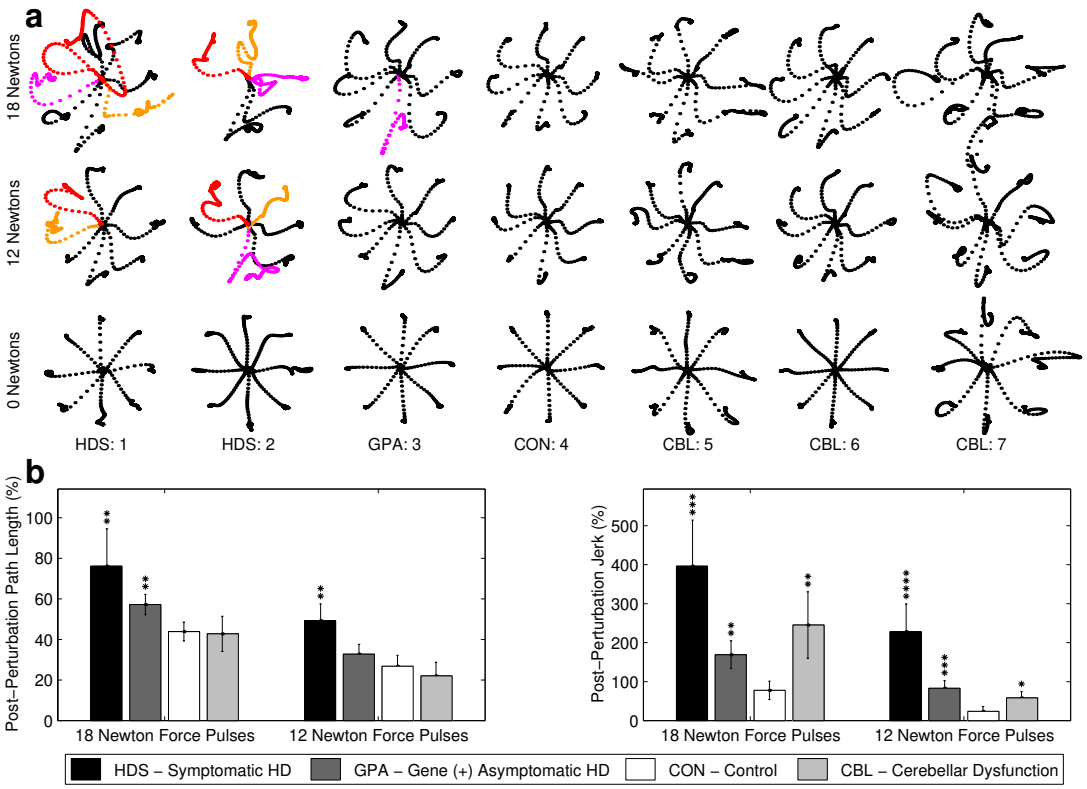

Figure 2.6: Force pulse perturbations disturb the movements of HD subjects more than controls or cerebellar subjects. a, Sample movement trajectories during the perturbation task. Top two rows: movements during which an 18 or 12 Newton force pulse was applied in the 7:30 direction. Bottom row: typical unperturbed movements interspersed within the perturbed movements. Some of the movements made by HD subjects become dramatically disturbed after a perturbation is applied. A few of the most greatly disturbed trajectories are highlighted. Note the trajectory towards 10:30 for HD subject 1. Here the movement begins in the correct direction but is perturbed to the left. The 'correction' then brings the movement quickly back all the way past the original starting location, turns around and heads roughly toward the target, then makes a final turn, moves toward the target and stops. **b,** Change in movement properties in response to force pulse perturbations (% change with respect to unperturbed movements). Right panel: normalized post-perturbation path length. Left panel: normalized post-perturbation jerk. Asterisks indicate significant increases above control disturbance. * p<0.05. ** p<0.025. *** p<0.01. **** p<0.001.

The 'correction' then brings the movement quickly back all the way past the original starting location, turns around and heads roughly toward the target, then makes a final turn, moves toward the target and stops. This movement was one the most dramatic examples of disturbed correction that we saw, but many other perturbed movements display clearly disturbed correction.

Several movements made by cerebellar subjects appear to have irregular and inefficient corrections, but close inspection of many of these trajectories reveals a striking similarity between the pattern of overshoots in these movements and the overshoots that are present in unperturbed movements in the same direction. This suggests that much of the irregularity that exists in these perturbed movements has a stronger relationship to the direction of movement than to the presence of perturbation. Note the movements toward 3:00, 4:30, and 7:30 for subjects 5 and 7.

HD subjects appear to have dysfunctional reactions to movement errors caused by external perturbations. During the post perturbation movement segment (the corrective period), relative jerk and path length are increased over the corresponding periods in unperturbed movement significantly more for HD subjects than controls (see figure 5b) for both 12 and 18 N perturbations. The error-correction performance of presymptomatic subjects generally falls between that of controls and subjects with manifest HD. Cerebellar subjects, like symptomatic HDs , had worse baseline (unperturbed) movement performance than controls, but the decrement in their performance when perturbations were given was generally more like that of controls than HD subjects. This suggests that subjects with HD generally have greater deficits in error feedback control than do cerebellar patients.

Discussion

The existence of performance deficits on tests of behavioral function before the clinical onset of HD is controversial. To date, assessments of motor, cognitive, or psychiatric function in HD have revealed only subtle deficits in presymptomatic subject

groups[6,7,8] if any[9,10,11]. Even when changes have been detected, they were not sufficiently specific to permit discrimination between mutation positive and mutation negative individuals, or even reliable identification of people with early stage manifest HD. In contrast, functional imaging of the basal ganglia reveals low glucose metabolism in about two thirds of asymptomatic at risk individuals[**15**,12,13,14] and basal ganglia volumes may be reduced years before clinical onset[4], suggesting that brain pathology may substantially precede manifestation of the behavioral dysfunction previously studied. However, end-movement jerk appears to be a fairly sensitive task-performance based indicator of Huntington's Disease progression, suggesting the existence of a direct behavioral correlate to the early brain pathology of HD.

The findings that movement completion is much more impaired than initiation and that the sensitivity of movement jerk to errors is increased, point to relatively spared feedforward control, but dysfunctional feedback control processes in HD. Movements that lack feedback control, as in deafferented subjects, are smooth but inaccurate[36] whereas the HD movements we measured are accurate but high in jerk. Thus, feedback corrections are not missing in HD, but rather are inappropriate. Force pulse perturbations do not cause movement trajectories to pause at locations related to the perturbation direction, rather successive target overshoots and corrective movements in apparently inappropriate directions seem to characterize the disturbed corrections made by HD subjects.

The feedback control dysfunction that we observe may help explain the pattern of motor learning deficits reported in HD. Individuals symptomatic for HD show intact learning of mirror tracing[37], but impaired learning on rotary pursuit tasks[37,38]. Our results

suggests an interpretation of these findings in a feedforward / feedback control framework. Rotary pursuit tasks involve long continuous movements, which are largely under closed-loop feedback control. In contrast, mirror tracing of polygons involves multiple short, discrete movements, which rely more heavily on open-loop feedforward control processes. Therefore, intact feedforward, but impaired feedback control learning may also characterize HD.

Real time error feedback control presents a formidable challenge to the CNS because of the large sensorimotor delays that occur (100-300ms). The stability of simple linear negative error feedback controllers decline quickly as loop delays increase. These systems must respond very slowly to preserve stability as delay increases[39]. One way to improve the performance of such a feedback control system is to include a component which can effectively predict away the delay. This component could combine delayed sensory information with a knowledge of system's physical dynamics and of the motor output which would influence motion since the acquisition of that sensory information to predict the current or future motion state. This sort of predictor has been referred to as a forward model of system dynamics[40,41]. Neurons in the basal ganglia have been shown to predict reward[42] and predictive capacity may be a general feature of some basal ganglia structures. The main output of the basal ganglia modulates the action of the thalamus, which relays sensory information to the cortex. This information stream is likely to participate in error feedback control, thus the error correction process may be modulated by the basal ganglia, although the mechanism through which this occurs, including whether the predictive capacity of basal ganglia structures is involved, is not yet understood.

Chapter 3 – Visual Reaction Times for Arm Movements in Huntington's Disease

Introduction

By studying self-initiated movements, both with and without the application of external force perturbations, we were able to provide evidence for dysfunctional feedback control for both internally and externally generated errors in HD. Error correction involves the use of online (although delayed) sensory feedback in the guidance of movement. Correcting for error requires an initial evaluation of sensory input to estimate error, and the subsequent formulation of a response. In this chapter we ask the question of whether online and immediate use of sensory feedback is generally disturbed in HD, even when error correction is not directly involved. We approach this by studying the ability to evaluate visual input using a visual reaction time paradigm.

In our previous experiments, subjects were instructed to move to a target when they felt ready, not as soon as it appeared. They were instructed that the reward was given based on the duration of the time interval between movement onset and movement completion, and was independent of the time between target appearance and movement onset. In the perturbation experiments there was even an additional instructed delay period between target appearance and movement onset (see Chapter 2 methods). Using this paradigm, we found that movements began becoming disturbed 200-300ms after onset – corresponding to the time at which online sensory-based correction of movement should begin to occur.

It is likely that online sensory feedback only plays a small role during the beginning of self-initiated movements. In contrast, a reaction time task requires movement initiation to be guided by online sensory feedback about the movement stimulus. Reaction times for both eye and arm movements have been previously studied in HD. Latencies of eye-saccades and arm movements are slowed in manifest HD. HD subjects have been shown to have great difficulty in an anti-saccade task – during which they were instructed to saccade in the opposite direction from a peripheral LED after it was lit (Zee et al.). However, asymptomatic subjects who were gene-positive for the HD mutation performed normally on this task. A large study of almost 200 pre-symptomatic HD subjects found statistically significant, but only very small (5%) increases in reaction time (RT) for arm movements (Seimers et al). Since we were able to demonstrate substantially dysfunctional error correction in pre-symptomatic and clinically manifest HD patients, we hypothesized that careful study of a reaction time task on many of these same subjects might reveal additional deficits associated with sensory processing and integration in HD and shed light on the relationship between the neural processes underlying error feedback control and sensory guided movement initiation.

Methods

Task

We administered a reaction time task to seven patients with manifest HD and 14 individuals positive for the HD mutation, 3 individuals from HD families who were gene-negative and 13 other control subjects. The system we used for displaying targets and recording movements was described in Chapter 2. During the first set of reaction time trials (set F), which consisted of 60 to 90 movements, 1cm red-colored targets were

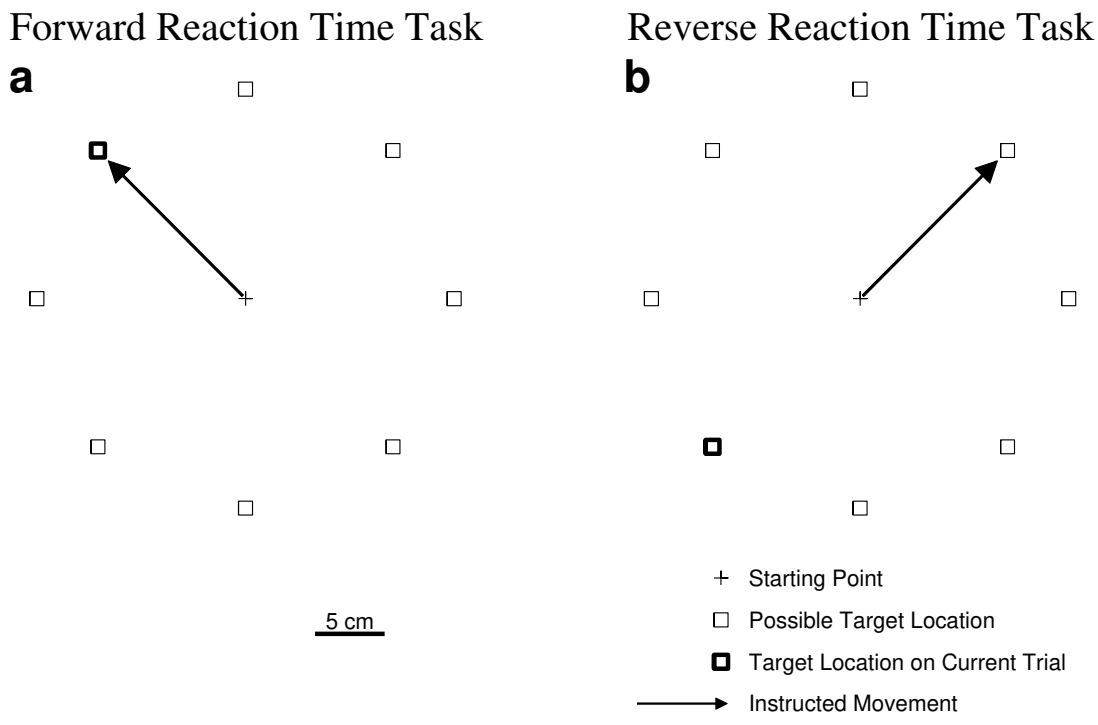

Figure 3.1 Illustration of Forward and Reverse Reaction Time Tasks. Subjects started in the center and attempted to make the instructed movement (forward or reverse) as soon as the target appeared. The first set (set F) consisted entirely of forward movements, the second set (set R) consisted entirely of reverse movements, and the third set (set FR) had forward and reverse movements randomly intermixed, with the target color signaling movement type. As shown, the target could appear in any of eight positions equally spaced 15cm from the staring point.

flashed in one of eight positions in the periphery of the workspace (see figure1a). Each subject grasped a robotic manipulandum with her dominant hand and was instructed to move this hand toward the target as soon as it appeared. Shortly after the subject reached the target it disappeared, after which the subject returned her hand to a cross-hair marking the center of the workspace to await the appearance of the next target. During the second set of trials (set R), also 60-90 movements, targets were flashed to the screen as before, but were instead yellow in color. Subjects were instructed to move in the direction opposite the target as soon as it appeared, and stop in the mirror of the target's location as

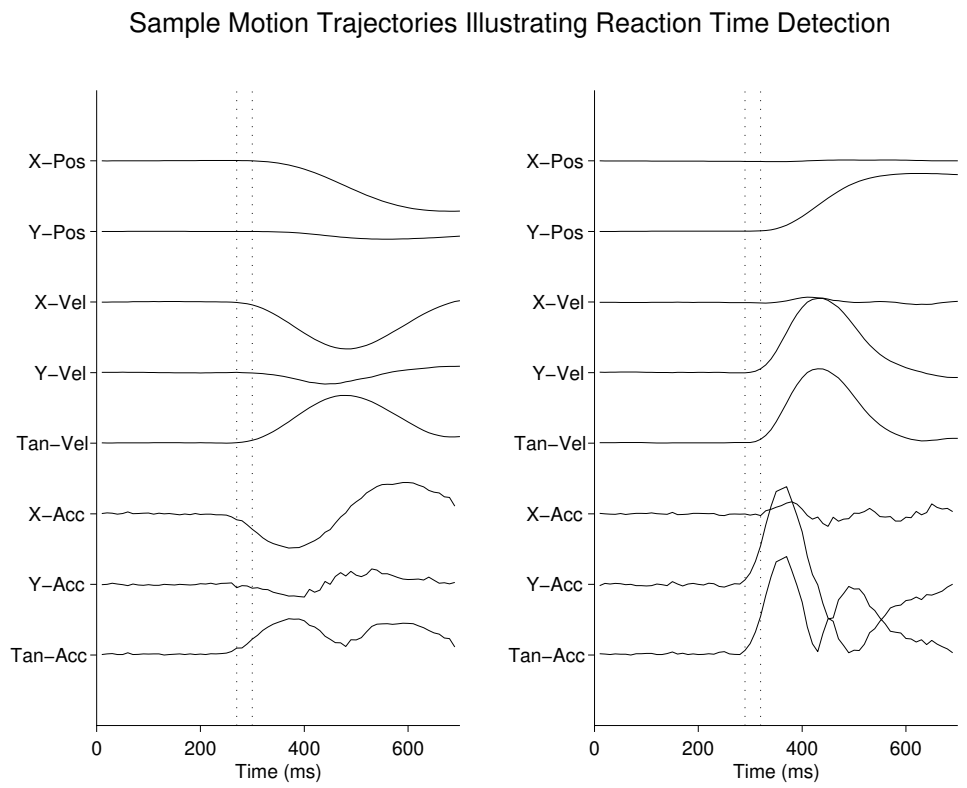

Figure 3.2 Motion Trajectories for Two Selected Trials Illustrating Reaction Time Detection. Time functions of position velocity and acceleration are displayed for each movement. The dotted lines represent the reaction time estimates obtained by tangential acceleration and velocity thresholding. In both cases, the first line corresponds to the threshold crossing of tangential acceleration and the second line corresponds to the threshold crossing of tangential velocity. These reaction times are referred to initial direction reaction times. Appropriate direction reaction times were computed similarly by determining the threshold crossings of the component of motion in the instructed movement direction. Since the initial motion is in the instructed direction for these two trials, the appropriate direction react times would be almost identical to the initial direction reaction time.

illustrated in figure 1b. During the third set (set FR), red and yellow targets were randomly interspersed with red targets appearing on two-thirds of the 90 trials.

Analysis

Reaction time to movement onset was measured by thresholding velocity or acceleration. Thresholds of 4cm/s and 50cm/s^2 were used. The time-point of threshold crossing was determined by linearly interpolating each trace between the samples

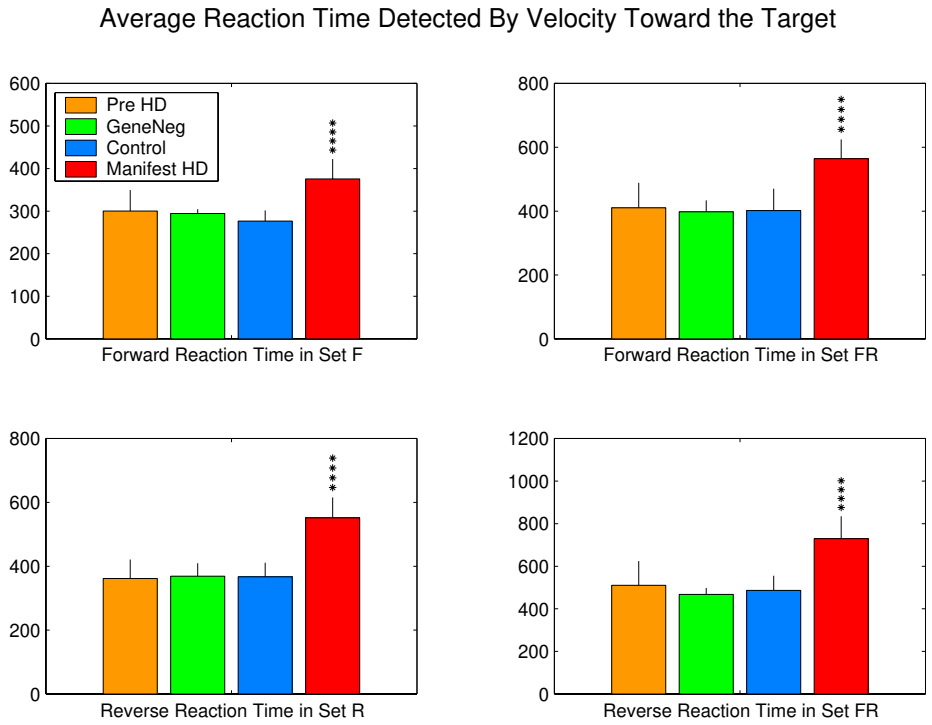

Figure 3.3 Appropriate Direction Reaction Times Detected by Velocity Thresholding. Average reaction times are displayed for all subject groups in sets F, R, and FR. Asterisks indicate significant increases from controls. Symptomatic but not presymptomatic HD subjects had reaction times which were significantly increased over controls in all sets. **** $p < 0.0001$.

immediately before and after threshold crossing. For each movement, both the raw reaction times to movement in any direction and the reaction times to motion directed toward the target were determined (see figure 2). The direction of the initial reaction was gauged by determining the direction of the acceleration vector with respect to the target at the first supra-threshold sample.

Results

Comparisons of Reaction Times Between Groups

Figures 3 and 4 show the average reaction times to motion in the appropriate direction for each group. The majority of control subjects had average velocity-threshold

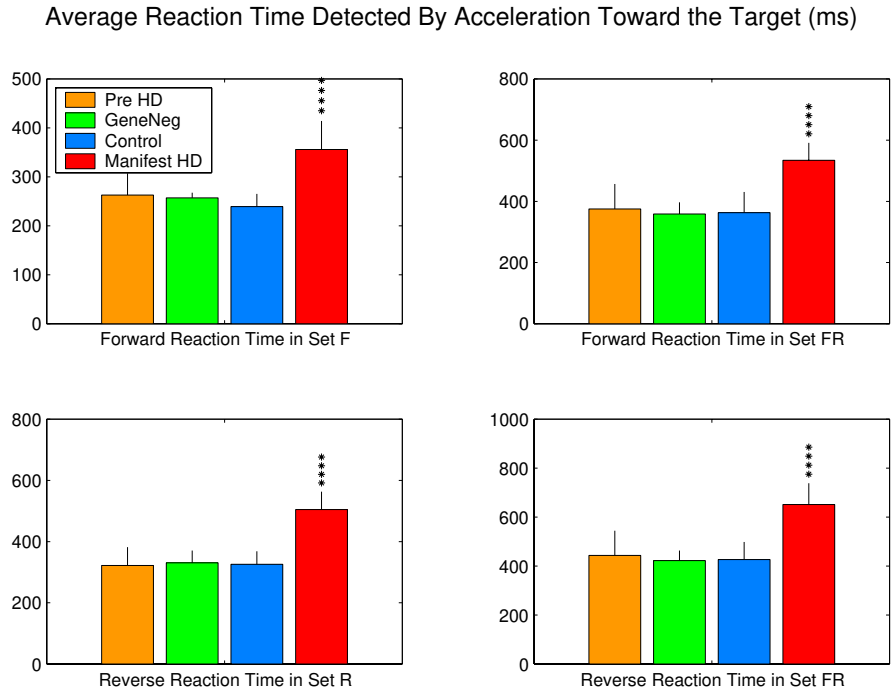

Figure 3.4 Appropriate Direction Reaction Times Detected by Acceleration Thresholding. Average reaction times are displayed for all subject groups in sets F, R, and FR. Asterisks indicate significant increases from controls. Symptomatic but not presymptomatic HD subjects had reaction times which were significantly increased over controls in all sets. **** $p < 0.0001$.

detected reaction times which varied between 260 and 320ms for forward movements in set F. Subjects with HD had average reaction times that were significantly increased over controls ($p<0.00001$); 100ms greater than controls on average. The difference in average reaction times between control and HD subjects increases to 160ms for forward movements in set FR, during which forward and reverse movements are intermixed, and is even greater for the reverse movements. HD subjects display significantly increased reaction time for both forward and reverse movement trials in all sets ($p<0.00001$ in all cases). Reaction times toward the target detected by acceleration (Figure 4) show the same trends between groups as the velocity-detected reactions, but appear uniformly lower by about 40ms across all groups and conditions.

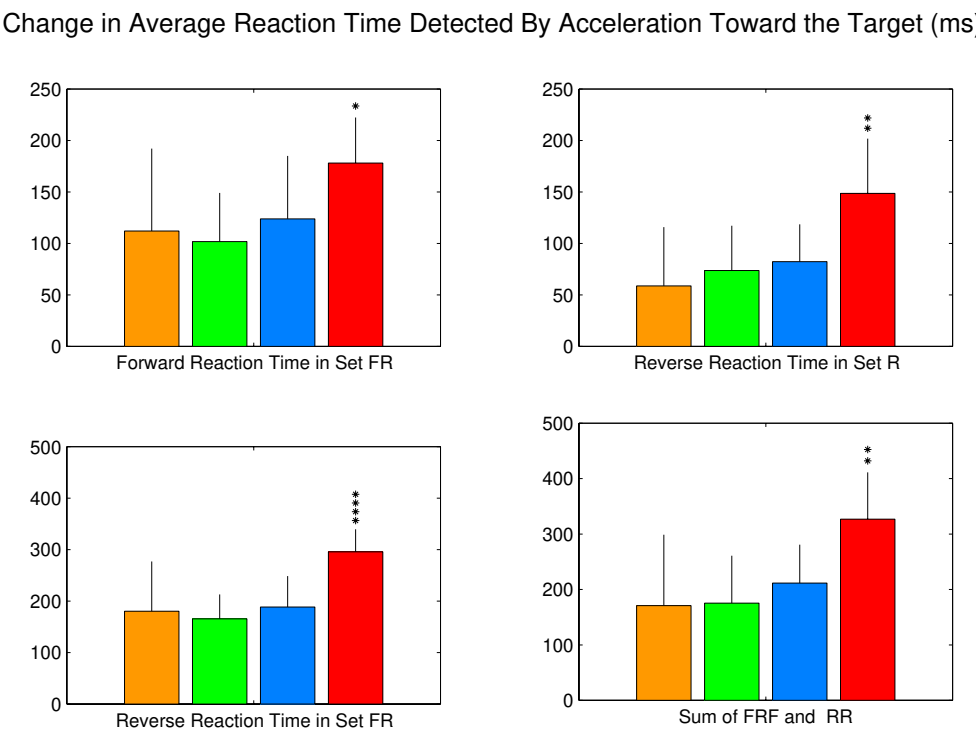

Figure 3.5 Changes in Reaction Time Relative to Baseline. The mean reaction time in set F (only forward movements) was deemed baseline for each subject, and reaction times in the other sets were compared to this baseline. The mean and standard deviation of the increase in reaction times from baseline across subjects are plotted for each group. Asterisks indicate significant increases from controls. **** $p<0.0001$, ** $p<0.01$.

In set FR, during which forward and reverse movements are intermixed, the average reaction times for forward movements for control and presymptomatic subjects increased by 110-120ms over the reaction times in set F (Figure 5a). During set FR, both the target's color and location were salient to the subjects' response, whereas in sets F and R only the target's location was salient. Subjects with manifest HD displayed reaction time increases that averaged 180ms - significantly greater than controls ($p<0.02$), but expressed as a percentage of the reaction times in set F (Figure 6a) the increase seen in subjects with manifest HD was no different than controls (52% versus 50%, $p>0.4$).

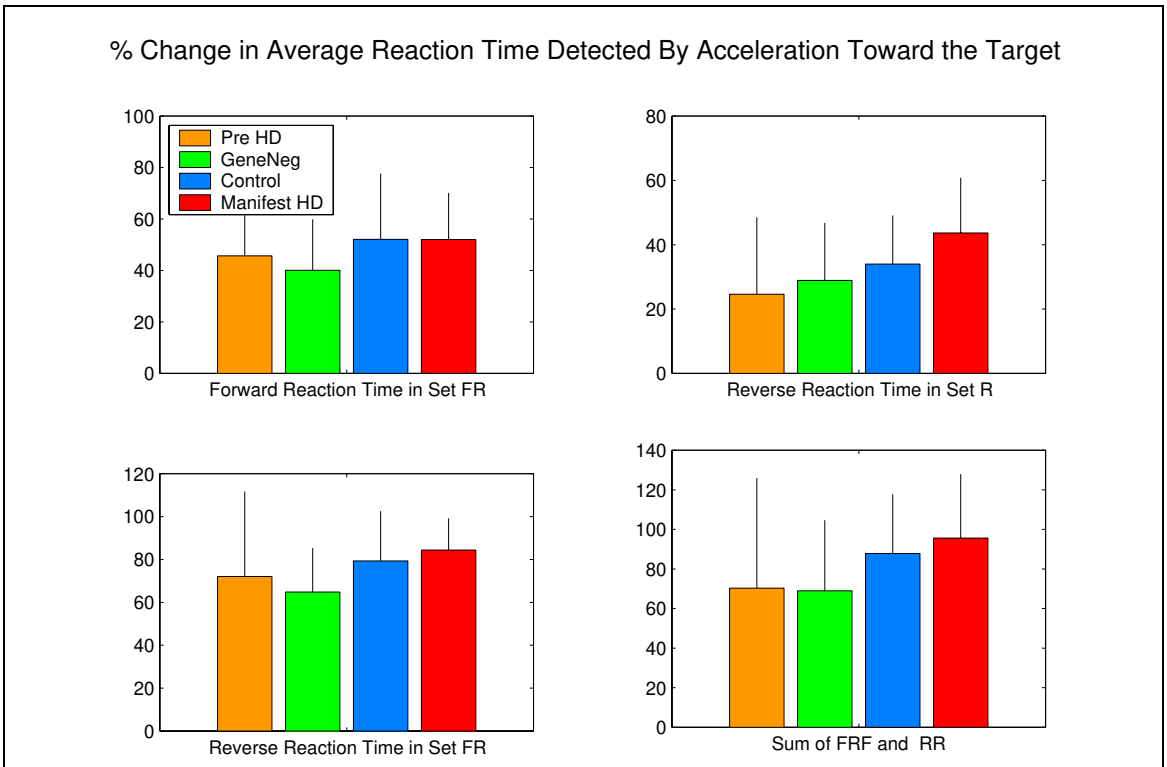

Figure 3.6 Relative Changes in Reaction time from baseline. The mean reaction time in set F (only forward movements) was deemed baseline for each subject, and the percentage change form baseline of the reaction times in the other sets was found. The mean and standard deviation of the percent increase in reaction times from baseline across subjects are plotted for each group.

Reaction times for reverse movements in set FR (Figure 5c) were increased by 180ms on average for both presymptomatic and control subjects, and by 300ms for patients with manifest HD. These raw increases in reaction time correspond to fractional increases of 76%, 72%, and 84% for control, presymptomatic, and symptomatic HD subjects, respectively (Figure 6c). The difference in these relative reaction times between symptomatic HD and control subjects is statistically significant ($p<0.0001$), but the difference between the percentage increases in reaction times is not ($p>0.2$).

The raw reaction time increases, from set F, for reverse movements in set R are 80, 60, and 150ms (Figure 5b), which correspond to changes of 33%, 25%, and 44% (Figure 6b) for control, presymptomatic, and symptomatic HD subjects, respectively.

Similar to the increases from baseline reaction times for the movements in set FR, the raw changes in reaction time are significantly different between symptomatic HD subjects and controls ($p=0.001$), but the fractional increases from baseline are not significant ($p>0.05$). In summary, subjects with manifest HD display reaction times which are increased in the baseline task, and they display incremental changes in reaction time in the secondary tasks (those tasks in which reverse movements or color-based decisions were required) which are also significantly increased over healthy control subjects. Furthermore, none of the incremental changes are of significantly different relative magnitude than the corresponding changes in control subjects. Since performance on the baseline task and on the secondary tasks involves processing of visual sensory information in different, non-reflexive ways, these data suggest that, on average, subjects with HD display a fairly uniform deficit in non-reflexive processing of visual information. The average reaction times of presymptomatic subjects were not significantly increased over control subjects in any of the tasks, however the same presymptomatic subjects displayed significantly increased signs of feedback control dysfunction, such as end-movement jerkiness and sensitivity to early movement errors (Smith et. al., 2000). This suggests that changes in average reaction time are not as sensitive as measures of feedback control dysfunction in detecting the early progression of Huntington's disease.

Components Within Reaction Time

For all groups, reaction times for reverse movements in set R, and for forward movements in set FR were greater than the reaction times in set F (Figures 3 & 4). Additionally, reaction times for reverse movements in set FR were greater than the

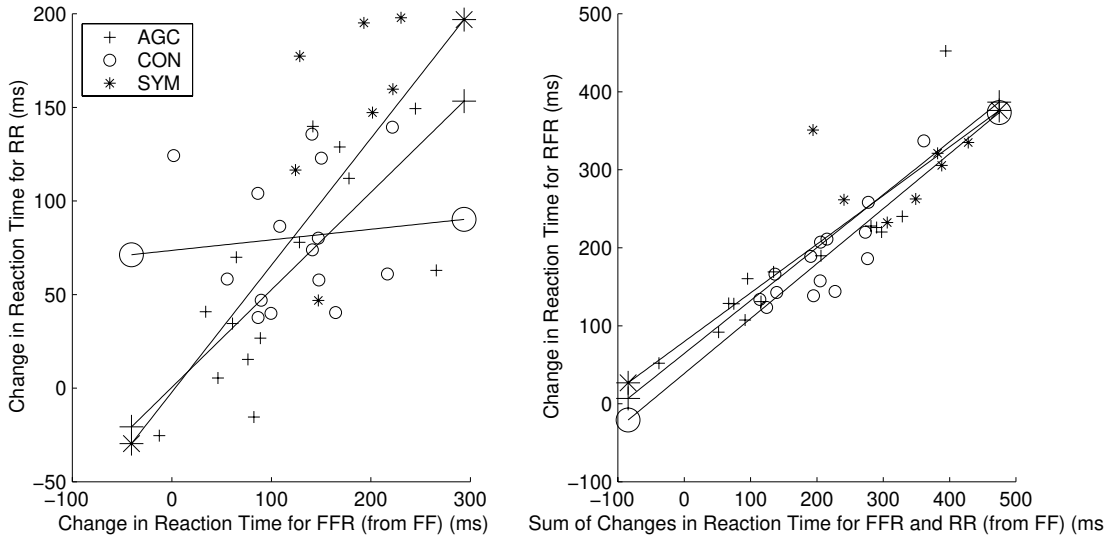

Figure 3.7 Components Within Reaction Times.

reaction times for either forward movements in set FR or reverse movements in set R. In fact, the raw increases in reaction time from baseline for reverse movements in set FR correspond closely to the sum of the raw increases for forward movements in set FR and reverse movements in set R for all groups (compare figure 5c and 5d).

This correspondence is also strong for the individual subjects within each group as shown in figure 7b. The correlation coefficient between the raw increases in reaction time from baseline for reverse movements in set FR and the sum of the raw increases for forward movements in set FR and reverse movements in set R is 0.85 for control subjects ($p<0.0001$), 0.90 for presymptomatic subjects ($p<10^{-5}$) and 0.86 for all HD subjects taken together, both pre- and symptomatic ($p<10^{-6}$). These results suggest an additive quality to certain distinct components within the reaction time. Specifically, the reaction time for making reverse movements when a color-based decision is required appears to correspond closely to the sum three components: (1) the simple, baseline forward reaction time, (2) the extra time from baseline for reverse movements when color-based

decision is not required (set R), and (3) the extra time from baseline for forward movements when a color-based decision is required. Additivity between these components suggests the existence of some degree of serial processing of the physiologic bases of these components. Note that although strong correlations exist between the extra time above baseline required for reverse movements in set FR and the sum of components 2 and 3, the slope of the best fit straight lines shown in figure 7b are all less than unity. To explore the contributions of components 2 and 3 more closely and examine whether components 2 & 3 had demonstrably different contributions to the compound reaction time, the model:

$$\{y = x_1 + \mathbf{a} * (x_2 + x_3) + \mathbf{b} * (x_2 - x_3) \qquad \text{Equation (1)}\}$$

was fit to the data, where y represents the average reaction time for making reverse movements in set FR for each subject, and x_i represents the estimate for each component for each subject: x_1 - the average reaction time in set F, x_2 - the average extra reaction time above baseline in set R, x_3 - the average extra reaction time above baseline for forward movements in set FR. The best-fit coefficients are: a=0.673, b=0.141 for controls, a=0.749, b=-0.138 for presymptomatic HD subjects, and a=0.615, b=0.188 for all HD subjects taken together. These model fits are all significant ($F>30$, $p<0.0001$ in all cases) and in all cases the 95% confidence intervals for **a** (at the best-fit **b**) lie above zero but below one: [0.39, 0.96] for controls, [0.46, 0.93] for presymptomatic subjects, and [0.44, 0.79] for all HD subjects taken together. The confidence intervals for **b** all include zero: [-0.27, +0.56], [-0.63, +0.46], and [-0.27, +0.64] for controls, presymptomatic HD, and all HD subjects, respectively. Taken together these data suggest that components 2 and 3 are substantially, yet not completely (**a**<1), additive in

their contribution to the compound reaction time (reverse movements with color-based decision) and that there is no significant preferential effect of one component over the other on the compound reaction time. Furthermore, the way these components combine: the degree of their additivity and the similarity of their effects on the compound reaction time, appears fairly well preserved in HD, despite the increased magnitude of each component in subjects with manifest HD.

In HD subjects, the magnitudes of the reverse movement component (RR-FF) and the color-based decision component (FFR-FF) are strongly correlated with one another, whereas the magnitudes of these components appear uncorrelated among controls as shown in figure 7a. Interpretation of this finding is difficult however, because although presymptomatic subjects show this high inter-component correlation, the average values of these reaction time components are no higher than normal (see Figure 5). The large correlation between these components among HD subjects may suggest that they deteriorate together as the disease progresses, but if this were true, the starting point for this deterioration would be at component times much faster than controls. This seems somewhat unlikely however, and so a clear explanation for this effect currently eludes us.

Mistakes

Figure 8 shows the hand paths of the forward movements in set FR for two symptomatic HD subjects, one presymptomatic subject, and one control. Most movements proceed directly toward the target as they begin, but several movements start in the wrong direction. In set FR, both symptomatic and presymptomatic HD subjects made mistakes in initial movement direction on about 11% of trials while controls made mistakes on only 5% of trials (see Figure 9). All subjects made at least a few mistakes in

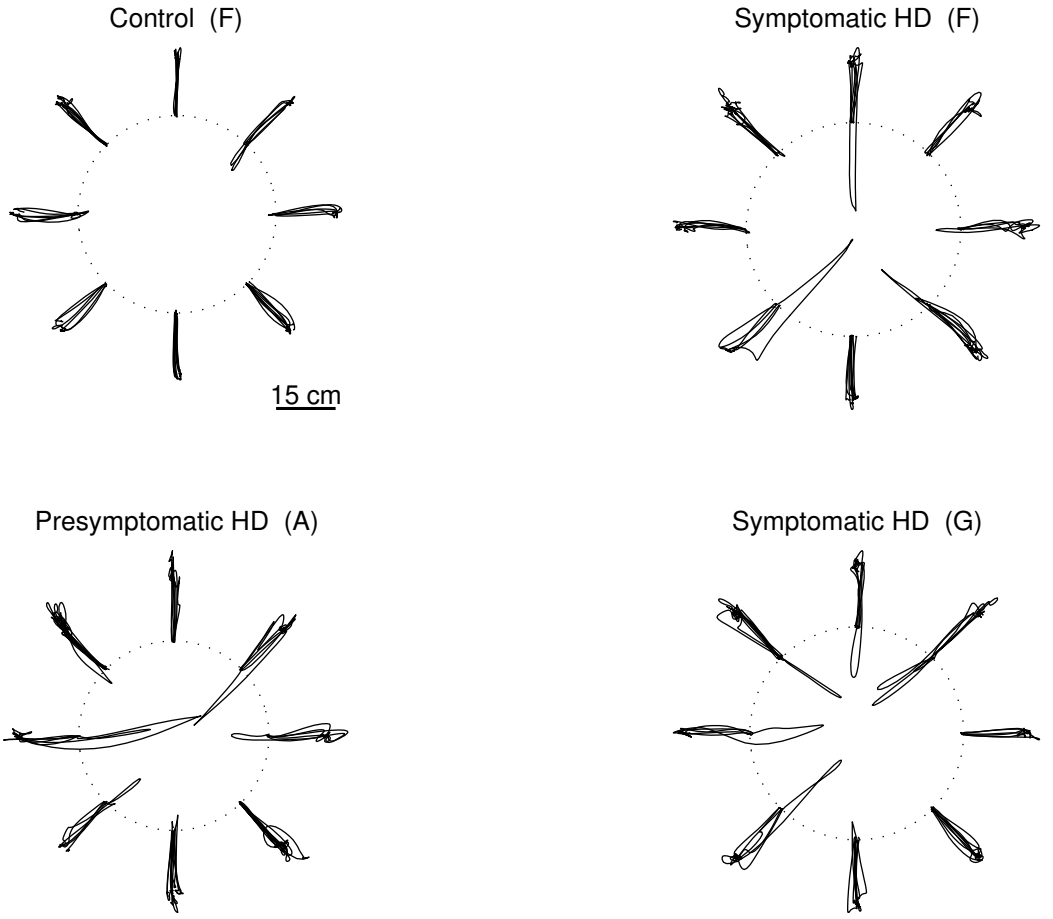

Figure 3.8 Sample Hand Paths Including Mistakes. Hand Paths are plotted for several subjects in set FR. Hand paths for all forward movements in set FR made by two symptomatic, one presymptomatic, and one control subject are shown. Paths are exploded out from the center for clarity: all movements actually begin from the same center point, but the starting points shown are plotted along the dotted circle so that wrong direction movements can be clearly seen.

the direction of initial motion during the course of the experiment. Movements were classified as mistakes based on the direction of their initial acceleration. The direction of the acceleration vector was determined at the first supra-threshold sample (threshold = 50cm/s^2), and movements with initial acceleration more than 45 degrees from the target direction were classified as mistakes.

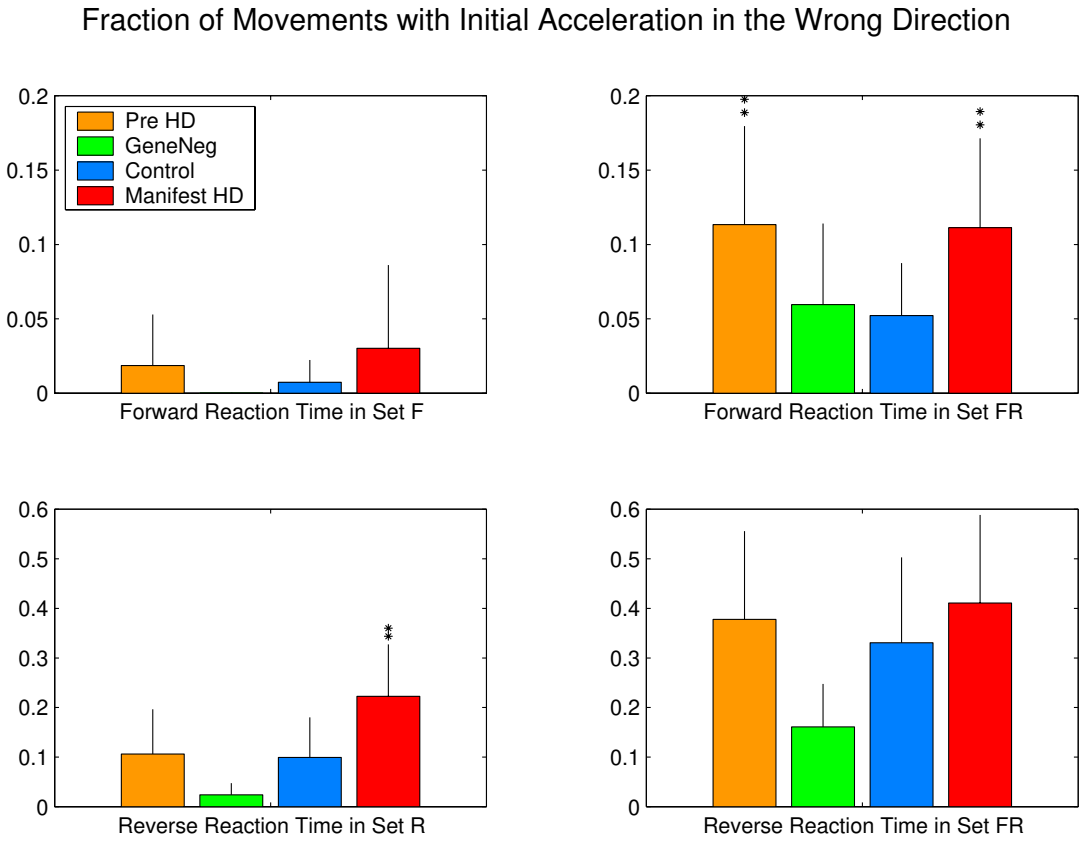

Figure 3.9 Likelihood of Occurrence of Mistakes in the Direction of Initial Reaction. The mean and standard deviation of the fraction of movements for which the direction of initial acceleration is greater than 45 degrees from the instructed movement direction for each subject group for each movement type. Asterisks indicate the occurrence of significantly more mistakes than controls. ** $p<0.01$.

Figure 9 shows that, for all groups, the fewest mistakes were made in set F, and the most mistakes were made for the reverse movements in set FR. Subjects with manifest HD made significantly more mistakes in set R and for forward movements in set FR than control subjects ($p<0.01$ in both cases). Subjects presymptomatic for HD made more than twice as many mistakes on average as control subjects for forward movements in set FR. They also made a few more mistakes than control subjects for the other three movement types, but none of these increases were significant. All groups made mistakes in fewer than 3% of their movements during set F, and the differences in the occurrence

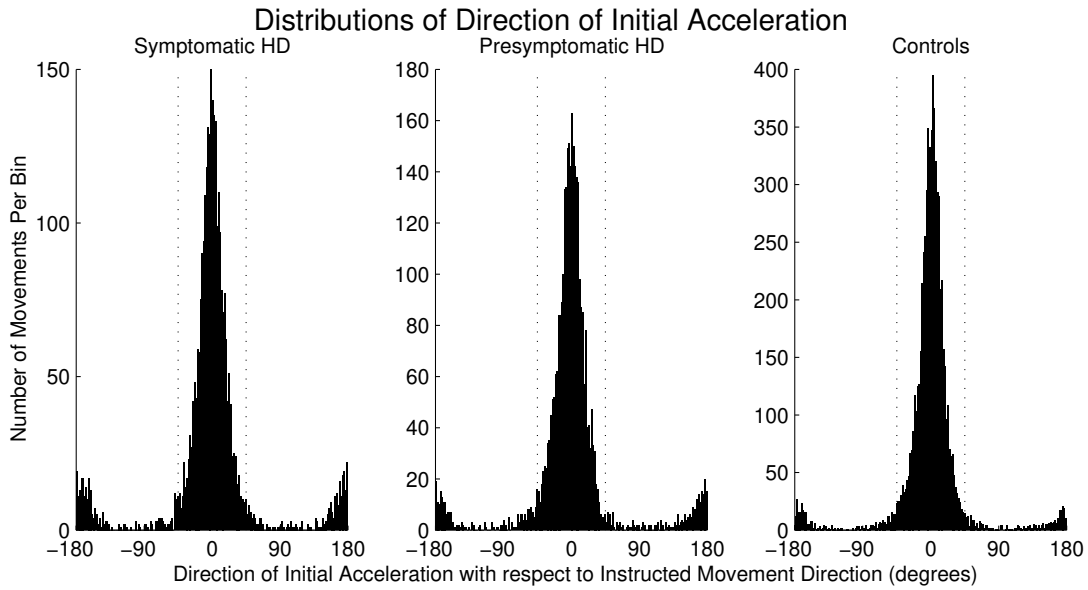

Figure 3.10 Initial Motion Direction Distributions for Symptomatic HD, Presymptomatic HD, and Control Subjects. Vertical dotted lines are at +/- 45 degrees from the instructed movement direction. Movements with initial acceleration directions outside these lines were classified as mistakes.

of mistakes between groups were all insignificant in this set. In contrast, mistakes were made on a full third of the trials during which subjects were instructed to make reverse movements in set FR by both HD and control subjects.

The distributions of initial acceleration directions show two clear peaks in all groups: a large peak centered at the instructed direction of motion, and a smaller peak 180 degrees away. The direction of initial acceleration was within 45 degrees of target on most trials, but when mistakes were made (|direction| > 45 degrees), the initial acceleration direction was usually close to 180 degrees as shown in Figure 10. Mistakes were not uniformly distributed across directions, but rather, when they occurred, often corresponded to a movement opposite to the correct direction. Since all movements in this task were either forward or reverse with respect to the target, it appears that the majority of mistakes resulted in programming a forward movement when a reverse movement was required or vice-versa.

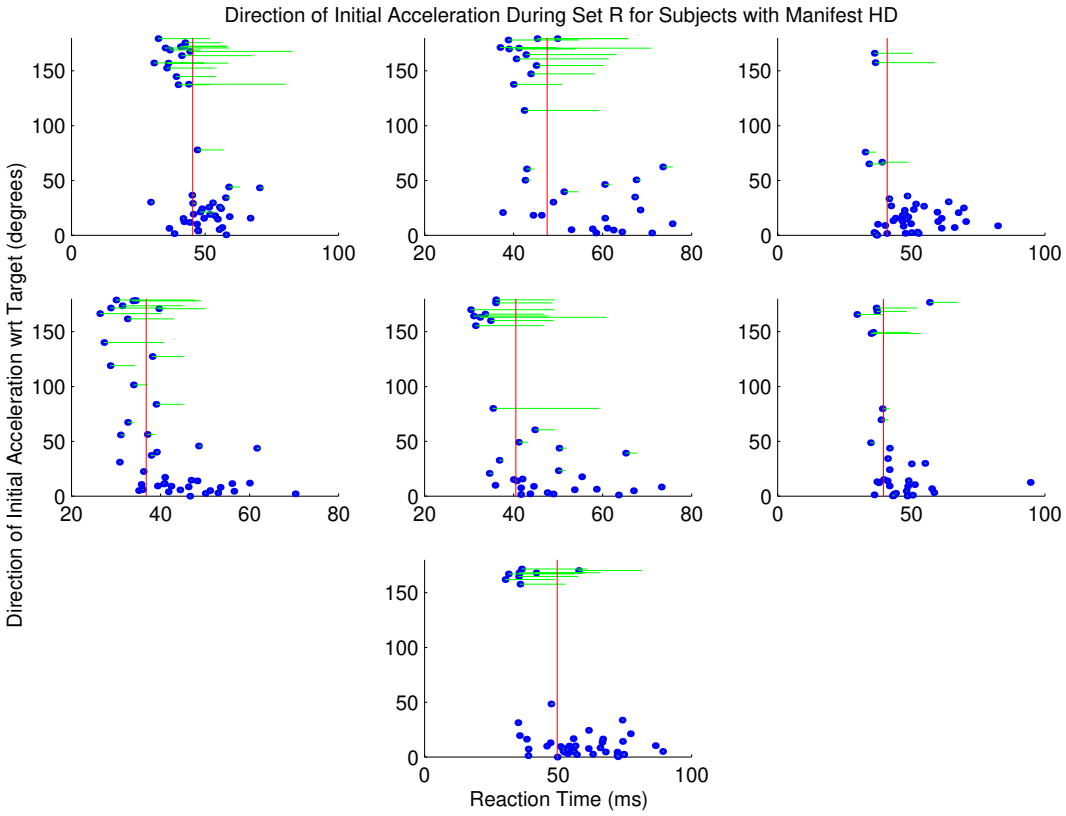

Figure 3.11 Relationship Between Direction of Initial Acceleration and Reaction Time. Reaction time is plotted against Initial acceleration direction on a trial-by-trial basis for all subjects with manifest HD in set R. Blue dots represent the initial reaction time, and the green horizontal lines extend forward from the initial direction reaction time to the appropriate direction reaction time.

Figure 11 shows reaction times for individual movements made by symptomatic HD subjects in set R. Notice that the movements with the fastest reaction times were often mistakes, and that below a certain reaction time almost all movements were mistakes (forward movements instead of the reverse movements called for). The green lines extend for the initial (any direction) reaction time to the appropriate direction reaction time. The initial reaction time is the time at which the tangential acceleration first exceeds 50 cm/s^2, and the appropriate direction reaction time is the time at which the acceleration in the target direction first exceeds 50 cm/s^2. The distributions of

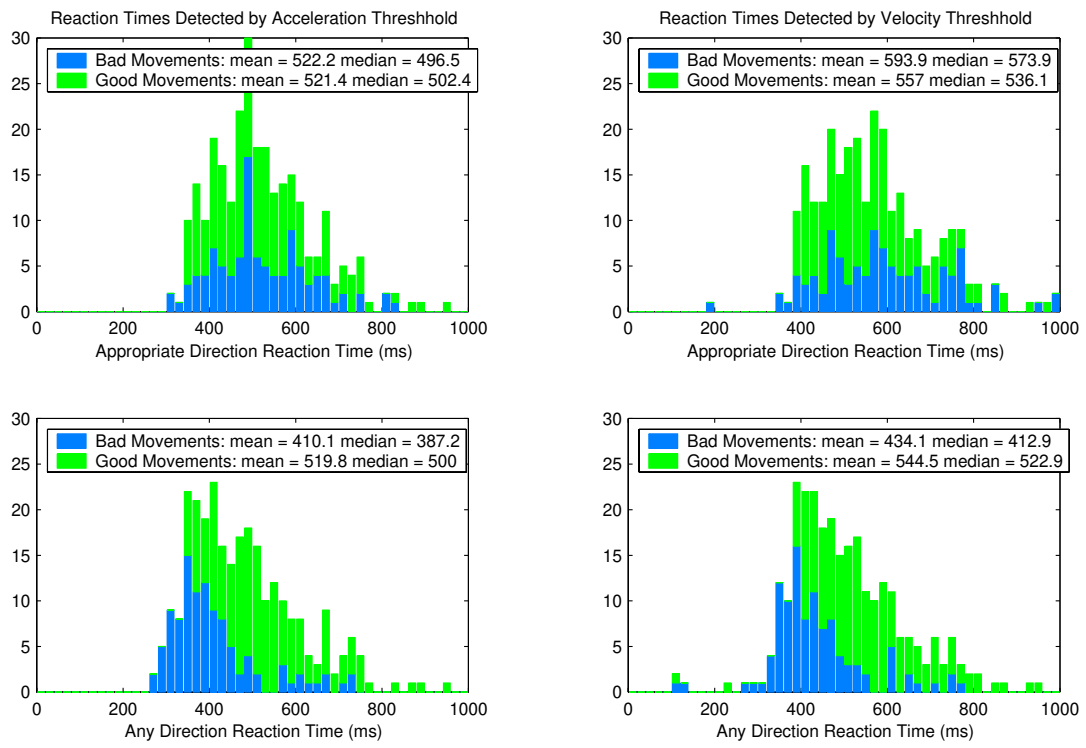

Figure 3.12 Distributions of Initial Direction Reaction Times and Appropriate Direction Reaction Times for HD Subjects Computed by Velocity and Acceleration Thresholding for Good and Bad Movements. Movements with direction of initial acceleration with more than 45 degrees from the instructed movement direction were deemed 'bad'. Green bars representing the distributions of good movements are stacked atop blue bars representing the distributions of bad movements.

appropriate direction reaction times appear very similar for mistakes and non-mistakes, although the initial reaction times are much lower for mistakes than non-mistakes (direction of initial acceleration within 45 degrees of target direction) suggesting that the timing of appropriate reactions are independent of whether or not mistakes occur.

The histograms shown in Figure 12 illustrate that the distributions of appropriate direction reaction times are nearly identical for mistakes (blue) and non-mistakes (green) in set R, while the initial reaction times are more than 100 ms earlier for the mistakes than good movements when reaction times are detected by acceleration thresholding in

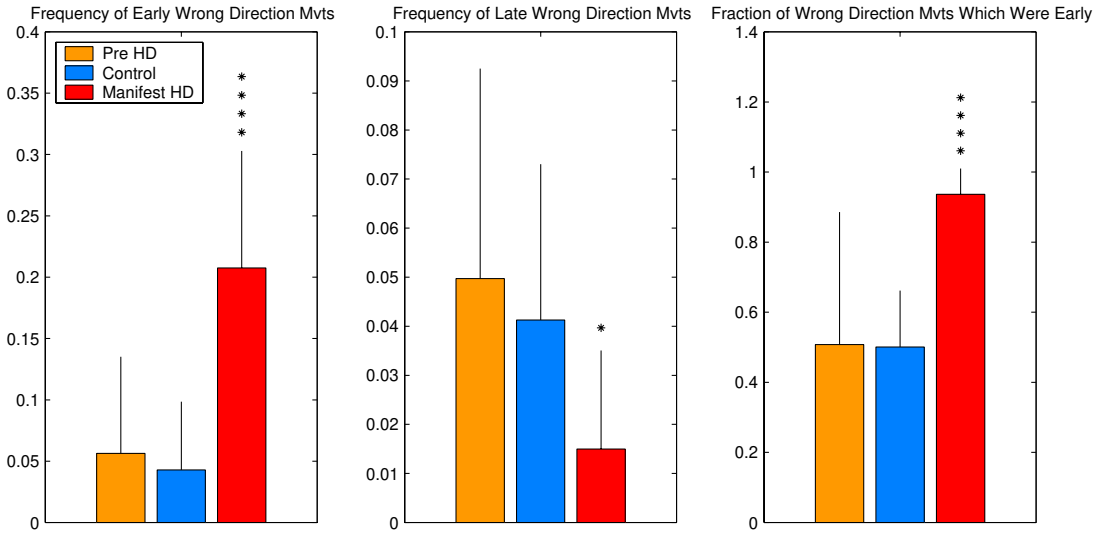

Figure 3.13 Mistakes Made by Subjects with Manifest HD in Set R Have Very Early Reaction Times Compared to their Good Movements. A reaction time in or below the lowest quintile (20%) of good movements was considered early, above the lowest quintile considered late. More than 20% of HD movements were early and initially in the wrong direction, and more than 90% of the mistakes had early reaction times. **** $p<0.0001$, * $p<0.05$. Both control groups are pooled.

this set (left panels). This indicates that the time at which the first acceleration away from the target (appropriate) occurs, is the same whether or not this acceleration was preceded by an initial inappropriate acceleration in the target direction.

For this reverse-movement task two types of motor actions were common: forward movements (inappropriate) and reverse movements (appropriate). Mistake-free execution of this task requires inhibition of the motor action corresponding to forward movement and discharge of the motor action corresponding to a reverse movement. Appropriate direction reaction times detected by acceleration thresholding are nearly identical for mistakes and non-mistakes in set R, suggesting that the activation of task-appropriate motor actions is independent of the successful inhibition of inappropriate motor commands in HD. Thus the average reaction time detected in this way should not depend on the number of mistakes made. Therefore as performance measures, the

appropriate direction reaction time detected by acceleration thresholding and the number of mistakes made should be independent of one another in set R, and so the increases in raw appropriate-direction reaction time that symptomatic HD subjects display over controls (Figures 3&4) and reaction time relative to baseline (Figure 5) cannot be attributed to the increase in mistake likelihood which occurs. By using acceleration thresholding to determine reaction times we can measure the inhibition of inappropriate motor actions and generation of task-appropriate motor commands independently, at least when reverse movements are required (using the appropriate-direction reaction times and initial movement directions), even within the same movement. This allows assessment of motor inhibition and motor command generation in the same data set.

Since it takes time for acceleration to accumulate into large changes in velocity, when velocity thresholding is used instead of acceleration thresholding for reaction time detection (right panels), the appropriate direction reaction time for mistakes exceeds that for good movements, because during bad movements the velocity in the inappropriate direction must be reversed before a supra-threshold appropriate velocity is detected.

Figure 13 shows that the predominance of mistakes in early reaction movements is greater for subjects with manifest HD than controls or presymptomatic subjects. The rate of occurrence of early reaction mistakes in manifest HD subjects is fives times greater than that of controls (left panel, $p < 0.01$). Greater than 90% of the mistakes made by subjects symptomatic for HD occur with early reaction times compared to just 50% for controls and presymptomatic subjects as shown in the right panel ($p<0.01$).

Summary

Overall, subjects with HD, particularly presymptomatic subjects, were less disturbed on the reaction time tasks, than in completing simple point to point movements or responding to externally produced perturbations. We found that HD subjects had elevated simple forward reaction times, and elevated increments in that baseline reaction time for making reverse movements, or for making forward movements when color-based decisions were required. Additionally, the baseline reaction time and the incremental increases from baseline that symptomatic HD subjects displayed were proportionately equivalent to one another, suggesting that the pathology in symptomatic Huntington's Disease affects the baseline reaction time and all the component increases studied in our tasks in a fairly uniform manner. There was no clear disturbance specific to the reaction time for reverse movements or movements requiring a color-based decision. The reaction times for both of these components were disturbed, but not disproportionately to each other or to the baseline reaction time. However, the degree of additivity of these two components in predicting the reaction time for reverse movements when color-based decisions were required was preserved in HD, indicating that whatever mental processes that account for the serial combination of these components is spared in HD. Thus in our experiment, we see no specific effect of task complexity on the performance of subjects with Huntington's Disease. Presymptomatic subjects showed no increases in baseline reaction time or any increments in that reaction time compared to controls. They also displayed the same degree of component reaction time additivity found in symptomatic HD and control subjects. This suggests that the processes

responsible for visual reaction times are largely spared early in the course of HD, but they do deteriorate later in the symptomatic disease progression.

By using acceleration measurements to assess reaction time, it appears that we are able to measure directional reaction times independently of whether mistakes were made. We found that all subjects occasionally made mistakes on our reverse movement or decision tasks, but that the directions of these mistakes were not random. When mistakes were made the initial motion direction was usually 180 degrees from the instructed direction of motion, indicating a response inappropriate for that trial, but not inappropriate for the task as a whole. Thus for all subjects, experience on the task appeared to influence the types of mistakes that were made. HD subjects made more mistakes than controls for both reverse movements in set R and forward movements in set FR. Presymptomatic subjects made more mistakes than normal for forward movements in set FR despite displaying normal reaction times in all sets, suggesting that the occurrence of mistakes may begin earlier in the disease course than reaction time increases on this task because dysfunctional inhibition of motor actions precedes deficits in the timing of motor command generation. Keep in mind however, that the vast majority of these movements were mistake free for all subjects. Presymptomatic and symptomatic HD subjects only made mistakes on about 11% of trials for forward movements in set FR while control subjects made mistakes on 5% to 6% of these trials.

Although it is quite difficult to fairly compare the degree of dysfunction between subjects on different task paradigms, it appears that we find somewhat less disturbance, particularly early in the disease course, on our reaction time tasks than on the tasks we studied which were more sensitive to dysfunctional error feedback control. The online

processing of visual information is important in both tasks. However, online processing of error signals and the processing of proprioceptive sensory information were important features of tasks we used to study error feedback control dysfunction, but not for the aspects of the reaction time tasks that we studied. So the difference in task performance seen in HD subjects may stem from the specific processing of visual error signals versus the processing of other types of visual signals, or from dysfunctional processing of proprioceptive sensory information in HD, or a combination of these.

Chapter 4 - Perturbations, Patterns, and Darkness - Analysis of the effects of external force perturbations and the withholding of visual feedback on point to point movements in patients with Huntington's Disease and Cerebellar Dysfunction.

Introduction

Previously, we looked very closely at the properties of voluntary point-to-point arm movements in subjects with HD. This revealed three important points. (1) HD subjects made movements that began normally but often ended in an irregular, jerky fashion. (2) That this elevated end-movement jerkiness seemed to be caused by poor error feedback correction. Specifically, we found that end-movement jerk, which was greatly increased overall in HD, varied substantially from trial to trial, but a large part of this variability was predicted by the magnitude of subtle, self-generated early-movement errors, and that the sensitivity of end-movement jerk to early-movement error was greater in HD subjects than controls. (3) Individuals gene-positive for HD who were clinically presymptomatic for the disease had both increased end-movement jerk, and increased error sensitivity compared to controls, suggesting that dysfunction in error feedback control begins very early in the disease course, perhaps 7-10 years before clinical onset.

To corroborate our findings of the dysfunctional responses to self-generated errors, we used our robotic manipulandum to apply well-controlled, but unexpected force pulses on a few randomly selected trials during a point-to-point reaching task. A preliminary analysis of the results from this experiment was presented in Chapter 2. This preliminary analysis showed that unimodal bell-shaped force pulse perturbations

delivered near movement onset disproportionately increased the end-movement jerk in subjects with manifest HD and in individuals presymptomatic for the disease, and that these perturbations were occasionally able to completely destabilize the movements of some of the subjects with manifest HD. Here, a more thorough treatment of the data gathered during the perturbation experiment is presented. In general, this data will address the scope of the error feedback control dysfunction that we reported in Huntington's disease. We will attempt to understand the dependence of this dysfunction on the nature of the time course of error, on the modalities involved in sensory feedback, and on the directions of error and movement. Specifically, in this chapter, we will compare the effects of bimodal and unimodal force pulse perturbations, and of early and late-movement perturbations; we will explore the role that visual feedback plays in the error-correcting response by looking at perturbed movements during which visual feedback was withheld; and finally, we will try to understand if the error feedback control dysfunction in HD is specific to certain directions of motion, certain directions of perturbation, or any combinations of these, or alternatively, whether it was generalized across all directions.

The basal ganglia are thought to play an important role in motor control, but characterization of this role has been difficult. The prevailing view is that the basal ganglia are involved in the selection and inhibition of motor programs. This idea is related to the symptoms in diseases of the basal ganglia and its anatomy: the complex multi-joint involuntary movements seen in Huntington's Disease (HD) may result from disinhibition of inappropriate motor programs, and the difficulty with movement initiation evident in Parkinson's Disease may correspond to insufficient activation of

appropriate motor programs. However, this characterization is at best incomplete as basal ganglia damage also affects the ability of individuals to integrate ongoing sensory information into their actions.

Perhaps the simplest form of this appears in voluntary control of reflexive behaviors. When a perturbation displaces the hand, stretch-reflex mechanisms originating in the spinal cord provide a short-latency compensatory response, but a secondary, long-latency response is also observed. It is believed that this response involves a pathway from the spinal cord to the thalamus, to the somatosensory cortex, to the motor cortex, and then back to the spinal cord[43,44,45]. Importantly, one function of the basal ganglia may be to modulate this pathway. In HD, short-latency responses are normal, but long-latency responses in some muscles are reduced or absent[25,46,47]. Intriguingly, cortical responses to peripheral nerve stimulation as measured by evoked potentials from the somatosensory cortex are also reduced in HD[24,26]. These results suggest that while the afferent system of the spinal cord may be relatively intact in HD, the systems that relay somatic information to the cortex are inappropriately modulated.

While previous work had considered long-latency reflexes generally as a part of the system that allows maintenance of steady posture[48], we thought that it might also play a fundamental role in control of voluntary movements. When subtle errors occur in the execution of simple reaching movements, the errors must first be detected among the large amount of sensory feedback to the brain. Successful detection should then result in the selection of the appropriate motor response and the modification of ongoing descending motor commands. Because of the large delays in sensory feedback, this is a difficult computational problem, but one that may be solved with a system that predicts

sensory consequences of motor commands[49,41]. When we closely examined reaching movements of HD patients, we found that like normal controls, they sometimes made movements that began with small errors[78]. However, unlike control subjects, movements of HD subjects often ended in an irregular, jerky fashion. Indeed, we observed increased end of movement jerkiness in asymptomatic gene carriers of HD (AGCs) who were up to 10 years away from predicted clinical onset of symptoms. This increased jerkiness did not occur in every movement, but when it occurred it came at the end of movements that had begun with subtle errors. The results suggested that the motor disorder in HD began as a dysfunction in the error feedback pathway.

Here we performed experiments to uncover the nature of error feedback problems in HD. Is the problem one of gain control, i.e., disproportionately large response to a small error, as might be expected if HD results in a general disinhibition of motor programs? Alternatively, is the problem more fundamentally related to selection of motor actions based on an incorrect evaluation of the ongoing sensory feedback?

Methods

Subjects

5 symptomatic and 9 presymptomatic HD subjects, 8 age-matched controls, and 6 subjects with cerebellar lesions participated in this experiment. All subjects were right handed and used their dominant hand. The direct gene test for IT-15 mutation was conducted at the Johns Hopkins Huntington's Disease Project. The length of the CAG trinucleotide repeat was determined, and subjects with a CAG repeat length of at least 37

were called mutation-positive. Subjects with CAG repeat length less than 34 were called mutation-negative.

The genetic testing was part of the HD Presymptomatic Testing Program headed by Jason Brandt at Johns Hopkins School of Medicine. In this program, mutation-positive individuals participated in a longitudinal study that included annual psychiatric and neurological evaluations, along with a brain MRI. AGCs that participated in our study were part of this program. Their participation in the current study of motor function was for a single visit that lasted about 4 hours.

Clinical evaluation of the AGCs and HD subjects included a quantitative neurological exam (QNE, Folstein et al. 1983). This examination includes an assessment of voluntary motor function via a motor impairment score (MIS) and an assessment of involuntary motor function via a chorea scale. Preliminary results from 17 AGC subjects who were studied annually at the Johns Hopkins Huntington's Disease Project show that individuals who are 5 or more years from predicted onset of the disease have QNE scores of 6 or less. This score gradually increases so that by the year of the onset QNE is about 15. In the early years of the disease development when the motor symptoms are mild, QNE is less than 30.

All cerebellar subjects that we studied had been diagnosed clinically with cerebellar dysfunction, and all had lesions localized to the cerebellum on MRI. 4 patients had generalized cerebellar atrophy, and 2 had suffered strokes of the right posterior inferior cerebellar artery (PICA). One of these patients also had a left PICA and a right superior cerebellar artery stroke.

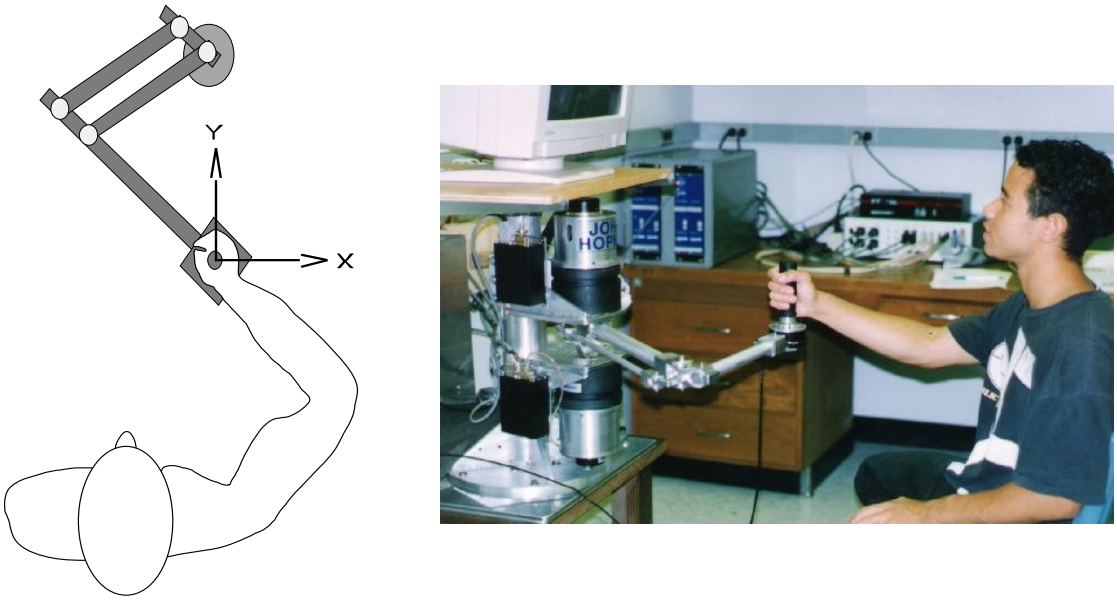

Figure 4.1: Diagram and photo of subject grasping manipulandum.

Task

Subjects made quick reaching movements to targets spaced 10cm away while grasping a lightweight two-joint manipulandum. The 1cm square targets and a small cursor (4mm) indicating the subject's hand position were displayed on a vertically-oriented computer monitor in front of the subject as shown in Figure 1. Position and velocity data from the manipulandum were sampled at 100Hz and the computer monitor was refreshed 60 times per second. The robot produced force pulses on a minority of randomly pre-selected trials (with a probability of 1 in 4). The force pulse could be any one of three types, in any of 8 directions, and of magnitude 6, 12, or 18 Newtons peak force. The three types of force pulses were unimodal-early, bimodal-early, and unimodal-late. Unimodal-early perturbations consisted of 70 ms bell shaped (minimum jerk velocity shape) force pulses triggered when the subject had moved 2cm of the way to the target. Bimodal-early perturbations consisted of 150 ms S-shaped bimodal force

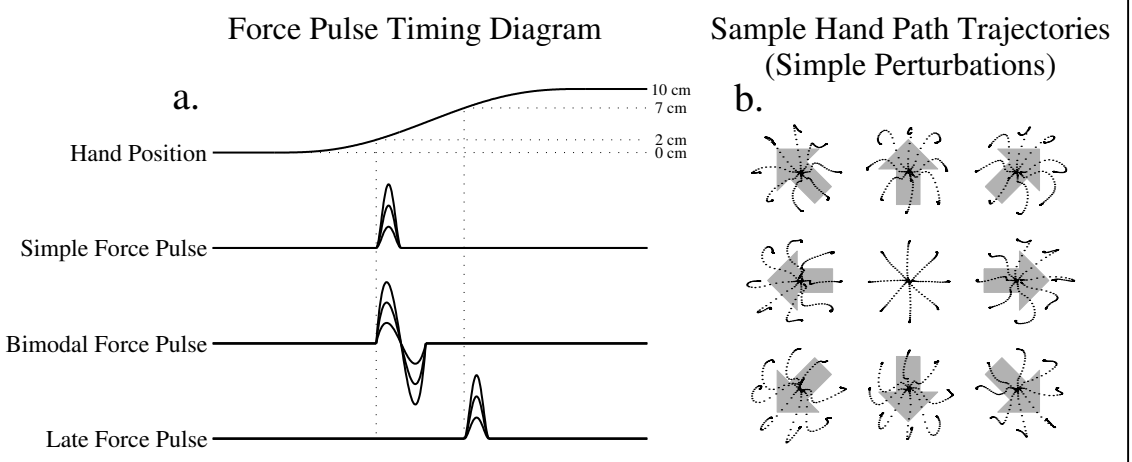

Figure 4.2: Illustration of Force Pulse Application. a. Diagram of force-pulse timing. As shown three types of force pulses could be applied. The lines at different heights within each trace represent 6, 12, and 18N force pulses. **b.** Hand paths resulting from the application of simple (unimodal) 18N force pulses for a control subject. 72 movements are displayed in all, grouped into 9 pinwheels of 8 movements each. The gray arrows overlaid on each pinwheel of plots indicate the direction of the applied force pulses. The center pinwheel shows the hand paths of typical unperturbed movements in each direction. The 64 movements in the peripheral pinwheels correspond to all combinations of movement direction and perturbation direction.

pulses (minimum jerk acceleration shape) triggered when the subject had moved 2cm of the way to the target. Unimodal-late perturbations consisted of 70 ms bell shaped application of these force pulses is displayed in Figure 2a. Figure 2b shows typical hand-path trajectories resulting from the application of 18N unimodal-early force pulses. During the course of the experiment, one unimodal-early force pulse in each direction and of each magnitude was given for each direction of movement with visual feedback (192 perturbed trials, 64 at each magnitude). 16 trials at each perturbation magnitude were administered with each of the other perturbation types, bimodal-early and unimodal late. Additionally, 192 trials were administered without visual feedback. Of these, there were 16 trials at each magnitude of the unimodal-early perturbations, leaving 144 unperturbed trials without visual feedback. No unimodal-late or bimodal perturbations were administered on trials without visual feedback. We removed visual feedback by

blanking the screen cursor after the point at which the velocity threshold (0.03m/s) marking movement onset was first exceeded. In this way, subjects were prevented from knowing whether visual feedback would be provided prior to movement onset, however a small amount of the initial cursor motion was visible near movement onset, but the cursor was generally extinguished before 5mm of motion, about the cursor's diameter and approximately 5% of the target distance.

During the experiments, subjects were seated and we used a sling suspended from the ceiling to support the subject's upper arm in the horizontal plane. This helped regularize each subjects' arm position and minimize the effort required to support his or her arm in this posture against gravity for the experiment's duration. In all, the experiment consisted of 19 sets of 96 movements, and was carried out in a single 3 to 4 hour session. Each set consisted of 12 movements in each of the 8 target directions. During the first four sets all movements were unperturbed and visual feedback was always provided. The next fourteen sets contained a random mix of perturbed and unperturbed movements with and without visual feedback as described above. The final set consisted entirely of null movements, like the first four.

Analysis

Perturbed and unperturbed movements were quantified using movement time, post perturbation path length, and post perturbation jerk efficiency. We defined the end of a movement as the end of the first time interval after movement onset when hand velocity remained below a threshold of 0.03m/s for 200ms. Jerk is the rate of change of acceleration with respect to time. In order to minimize the effect of discretization noise on the differentiation of the velocity signal, jerk was estimated by applying a fourth order

Savitsky-Golay filter on a 250 ms window of velocity data. This filter is equivalent to taking the second derivative at the window's center of the continuous least squares best fit fourth order polynomial. This fourth order polynomial fit is a low-pass filter with cutoff frequency of 6.83 Hz. Power spectra of mean subtracted velocity profiles of very fast 10 cm reaching movements show that 99.9% of the power is below 6 Hz.

We used three different measures to assess the dynamic performance of each participant's perturbation responses: movement time, post-perturbation path length, and post-perturbation jerk efficiency. All of these measures should increase with impairment in perturbation response and with increasing perturbation strength. To measure the efficiency and smoothness of the corrective movement that followed imposition of a perturbation, we computed its total squared jerk (TSJ). We normalized the TSJ measured after perturbation offset for a given movement by the minimum possible jerk required to make the movement state transition characteristic of that movement segment. We refer to ratio of the measured post perturbation TSJ to the minimum possible as the post-perturbation jerk efficiency. Similarly, we define post-perturbation path length as the path length between the point of perturbation offset and the end point of movement divided by the straight-line distance between these two points. We compare the values of these quantities for movements during which perturbations were given to unperturbed movements. For unperturbed movements, we define the time point of "perturbation offset" as that time when perturbation offset would have occurred had a perturbation been given.

We examined the accuracy and precision of movement endpoint position with respect to target location for movements during which visual feedback was withheld. To

assess endpoint precision we measured the spread of the distribution of endpoint positions by computing the standard deviations of these distributions in the axis of perturbation and orthogonal to it (for unperturbed movements the axis of perturbation was randomly assigned). To assess endpoint accuracy relative to precision we computed the overall eccentricity of the endpoint distributions defined as the Euclidean distance from the center of the movement endpoint distribution to the target location divided by the Euclidean norm of the standard deviations.

Two-way multivariate analyses of variance (MANOVAs) were performed on the average raw values and relative changes from unperturbed values of the set of dynamic performance measures for to determine the overall effects of subject group and perturbation condition on the perturbation response performance of our participants. For these analyses, responses were averaged across perturbation magnitude. To more directly compare the performance of HD subject groups with CBLs and controls, we followed up with two-way MANOVAs comparing pairs of subject groups (instead of all four groups at the same time). We made specific statistical comparisons between pairs of subject groups in different perturbation conditions using two-sample t-tests. One-sample t-tests were used to assess whether perturbation-induced changes in endpoint error precision were significantly greater than zero.

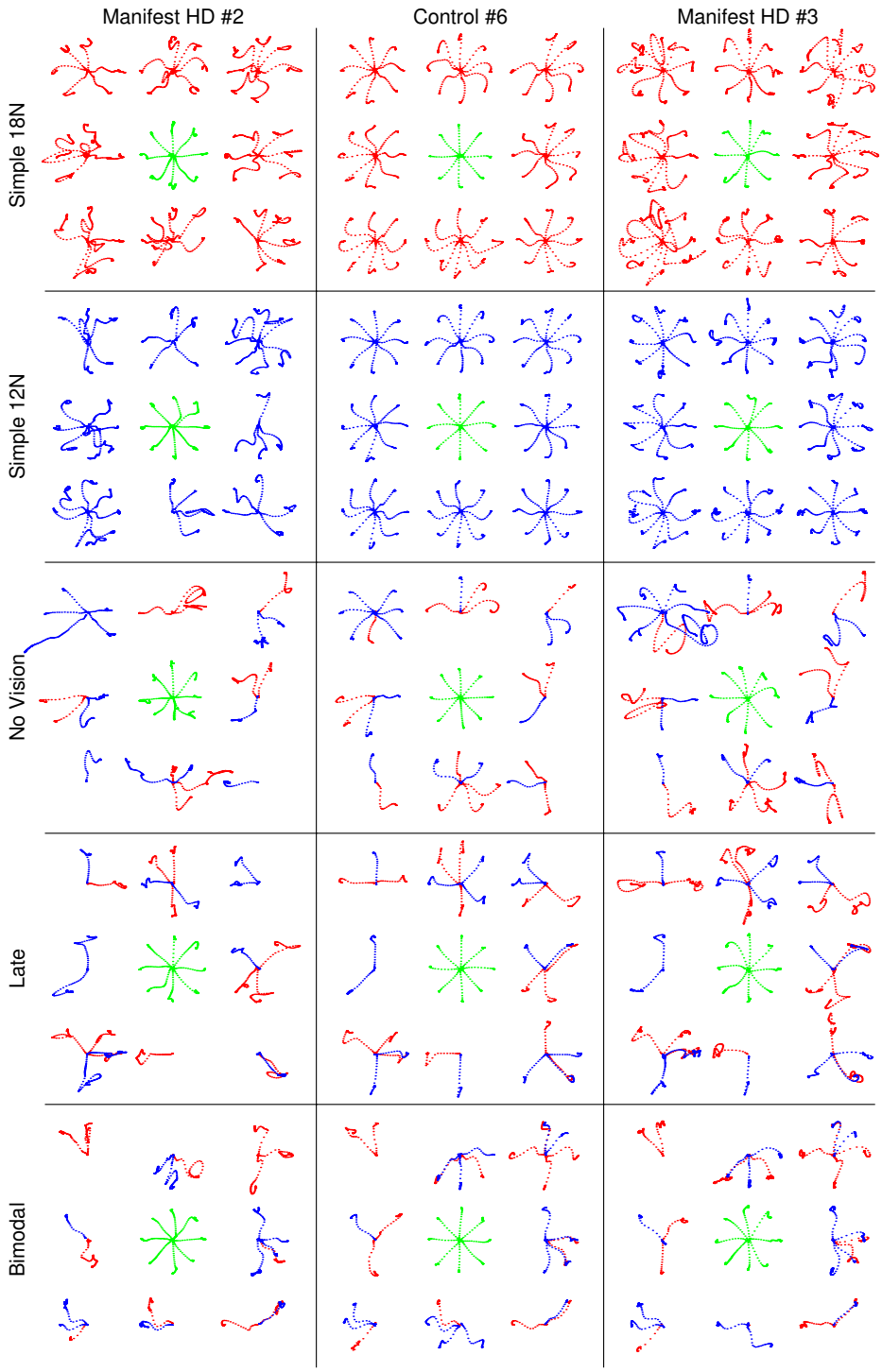

Figure 4.3: Hand Paths During the Perturbation Experiment for Two Subjects with Manifest HD and One Control. Red: Movements with 18N perturbations. Blue: Movements with 12N perturbations. Green: Unperturbed Movements. 6N perturbations are not shown. Each pinwheel shows movements in 8 different directions, and each 3x3 grouping of pinwheels represents a single perturbation type. In each grouping, the 8 peripheral pinwheels represent the movements with perturbations in each of the 8 directions. See Figure 4.2 for a full explanation of how the display is organized.

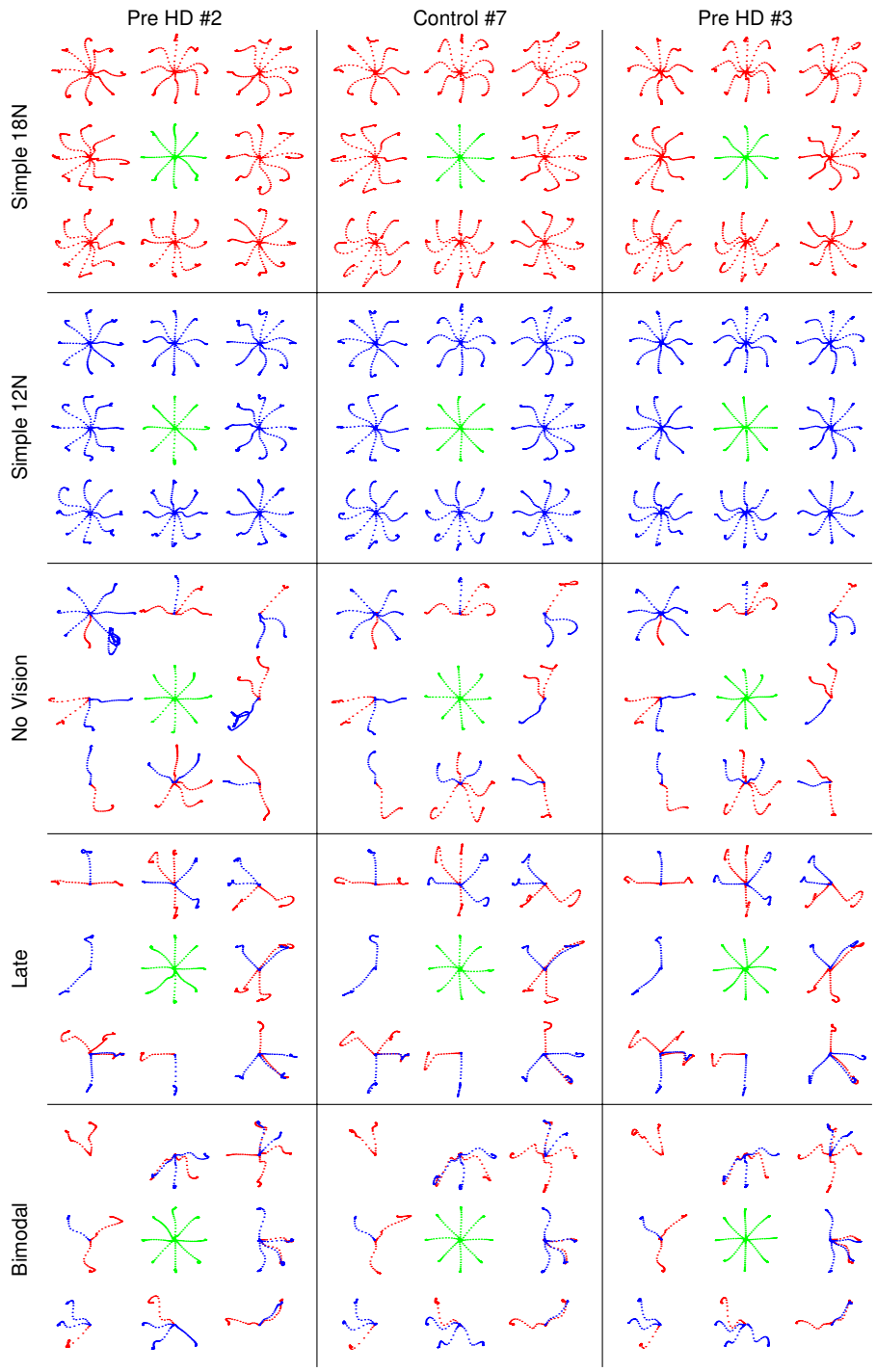

Figure 4.4: Hand Paths During the Perturbation Experiment for Two Subjects Presymptomatic for HD and One Control. Red: Movements with 18N perturbations. Blue: Movements with 12N perturbations. Green: Unperturbed Movements. 6N perturbations are not shown. Each pinwheel shows movements in 8 different directions, and each 3x3 grouping of pinwheels represents a single perturbation type. In each grouping, the 8 peripheral pinwheels represent the movements with perturbations in each of the 8 directions. See Figure 4.2 for a full explanation of how the display is organized.

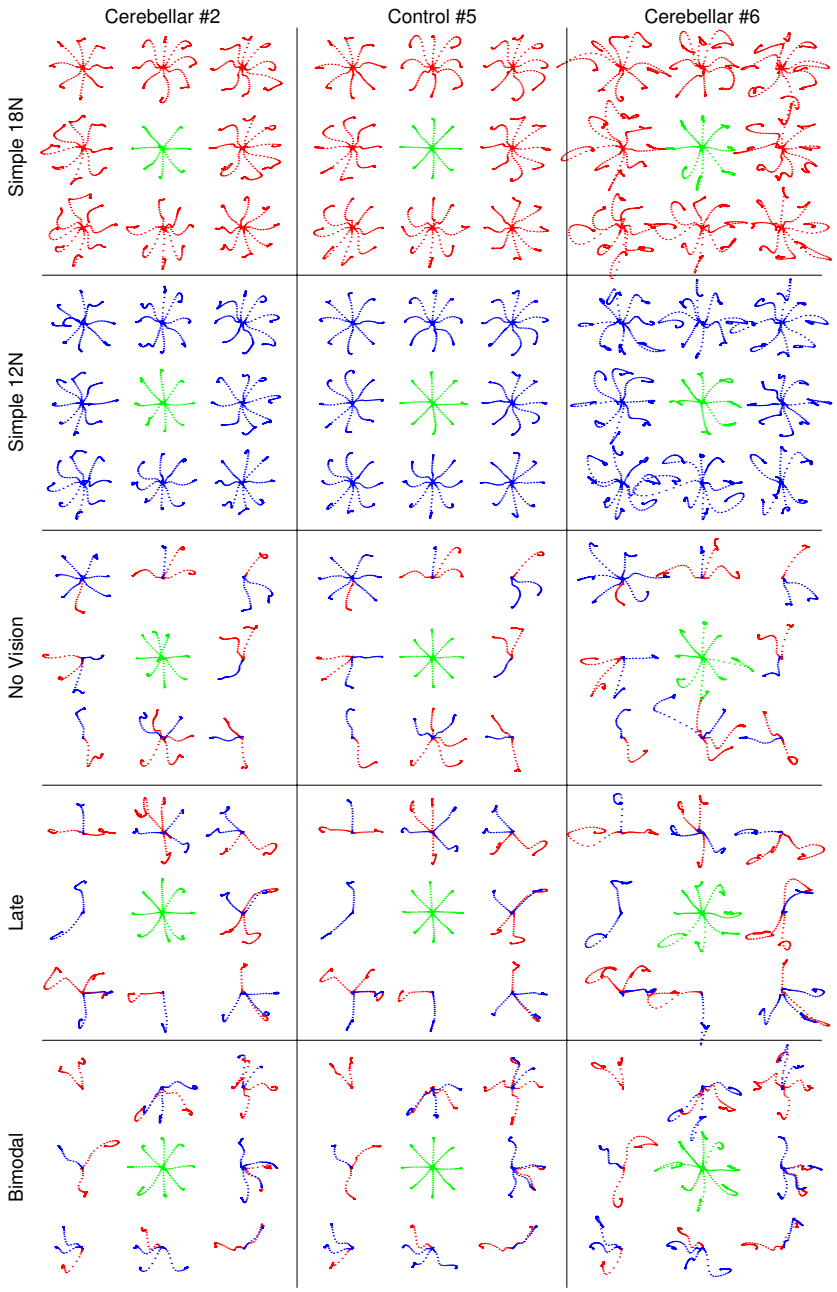

Figure 4.5: Hand Paths During the Perturbation Experiment for Two Subjects with Cerebellar Dysfunction and One Control. Red: Movements with 18N perturbations. Blue: Movements with 12N perturbations. Green: Unperturbed Movements. 6N perturbations are not shown. Each pinwheel shows movements in 8 different directions, and each 3x3 grouping of pinwheels represents a single perturbation type. In each grouping, the 8 peripheral pinwheels represent the movements with perturbations in each of the 8 directions. See Figure 4.2 for a full explanation of how the display is organized.

Results

Example Hand Path Trajectories and Quantification of the Dynamic Performance of Perturbed Movements.

To examine error feedback control function in individuals with HD and cerebellar disease, we used a robotic manipulandum to apply unexpected, randomly occurring perturbations on their reaching arm movements. We examined three different types of brief force-pulse perturbations and the effect of visual feedback at three different perturbation strengths in these subjects. Specifically, we looked at unimodal perturbations applied near the beginning or end of movement with visual feedback, bimodal perturbations near the beginning of movement with visual feedback, and unimodal perturbations near the beginning of movement without visual feedback. Figures 3, 4 and 5 display all movements perturbed by 12N or 18N force pulses as well as a few unperturbed movements for selected subjects from each group. Figure 3 displays the movements of two HD subjects alongside a control; Figure 4 shows two presymptomatic subjects and a control; and Figure 5 shows a control and two cerebellar subjects.

Overall Statistical Analysis of Perturbation Responses

Two-way multivariate analyses of variance (MANOVAs) were performed on this set of performance measures to determine the effects of subject group and perturbation condition on the perturbation response performance of our participants. A MANOVA on the percent changes in performance when perturbations were applied compared to unperturbed movements revealed significant main effects of subject group ($p<2*10^{-7}$) and perturbation condition ($p<10^{-10}$) as well as some interaction between these ($p<0.02$). To determine whether the HD subject groups displayed larger performance impairments than

controls and cerebellar subjects we followed up with two-way MANOVAs comparing pairs of subject groups. These MANOVAs showed that the perturbation-induced performance changes displayed by subjects with manifest HD were significantly different from both controls ($p<0.0001$) and cerebellar subjects ($p<0.003$) and the participants presymptomatic for HD were significantly different from the cerebellar subjects ($p<0.0002$). Similar MANOVAs performed on the average raw values of the performance measures (as opposed to their percentage changes from unperturbed movements) show significant overall differences between groups of participants ($p<10^{-10}$) and perturbation conditions ($p<10^{-10}$) and, in particular, between manifest HD subjects and controls ($p<10^{-10}$) but not between participants with manifest HD and participants with cerebellar disease ($p>0.05$). These analyses indicate that while the overall performance of manifest HD and cerebellar participants was similar when perturbations were applied, the relative change in performance induced by the randomly occurring perturbations was greater for HD than CBL or control participants. To examine in detail how participants responded to the individual perturbation conditions and how these responses depended on the perturbation strength for each performance measure, we conducted post hoc analyses that compared controls to all other subject groups and cerebellar patients with the HD groups. The results of these comparisons are displayed in figures 3 and 4, and are detailed below.

Unimodal-Early Force Pulse Perturbations

The 12 and 18 Newton force pulses perturb these movements substantially. When 18 Newton force pulses are delivered orthogonal to the target direction, the resulting movements are kicked as much as 4 to 5cm off the straight-line path to the target

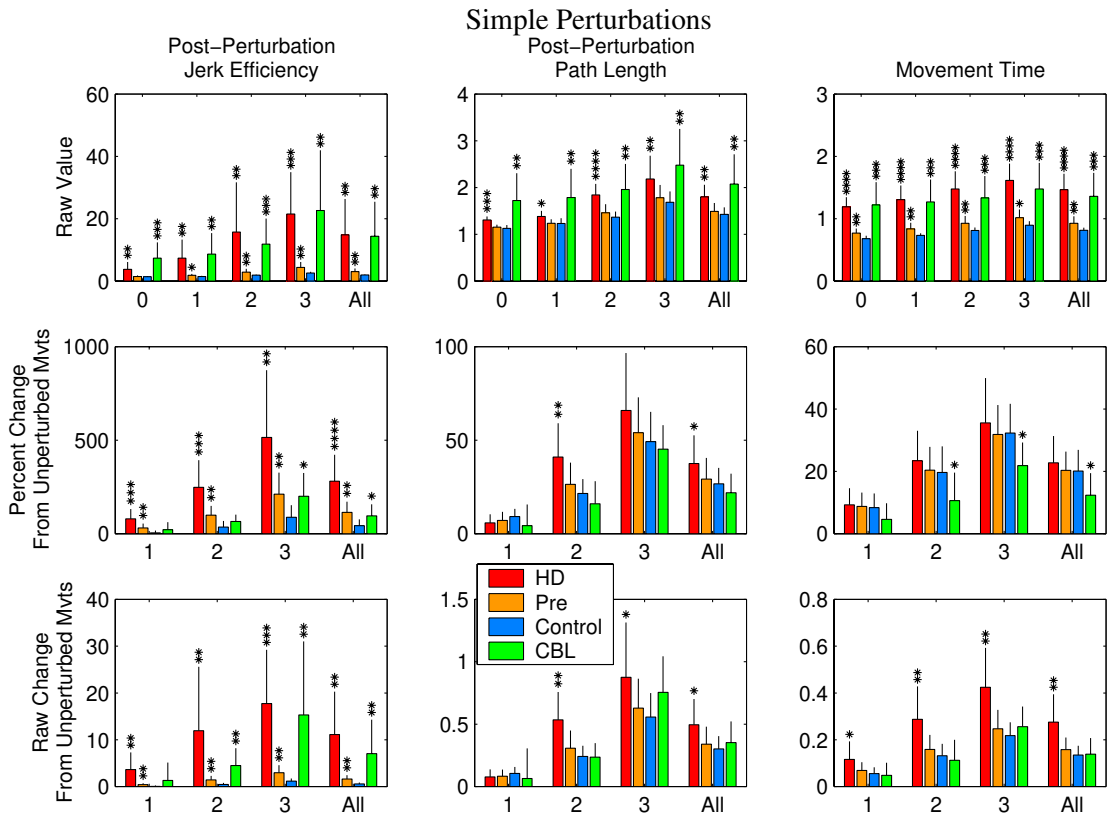

Figure 4.6: Movement Time, Post-Perturbation Path Length, and Post-Perturbation Jerk Efficiency for Movements Perturbed with Unimodal Force Pulses. Here all the different perturbation directions and movement directions are grouped together, and each score is averaged over this set of movements for each subject. The x-axis labels represent the perturbation magnitude. 0 : unperturbed movements, 1 : 6N force pulses, 2 : 12N pulses, 3 : 18N pulses, All : Mean of 6,12, & 18N force pulses. The error bars represent the standard deviation of each quantity across subjects. **** p<0.0001, *** p < 0.001, ** p< 0.01, * p<0.05.

(distance to target is 10cm). Control subjects correct these perturbations relatively smoothly and monotonically, but many of the corrections made by HD subjects seem somewhat unstable. Not all HD movement corrections appear disturbed, but some are so dramatically disturbed that their trajectories bear almost no qualitative similarity to any movements that we recorded from controls. Extremely large successive overshoots are seen during certain HD movement corrections that never appear during perturbed control movements, and occasionally perturbed movements appear to become somewhat unstable and make several turns in apparently wrong directions.

Several movements made by cerebellar subjects appear to have irregular and inefficient corrections, but close inspection of many of these trajectories reveals a striking similarity between the pattern of overshoots in these movements and the overshoots that are present in unperturbed movements in the same direction. This suggests that much of the irregularity that exists in these perturbed movements has a stronger relationship to the direction of movement than to the presence of perturbation. Note the movements toward 3:00, 4:30, and 7:30 for the two cerebellar subjects. Note also, that the unperturbed (green) movements displayed in rows 1,2,4, and 5 of the pinwheel groupings are fully comparable (they are all null movements with visual feedback, just different examples).

A quantitative comparison of the motion dynamics that occur in response to the different magnitudes of unimodal-early force pulse perturbations is presented in Figure 6. Both HD and cerebellar subjects have significantly increased movement time, post-perturbation path length, and post-perturbation jerk efficiency over controls for unperturbed movements and all magnitudes of perturbed movements. However, subjects symptomatic for Huntington's Disease display greater increases in these quantities from baseline in response to perturbations. Both the raw differences and the differences expressed as a fraction of baseline values were greater in symptomatic HD subjects than the cerebellar subjects in all cases. In contrast, the baseline movement time, path length, and jerk were all higher on average in the group of cerebellar subjects than the symptomatic HD group. This makes it seem unlikely that the changes from baseline were greater in the symptomatic HD subjects simply because they had a more advanced or more severe disorder in executing these voluntary reaching movements than did our group of cerebellar subjects. Instead, this data suggests that the motor disorder in Huntington's

Disease is more sensitive to the presence of the perturbations caused by these force pulses than is the motor disorder in subjects with cerebellar dysfunction.

Of the three measures presented, the post-perturbation jerk efficiency appears to offer the best quantitative characterization of the movement irregularity seen in HD. Jerk efficiency is the measure for which the difference between the distributions of the HD and normal subjects is greatest, and it is closely related to the post-peak jerk that we previously used very successfully to characterize the subtle differences between the unperturbed movements of presymptomatic HD subjects and controls (Smith et al, 2000). Both the average post-peak jerk and the sensitivity of post-peak jerk to internally generated early-movement errors were significantly increased over controls for both symptomatic and presymptomatic HD subjects. The third row of plots displays the changes in each quantity from unperturbed to perturbed trials, while the second row shows these changes normalized by their corresponding unperturbed values (the fractional change from baseline). Even the smallest force pulses that we delivered increased the jerk efficiency score of HD subjects substantially. Symptomatic HD subjects had jerk efficiency scores for 6N perturbations that were increased by 70% over unperturbed movements on average. In contrast, control subjects did not display any increase in their jerk efficiency scores for 6N perturbations. When unimodal-early perturbations of all magnitudes are averaged together, subjects with manifest HD show a 250% increase in jerk relative to unperturbed movements. This is 5 times greater than the average increase seen in control subjects and 3 times greater than the increase displayed by cerebellar patients ($p<0.0001$ compared to controls). Presymptomatic HD subjects show greater than a 100% increase in jerk for these movements – more than double that of controls

($p<0.01$). When the raw change in jerk (Figure 6: third row, first column) is examined, we see that symptomatic HD subjects display greater increases from baseline than all other groups including cerebellar subjects, although their margin over cerebellar subjects is smaller than for percent change because cerebellar subjects display almost double the jerk for unperturbed movements as do subjects with manifest HD.

Other Types of Force Pulses: Bimodal and Unimodal-Late Force Pulse Perturbations.

The fourth and fifth rows of pinwheel groupings in Figures 3, 4, and 5 show the hand paths of movements perturbed by unimodal-late and bimodal force pulses, respectively. Notice that the irregularities made by the HD subjects in the movements with unimodal-early perturbations appear to persist in these movements. Although the magnitudes of the overshoots generally appear somewhat smaller than what we saw with unimodal-early perturbations, the problems that HD patients displayed in stopping these movements cleanly are substantially greater than for unperturbed movements.

Figures 7 and 8 show quantitative characterizations of the motion dynamics that occur in response to the different magnitudes of bimodal-early and unimodal-late force pulse perturbations. It is difficult to intelligently compare the raw magnitudes of the post-perturbation measures (jerk and path length) between these types of perturbations and the unimodal-early perturbations previously discussed, because both of these perturbation types were terminated at later stages in the movement than were unimodal-early perturbations. Unimodal-early movements began at the 2cm point and terminated 70ms later. Bimodal perturbations also began at the 2cm point but terminated 150ms after onset. Unimodal-late perturbations did not begin until the movement covered 7cm of the distance toward the target, and they lasted 70ms. Even the measures for unperturbed

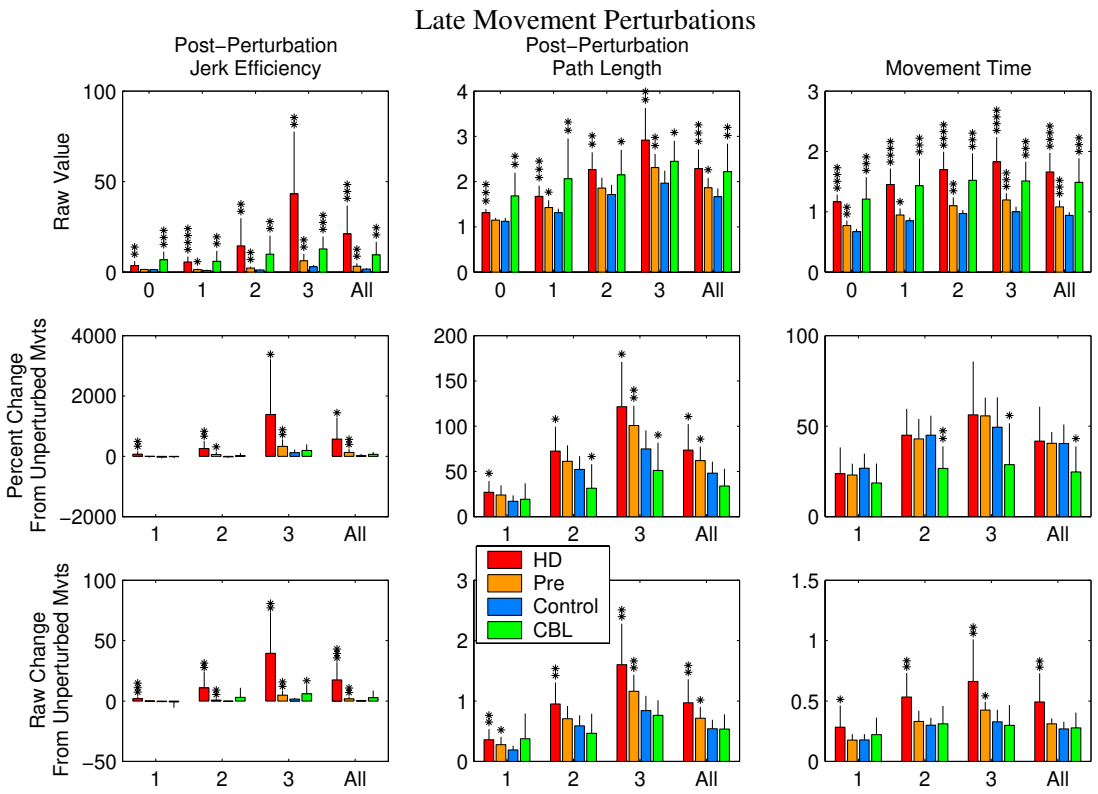

Figure 4.7: Movement Time, Post-Perturbation Path Length, and Post-Perturbation Jerk Efficiency for Movements Perturbed with Late-Unimodal Force Pulses. Here, force pulses were delivered at 7cm instead of 2cm of the way to the target. The format is the same as Figure 4.6. All different perturbation directions and movement directions are grouped together, and each score is averaged over this set of movements for each subject. The x-axis labels represent the perturbation magnitude. 0 : unperturbed movements, 1 : 6N force pulses, 2 : 12N pulses, 3 : 18N pulses, All : Mean of 6,12, & 18N force pulses. **** p<0.0001, *** p < 0.001, ** p< 0.01, * p<0.05.

movements are different because the interval of which they are measured begins later. Instead, the performance of HD and cerebellar subject groups on these measures must be compared to controls subjects and each other.

The late-movement unimodal perturbations appear to show the same patterns of disturbance as seen with the unimodal-early perturbations. Cerebellar subjects have slightly greater baseline jerk and path length than HD subjects, but both cerebellar and HD subjects have significantly increased scores over controls. As with the unimodal-early perturbations, the jerk is substantially increased relative to baseline in the HD

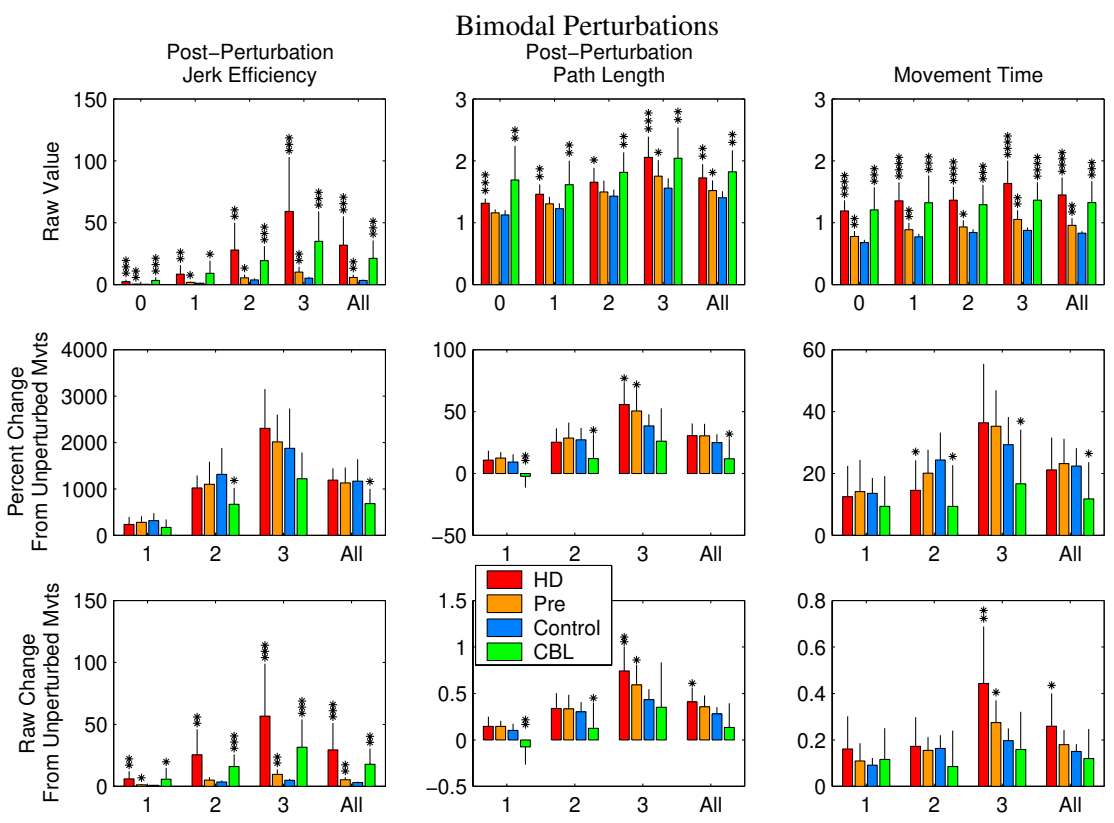

Figure 4.8: Movement Time, Post-Perturbation Path Length, and Post-Perturbation Jerk Efficiency for Movements Perturbed with Bimodal Force Pulses. All the different perturbation directions and movement directions are grouped together, and each score is averaged over this set of movements for each subject. The x-axis labels represent the perturbation magnitude. **0** : unperturbed movements, **1** : 6N force pulses, **2** : 12N pulses, **3** : 18N pulses, **All** : Mean of 6,12, & 18N force pulses. The error bars represent the standard deviation of each quantity across subjects. **** p<0.0001, *** p < 0.001, ** p< 0.01, * p<0.05.

subject group compared to both cerebellar subjects and controls. The relative changes in jerk are greater for both symptomatic and presymptomatic HD subjects than cerebellar subjects. For the largest perturbations, the post-perturbation path lengths of both symptomatic and presymptomatic HD subjects relative to unperturbed movements are significantly greater than those of controls. In contrast, the path length changes of the cerebellar subject group were less than controls.

The relative change in jerk in bimodally perturbed movements was less dramatically different from controls for HD subjects than with the other perturbations

types. However the significant increases over controls persisted for the raw changes in jerk relative to baseline (Figure 4.7: third row, first column) and for both the relative and absolute changes in path length. Cerebellar subjects had smaller relative changes in jerk, path length and movement time than controls. It is difficult to say whether HD subjects indeed performed better when bimodally perturbed movements were applied, but if real differences exist between this perturbation type and the others it may be an indication that lower order errors bring out the irregularities in HD movements more than higher order errors. In turn, if this was true, it may be that the error correcting response is greater for lower order errors than higher order errors, or there might be specific vulnerability in HD to lower order errors. Here order refers to order of differentiation, so position error is low order and acceleration error is high order, with velocity error in between. The unimodal and bimodal perturbations should produce the same magnitudes of acceleration error, but the second half of the bimodal perturbation helps to correct the position and velocity errors produced in the first half so that the magnitudes of these errors are smaller by time of perturbation offset. Keep in mind that in an intertio-viscous system position, errors will continue to grow after perturbation offset unless they are actively corrected. The human arm does indeed have some passive elasticity, but this has small effects on short, quick point-to-point movements compared to the effects of viscosity and inertia[41] (Todorov, 2k).

The movement times with different perturbation types were similar within each group. Symptomatic HD subjects take about 1.2 seconds to complete null movements. This rises to 1.6 seconds for 18N unimodal-early, and bimodal-early perturbations, and to 1.8 seconds for unimodal-late perturbations. Cerebellar Controls also complete null

movements in about 1.2 seconds. This rises to about 1.4 seconds for 18N unimodal-early, and bimodal-early perturbations, and to 1.5 seconds for unimodal-late perturbations. Control subjects have much lower movement times in all cases than the patient groups even though the peak speeds within movements are not higher. Their main savings in movement times compared to the patient groups arises because of their efficiency of motion.

Overall, the three different types of perturbations produced the same patterns in the measures that we used to characterize their effects on movements. Baseline, unperturbed, movements were slightly worse in cerebellar subjects than subjects with manifest HD, and subject with HD had worse unperturbed movements than controls. When perturbations were given, the decrement in performance was greater in HD subjects than cerebellar or control subjects. The raw decrement in performance caused by perturbation was generally greater for cerebellar subjects than controls, but when the performance decrement was assessed relative to baseline, as a percent change in each performance measure, cerebellar subjects often had smaller perturbation induced changes than controls.

Movements without Visual Feedback

Dynamic Properties of Movements Without Visual Feedback

When visual feedback was withheld from perturbed movements the irregularities seen in the movements with visual feedback persisted for HD subjects. The HD movements displayed in the third row of pinwheel groupings in Figure 3 show several trials with successive overshoots, loops, or reverses in direction. The character of these irregularities appears similar to that seen in movements with visual feedback, and the

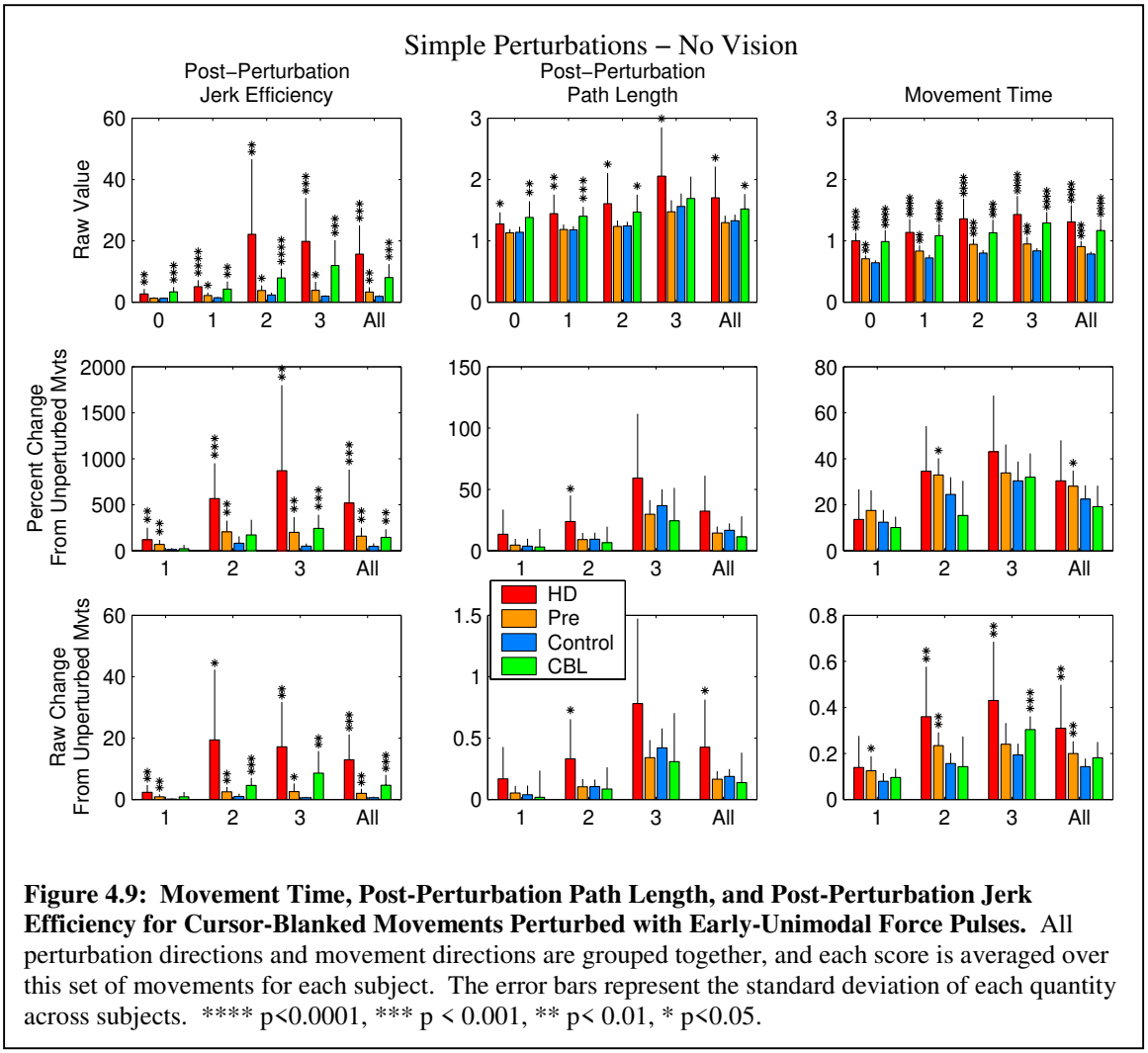

Figure 4.9: Movement Time, Post-Perturbation Path Length, and Post-Perturbation Jerk Efficiency for Cursor-Blanked Movements Perturbed with Early-Unimodal Force Pulses. All perturbation directions and movement directions are grouped together, and each score is averaged over this set of movements for each subject. The error bars represent the standard deviation of each quantity across subjects. **** p<0.0001, *** p < 0.001, ** p< 0.01, * p<0.05.

fraction of movements that appear to display extreme irregularity is comparable. Like those with vision, cursor-blanked unperturbed movements made by HD subjects did not display the extreme irregularities that sometimes occurred when movements were perturbed. The similarity between both the perturbed and unperturbed movements with or without visual feedback suggests that the presence of visual feedback is not primarily responsible for these irregularities. Because the instability seen in perturbed visually aided movements persists in perturbed cursor-blanked trials, visual signals are unlikely to be the main cause of the instability. Conversely, because the instability seen in perturbed cursor-blanked trials persists in visually aided movements, it appears that real-time visual

information about the movement progression is not sufficient to prevent instability from occurring.

A quantitative characterization of the motion dynamics resulting from force pulse application is presented in Figure 9. Like the trials with visual feedback, the presence of perturbing force pulses on cursor-blanked trials substantially increases the jerk, path length, and movement time over unperturbed cursor-blanked trials. Similar to the behavior seen when visual feedback of the cursor was provided, HD subjects had worse baseline performance than individuals with cerebellar dysfunction, but worse performance in trials with the larger perturbations. When visual feedback is withheld, the relative changes in jerk for 12N and 18N perturbations are 500% and 800%, respectively. These changes are 5 to 10 fold higher than the percent changes displayed by controls, and 3 fold higher than the changes displayed by cerebellar subjects. Changes in path length and movement time were similar to those seen in trials during which vision of the cursor was provided. Overall, the character of movement disturbance seen when visual feedback was withheld seems quite similar to what we observed when visual feedback was provided. This suggests that dysfunctional processing of visual signals is not primarily responsible for the dysfunctional error feedback control in HD. In fact, the relative changes in jerk are more than 50% higher for cursor-blanked movements than for cursor-sighted trials. Although the error margins on these jerk scores are large, this hints that visual signals might even help compensate for the primary disturbance in error feedback control present in HD. If indeed it occurs, this compensation is, however, clearly far from complete, because several of perturbed trials made by HD subjects with vision are dramatically disturbed.

Static Properties of Cursor-Blanked Movements: Distributions of Endpoint Errors

When visual feedback was provided, all subjects reliably ended their movements within a centimeter of the target center, even when perturbed. This was not the case when visual feedback was withheld. Inspection of the hand paths in Figure 3 reveals that several of the perturbed, cursor-blanked movements made by HD subjects appear to stop a few centimeters away from the target location. This suggests that characterization of the dynamic properties of cursor-blanked movements cannot provide a complete picture of the irregularities displayed in these movements, since endpoint positions (which are static in nature) seem to be affected by the perturbations.

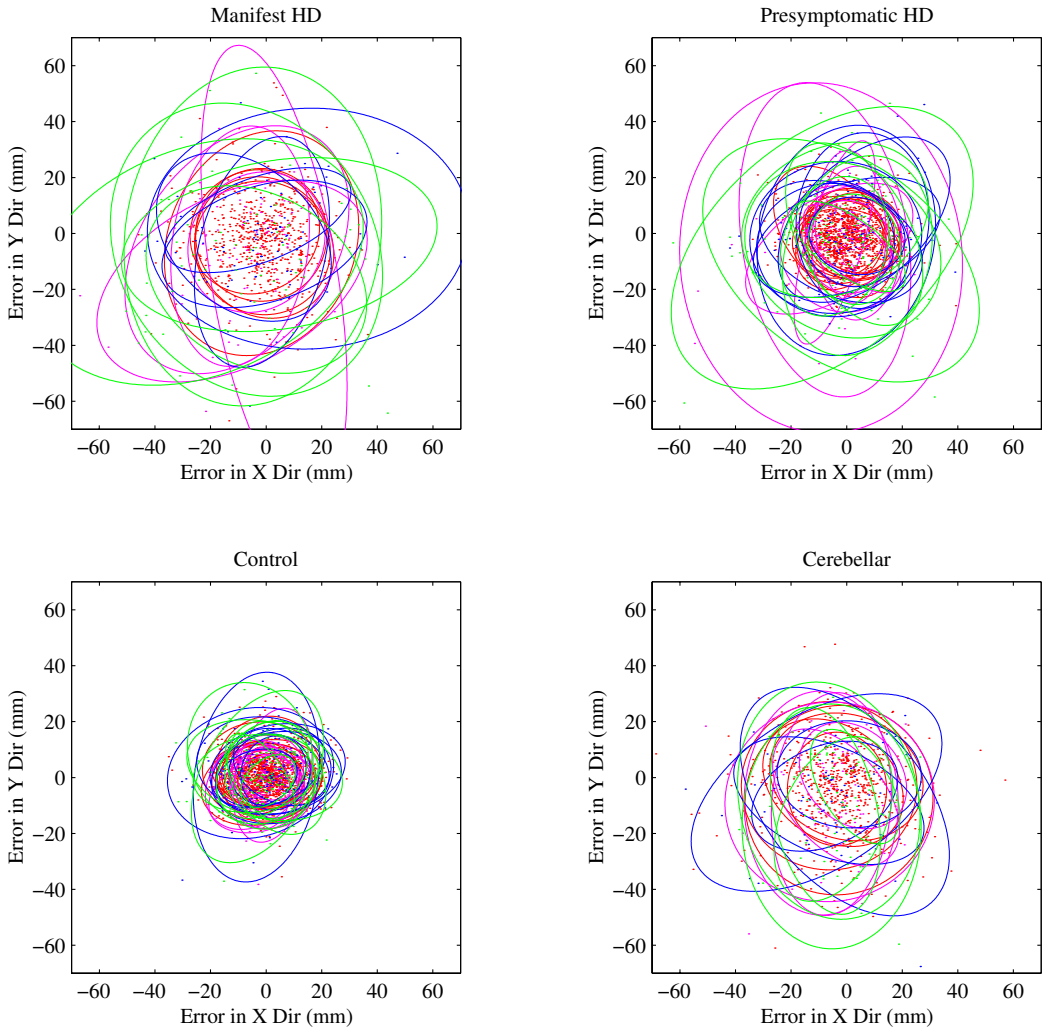

Figure 4.10: Distributions of End-Point Errors. The distributions of endpoint positions of all movements made without visual feedback are plotted. Each dot represents a movement's endpoint position relative to the target's center, and each ellipse represents an estimate of the 99% confidence limit for the distribution of endpoints of all the movements made with the same perturbation magnitude for each subject. The different groups are plotted on different axes. The color of each ellipse or dot corresponds to the perturbation magnitude. Red: unperturbed movements, magenta: 6N perturbations, blue: 12N perturbations, green: 18N perturbations.

Figure 10 shows the endpoint distributions relative to the target center of the different subject groups for different perturbation magnitudes when visual feedback was withheld. Each ellipse represents distribution of endpoint errors for a single subject at the perturbation magnitude coded by the ellipse's color. The vast majority of endpoint

errors are less than 2cm for control subjects, but the endpoint error distributions become much more spread for subjects in the other groups. Subjects symptomatic for HD have baseline (unperturbed) endpoint error distributions that are larger than control subjects, and the these distribution almost double in size when large perturbations are applied. In contrast, cerebellar subjects display unperturbed endpoint error distributions similar to HD subjects, but the sizes of these distributions change only to a small degree when perturbation are applied. Subject presymptomatic for HD have baseline distributions similar to those of controls, but, like symptomatic HD subjects, the spread of their distributions grow dramatically when perturbations are applied.

Figure 11 shows confidence ellipses representing the pooled endpoint error distributions of all subjects within each group. The distributions are represented in the coordinates of the original workspace, and in coordinate systems tied to the movement direction and perturbation direction. The ellipses appear fairly isotropic and unbiased (circular and zero-centered) in all three coordinate systems, suggesting that workspace-dependent, movement-dependent, and perturbation-dependent directional biases in endpoint error are small compared to its spread.

Close inspection of the distributions reveals that all groups except the cerebellar subjects display a slight elongation of the distributions in the movement direction that persists when perturbations are delivered, and cerebellar subjects show shift of their distributions in the movement direction (signifying a tendency to overshoot the target) whether or not perturbations are delivered. Presymptomatic and symptomatic subjects also show a small overshoot tendency (shift of distributions in the movement direction), but only for perturbed movements. There appear to be no clearly consistent changes in

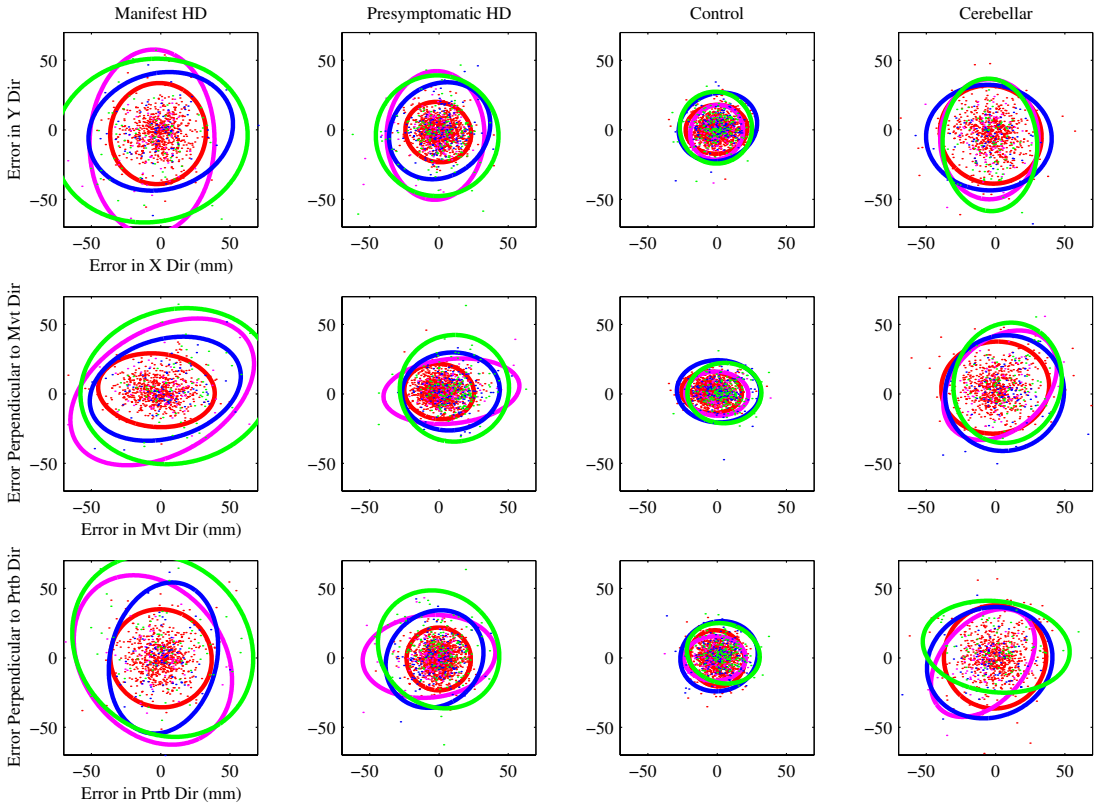

Figure 4.11: Distributions of End-Point Errors Expressed in Different Coordinate Systems. The distributions of endpoint positions of all movements made without visual feedback are plotted. Each dot represents a movement's endpoint position relative to the target's center, and each ellipse represents an estimate of the 99% confidence limit for the distribution of endpoints of all the movements made with the same perturbation magnitude for each group. The different groups are plotted on different axes. The color of each ellipse or dot corresponds to the perturbation magnitude. Red: unperturbed movements, magenta: 6N perturbations, blue: 12N perturbations, green: 18N perturbations.

the shapes or centers of the endpoint error distributions relative to the perturbation direction or the workspace coordinates, and the shape and center changes which occur in the movement direction appear small compared to the differences in spread within and between groups.

Analysis of the Spreads and Offsets of Endpoint Error Distributions

Figure 12 displays a quantitative analysis of the spread and offset of the endpoint error distributions for each group shown in Figures 10 and 11. We gauged spread by the

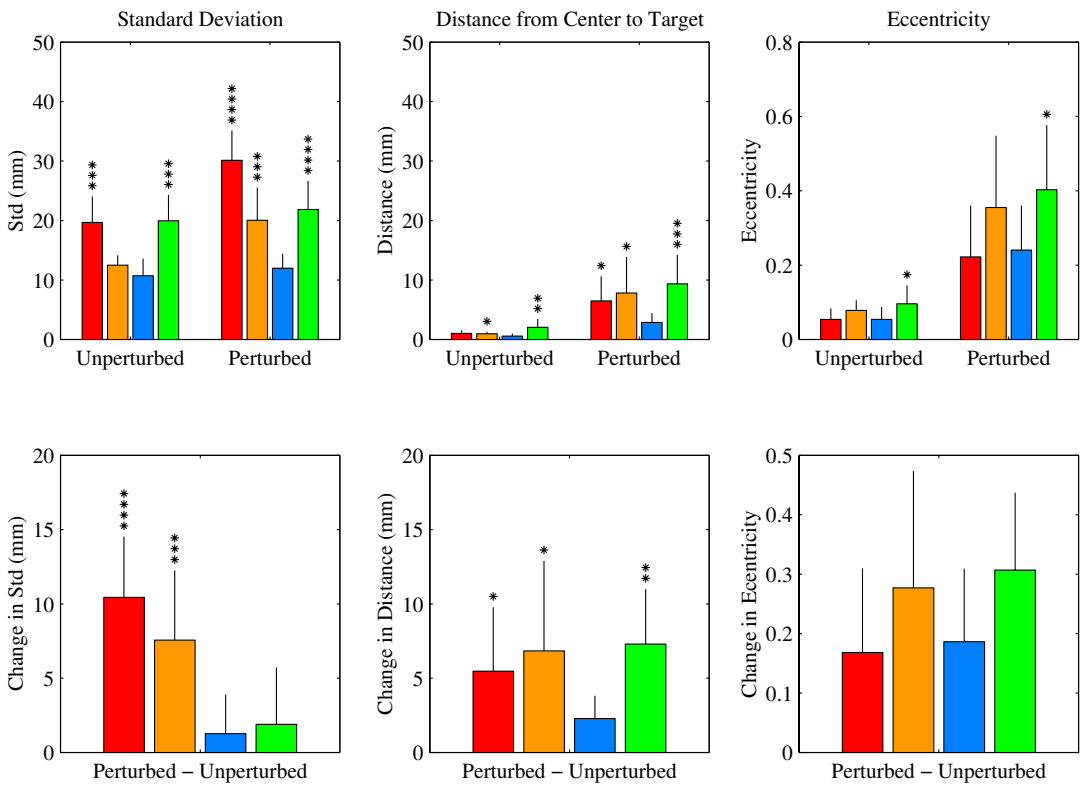

Figure 4.12: Analysis of the Properties of Endpoint Error Distributions for Movements without Visual Feedback. The standard deviation of each distribution characterizes its spread. The standard deviation shown here is the Euclidean norm of the standard deviations in the X and Y directions. Eccentricity is defined as the ratio of a distribution's offset from center to its standard deviation. Top row: the mean and standard deviation of each measure is shown for both perturbed and unperturbed trials. Bottom row: the difference between perturbed and unperturbed trials is plotted for each measure. **** p<0.0001, *** p < 0.001, ** p< 0.01, * p<0.05.

pooled standard deviations in the X and Y directions of the endpoint distributions. The pooled standard deviation was computed as the Euclidean norm of the standard deviations in the X and Y directions. For reference, the 99% confidence ellipses displayed in Figures 10 and 11 have radii in each direction of approximately 3 times the standard deviation in that direction. Each distribution's offset was characterized by the distance between its mean and the target center (zero error). The eccentricity of each distribution was defined as the ratio between its offset and its standard deviation.

Symptomatic HD and cerebellar subjects both display error distributions with spreads significantly increased over controls for both perturbed and unperturbed movements. However, the change in distribution spread due to the presence of perturbations was 4 times greater in HD than cerebellar subjects. Cerebellar subjects showed perturbation induced changes similar to controls; whereas the perturbation induced change in spread for symptomatic HD subjects was more than 5 times greater than that of controls ($p<0.0001$). Subjects presymptomatic for HD had spreads similar to controls for unperturbed movements, but their error distributions increased in spread by a 4-fold margin over controls when perturbations were applied ($p<0.001$).

All the non-control groups generally show greater offsets in their error distributions than controls, but of these, only cerebellar subjects display offsets in their distributions compared to their spreads that are disproportionately greater than controls to a significant extent ($p<0.05$ for both perturbed and unperturbed movements). For both perturbed and unperturbed movements, however, the eccentricity for cerebellar subjects is less than 2-fold greater than that of controls, and the change in eccentricity when perturbations are applied was not significantly greater for cerebellar subjects or either of the HD groups than controls.

Figure 13 displays the analysis of direction specific characteristics of endpoint error distributions in coordinate systems locked to the workspace or to the directions of movement or perturbation. The second column summarizes data for the widths of the distributions aligned to each coordinate frame. This data corroborates the conclusions that we drew about the distribution spreads shown in Figure 12. Cerebellar subjects display endpoint distribution widths in both the X and Y directions in all coordinate

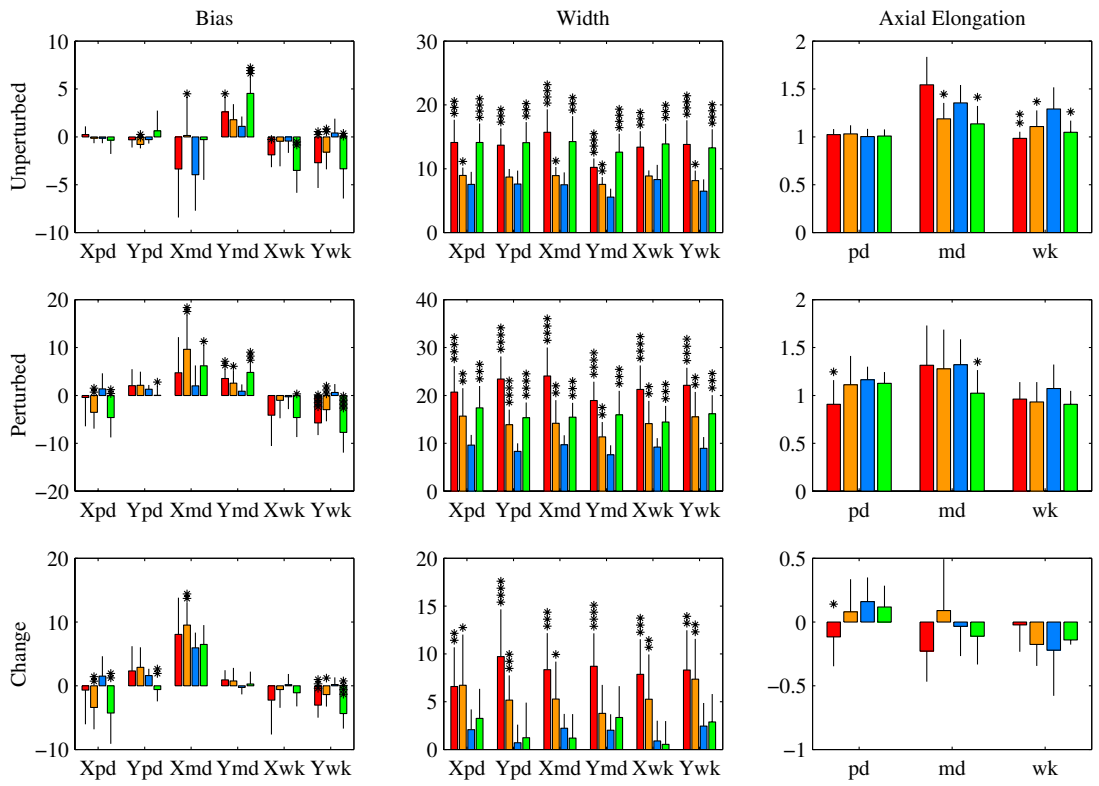

Figure 4.13: Direction Specific Characteristics of Endpoint Error Distributions for Movements without Visual Feedback. Distribution bias is simply the position of the mean compared to the target center, and width in a particular direction is the standard deviation in that direction. Axial elongation in a particular coordinate system is the ratio of X to Y widths in that coordinate system. The values displayed for bias and width are in millimeters. The third row of plots displays the raw change in each measure: the difference in each measure between perturbed and unperturbed trials. Data are aligned to three different coordinate systems: pd - perturbation direction, md - movement direction, wk – workspace coordinates. X is the primary direction of each coordinate system. For example, Xpd is in the perturbation direction, and Ypd is perpendicular to the perturbation direction. **** $p<0.0001$, *** $p < 0.001$, ** $p< 0.01$, * $p<0.05$.

systems which are significantly greater than controls for unperturbed movements (top row, m40iddle), but which increase to roughly the same extent as controls when perturbations are applied (bottom row, middle). In contrast, both presymptomatic and symptomatic HD subjects show changes in width that are substantially greater than control and cerebellar subjects for both directions in each coordinate system.

The Perturbation Response of the Endpoint Distributions of HD Subjects Is Less Direction Specific Than the Responses of Cerebellar or Control Subjects.

Interestingly, both cerebellar and control subjects show changes of the width of their endpoint distributions in the direction (Ypd) perpendicular to the perturbing force pulse that are almost identically zero (Figure 13 bottom row, middle, 2nd plot grouping); whereas HD subject groups display width increases in this direction which are as great as the width increases along the axis of the perturbation. This suggests that the response of cerebellar and control subjects to perturbations is almost completely direction specific whereas the perturbation response of HD subjects is not direction specific to the same degree. If the response to an external perturbation was entirely direction specific (i.e. the subject's response to a force pulse was to add a push in the direction exactly opposite to the force pulse to his original motor output), then one would expect almost no increase in endpoint variability in the direction orthogonal to the perturbation because no perturbing or compensatory forces would have acted in this direction. The original variability arising from errors in the originally planned motor output would remain essentially unchanged by the perturbation. There would, however, be an increase in endpoint variability in the direction of the perturbation. Even if the response to the perturbation was of the correct magnitude on average, trial to trial variations in magnitude of the response relative to the perturbation strength would add to the original endpoint variability in the perturbation direction.

A more detailed analysis of the dependence of endpoint error variability on perturbation direction is presented in Figure 14. The top right panel shows that the perturbation-induced changes in endpoint distribution width in the perturbation direction are significantly greater than zero for all groups, but the width changes orthogonal to the

perturbation direction are only significantly positive for the HD subject groups. The perturbation-induced width change orthogonal to the perturbation direction is large compared to the total width change for HD subjects, but quite small for cerebellar and control subjects (Figure 14, bottom left). Similarly, the difference between the width changes in and orthogonal to the perturbation direction were small compared to the total width change for the HD subject groups, but large for cerebellar and control subjects (Figure 14, bottom right). Taken together, this data suggests that the response of cerebellar and control subjects to perturbations is almost completely direction specific, but that HD subjects have substantially lost this normal direction specificity. The variability in endpoint error is almost entirely uniform for HD subjects. In fact, the only evidence that we see of preserved direction specificity in perturbation response for HD subjects is the lack of large perturbation dependent biases in the endpoint error distributions, indicating that HD subjects on average compensate for perturbing forces in their endpoint positioning. So while the mean responses that HD subjects display to perturbations on cursor-blanked trials are direction specific, the variability in these responses are not direction specific, but rather quite uniform.

To be honest, I don't really know what to make of all the data pertaining to the endpoint error biases presented in Figure 13. All of the biases do seem quite small. In fact, except for a tendency that all groups share to increase target overshoot in the movement direction when perturbations are applied, all biases and changes in bias are less than 5mm for each group. All the non-control subjects also display a slight (<5mm) tendency to undershoot the target in the direction of perturbation, and not fully compensate for the displacement caused by the force pulses. Although significant

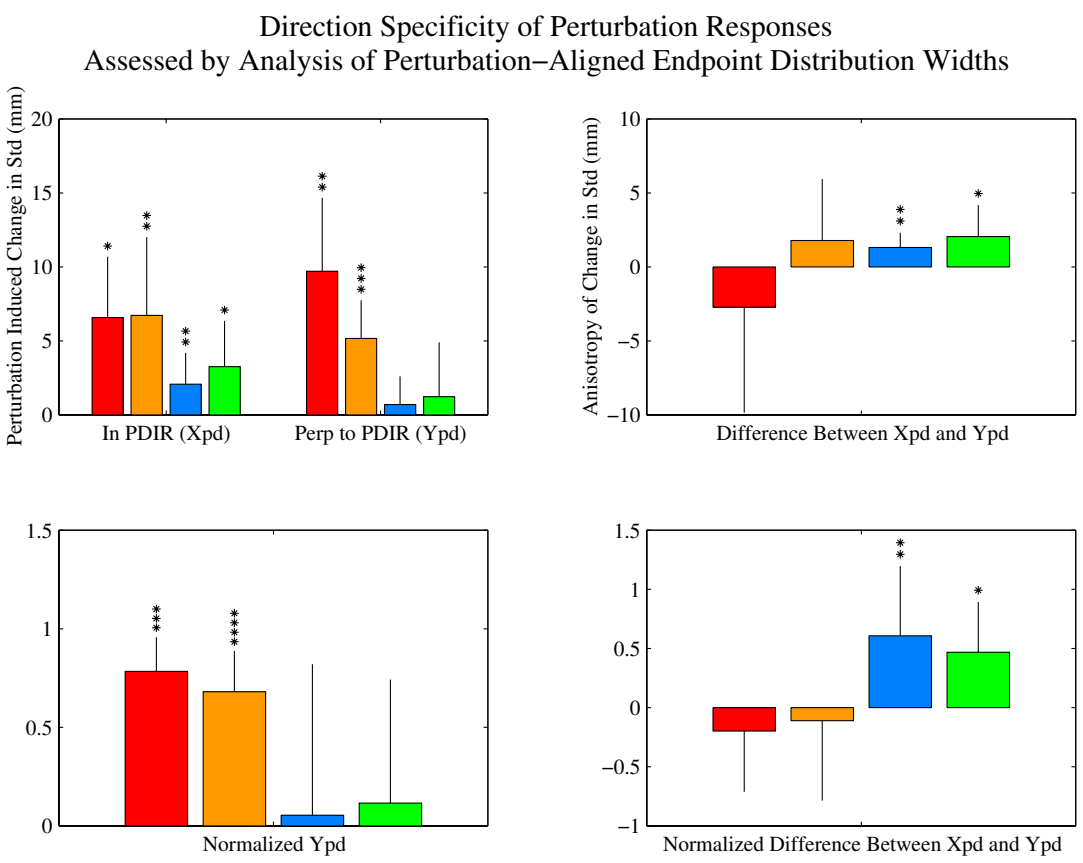

Figure 4.14: HD Subjects Lose Direction Specificity in Their Response to Error. Average endpoint error in cursor-blanked trials is more strongly aligned to the direction of the perturbing force for control and cerebellar subjects than subjects with HD. The distributions analyzed here are all anligned to the perturbation direction. Top left: The perturbation induced change in endpoint distribution width in (Xpd) and perpendicular to (Ypd) the perturbation direction. This is the same data plotted in the bottom center panel of Figure 13, but here and in the other panels of this figure, asterisks indicate behavior that is significantly different from zero. A value of about 0.7 ([√2]/2) indicates uniform change in spread in and perpendicular o the perturbation direction. Bottom left: The perturbation induced change in endpoint distribution width perpendicular to the perturbation direction (Ypd) normalized by the total magnitude of the change in endpoint distribution width subject by subject. This characterizes the fraction of the perturbation-induced width change that is orthogonal to the perturbation direction. Top right: Raw difference between Xpd and Ypd. Bottom right: Difference between Xpd and Ypd relative to the total magnitude of the change in endpoint distribution width subject by subject. **** $p<0.0001$, *** $p < 0.001$, ** $p< 0.01$, * $p<0.05$.

differences do exist between cerebellar and presymptomatic HD subject groups and controls ($p<0.01$ for both groups.), these undershoot biases are small enough to be within the target boundaries, and the symptomatic HD subject group fails to display significant biases.

These small undershoot biases might be the result of an intact optimization process. Harris and Wolpert have reported that signal dependent noise influences motor planning[30]. Specifically, they have shown that the typical trajectories of several eye and hand movements resemble those that would be predicted by a model which tries to minimize endpoint error given that motor activation signals exhibit noise proportional to their magnitude (constant signal to noise ratio). Their work suggests that movements tend to be smooth, because plans for such movements tend to minimize motor activation, and that the motor system attempts to complete tasks with minimal motor activation because the higher the planned motor activation the higher the associated variability. Undershot corrections may require slightly less motor activation than fully-compensating corrections and so movements with slightly undershot corrections may actually end closer to the target on average than those with fully compensating corrections. If this sort of argument were true then we might expect to find that unperturbed movements would tend to undershoot the target, there is a hint of this in the data but no clear effect. Error corrections may show a stronger effect than preplanned movements because error correcting motor commands must be based on noisy real-time sensory information, and thus may have a lower signal to noise ratio than preplanned movement commands. The idea that a biased plan might produce minimal error on average is somewhat counter-intuitive. As an example of this principle, recall from elementary statistics that the statistical estimator that approximates the variance from a sample best in the least squares sense is:

Vest = sum([xi-mean(x)]^2)/N

but that the expected value of this estimator is:

$$E(Vest) = V*(N-1)/N < V$$

Here we see that the best estimator is biased, and in practice the unbiased estimator:

$$Vest.unbiased = sum([xi-mean(x)]^2)/(N-1)$$

is often used, but the fact remains that an undershot estimator ($E(Vest)<V$) minimizes the expected value of the squared estimation error. The small undershoot biases displayed in perturbation response may result from an optimization process with similar properties.

Patterns Within the Perturbation Responses – Is the Error Feedback Dysfunction in HD More Prominent in Certain Movement Directions, Perturbation Directions, or Combinations of These?

Properties of Directional Performance Modulation

During the perturbation experiment, subjects made movements in eight different directions, and each of these target directions could be perturbed in eight different directions, yielding a total of 64 combinations of movement direction and perturbation direction. All the analysis presented so far lumped all the movements with a common force pulse type and magnitude together. We found that HD subjects had markedly disturbed error correcting responses on average, and that several of their movements were highly irregular, but that other movements made by the same subjects at the same perturbation magnitude appeared within normal limits. Here we explore the relationship between perturbation response performance and the direction of movement or perturbation. Specifically, we ask whether the trial-to-trial variability in error correcting performance is due to random trial-to-trial fluctuation, or whether it results from the direction of movement, the direction of perturbation, or a combination of the two? We aim to understand the scope of the error feedback control dysfunction in HD. Does this dysfunction affect only certain movement directions, perturbation directions, or

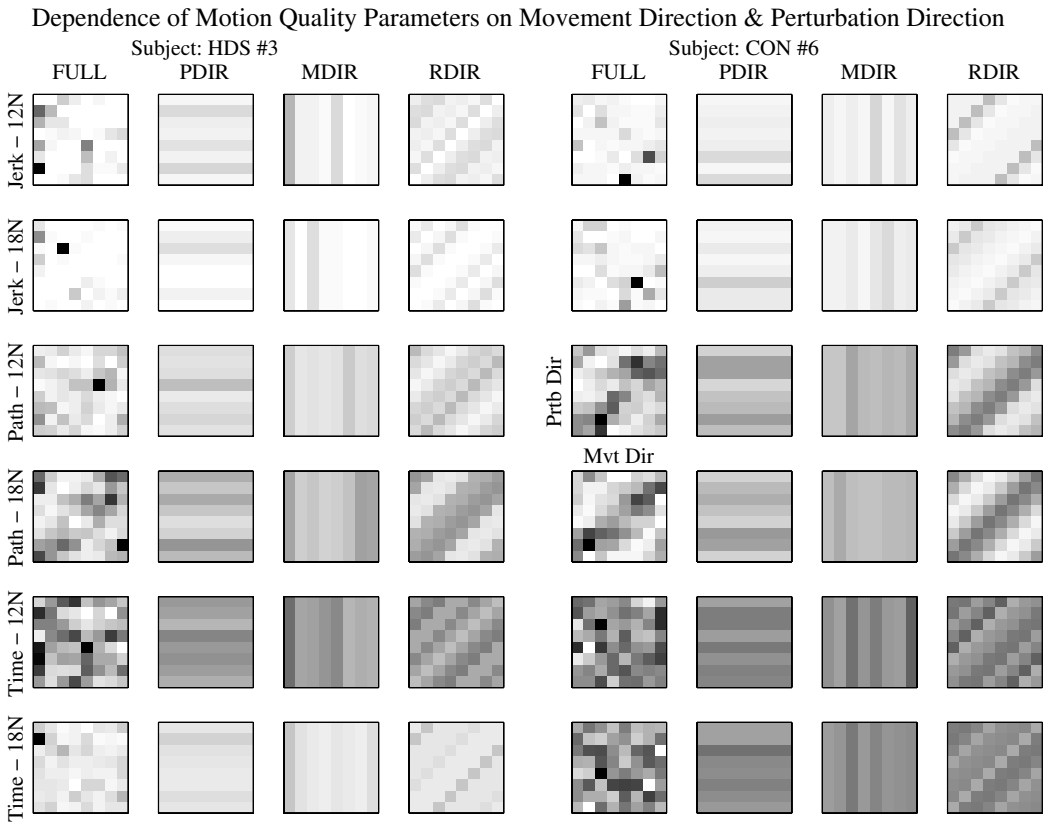

Figure 4.15: Pattern of Performance Measures in Relation to the Direction of Movement and Direction of Perturbation. The data for visually aided unimodal-early perturbations from two individual subjects are shown: an HD subject in the left 4 columns and a control in the right 4 columns. The **first column** for each subject consists of 8x8 images that code performance as a function of movement direction (MDIR) and perturbation direction (PDIR). Each square pixel represents a single movement and is colored to signify performance on a particular measure relative to other movements of the same perturbation magnitude. Dark pixels represent high scores and poor performance, while light pixels represent relatively good performance. The pixel location on the X-axis represents MDIR and on the Y-axis represents PDIR. The **second column** shows the average relationship between each measure and PDIR. Averaging together the pixels at a particular PDIR over the different MDIRs generates this plot. Similarly, the **third column** shows the average relationship between each measure and MDIR determined by collapsing across PDIR. The **fourth column** shows the relationship between each measure and the relative direction between perturbation and movement (RDIR) determined by collapsing across the PDIRs and MDIRs with the same RDIR. The **six rows** represent combinations of three performance measures: post-perturbation jerk, post-perturbation path length, and movement time and the two largest perturbation magnitudes: 12N and 18N. Large color variations in the collapsed images (PDIR, MDIR, and RDIR) signify the image's directional variable explaining a large fraction of the variance in the image's performance measure, indicating a strong relationship between the two.

combinations of these, or does is this dysfunction generalized enough to affect all directions to about the same degree?

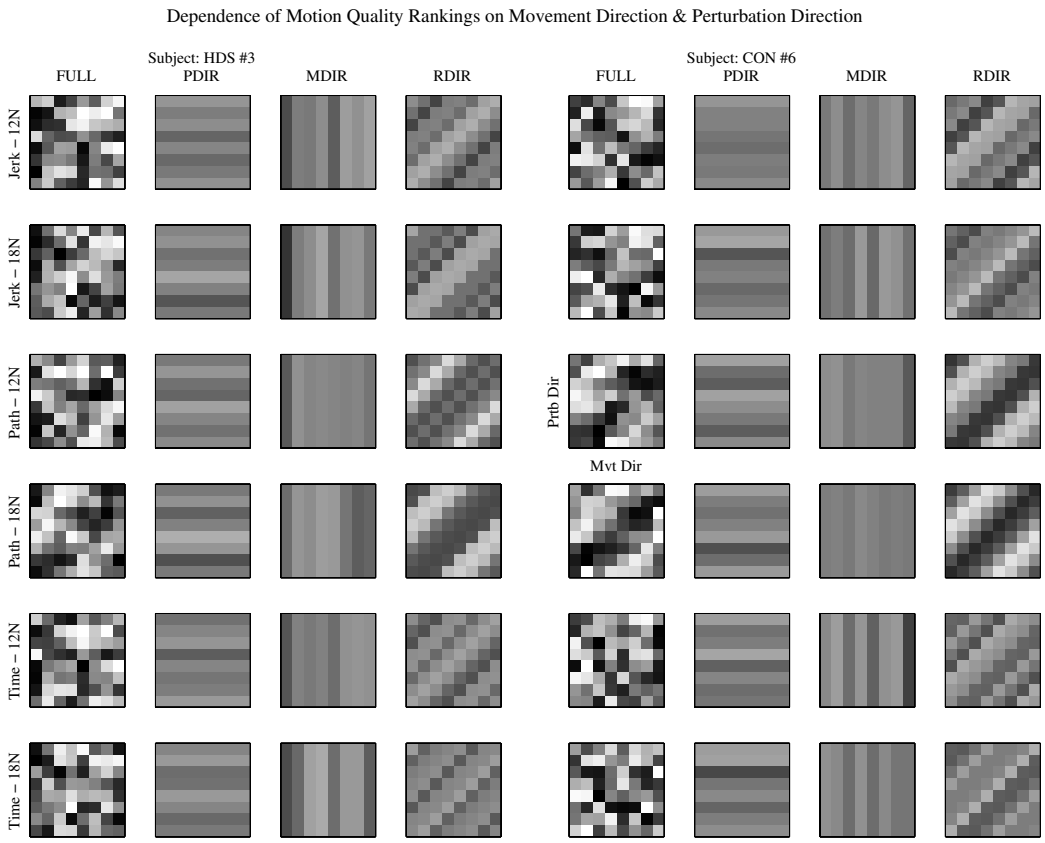

Figure 4.16: Pattern of Performance Measure Rankings in Relation to the Direction of Movement and Direction of Perturbation. The relationship between the self-rankings of three performance measures and the directions of movement and perturbation is illustrated. The format is like that of Figure 14 except that the movements at each perturbation magnitude are ranked from 1 to 64 and the pixel corresponding to each movement is shaded to represent its rank. Ranking performance measures removes extreme-value skews from their distributions. See Figure 14 an explanation of the format.

Figures 15 and 16 illustrate several representations of the relationship between movement performance and the directions of movement and perturbation for one subject with manifest HD and one control. Jerk, path length, and movement time scores (Figure 15) or score rankings (Figure 16) are plotted as images against movement direction (MDIR) on the x-axis and perturbation direction (PDIR) on the y-axis. The column of plots labeled FULL displays the performance score for each visually aided movement perturbed by a 12 or 18N unimodal-early force pulse. Each movement is represented by a score in each in the three performance measures. The corresponding pixels in each of

image are shaded proportionately to each performance score. High scores indicate poor performance and are darkly shaded. We only considered visually aided unimodal-early perturbation types because the other types had poor coverage of the PDIR/MDIR space since only 16 movements of each of these types was administered at each magnitude during the experiment.

If combinations of movement direction and perturbation direction strongly dictated the level of post-perturbation jerk for a subject, then the FULL images for 12 and 18N perturbations would share a pattern that reflected the combinations associated with low or high jerk. Low jerk combinations would be light in both images and high jerk combinations would be black. If however, no strong, consistent relationship existed between jerk and combinations of PDIR and MDIR then the jerk images for 12 and 18N perturbations would be independent of one another. Inspection of the FULL images reveals little consistency in the fine patterning of the pairs of 12 and 18N perturbation images for any of the three performance measures. This suggests that the trial-to-trial variations in jerk, path length, and movement time are not strongly dictated by combinations of movement direction and perturbation direction for these subjects.

The columns labeled PDIR, MDIR, and RDIR are simply collapsed and extruded versions of the data presented in the FULL images. These images show the average relationship the performance measures and perturbation direction (PDIR), movement direction, (MDIR), and the relative direction between perturbation and movement (RDIR). Large color variations in these collapsed images signify the image's directional variable explaining a large fraction of the variance in the image's performance measure, indicating a strong relationship between the two. If a very strong relationship existed

between PDIR and jerk, then FULL images for jerk would have large shade variations from one row (PDIR) to another, but small shade variations within rows. Thus these images would look like a series of horizontal lines, and would be almost unchanged in appearance when collapsed across MDIR to form the PDIR image. The PDIR image would retain almost all the variability and color range of the FULL image, signifying a strong relationship between jerk and PDIR. On the other hand, the associated MDIR image appear almost uniformly mid-gray because the different columns (MDIRs) of the FULL image would be nearly identical to one another, and therefore their means would also be quite similar, producing a uniformly gray MDIR image.

The relationship between path length and RDIR is the strongest of all the combinations of performance measures and directional variables for both subjects for both the rankings and the raw performance scores. It appears that the HD subject generally displays similar or somewhat weaker relationships between performance measures and directional variables than the control subject shown suggesting that these variables do not account for the large trial-to-trial performance variability displayed by HD subjects.

The average relationships between the three performance measures and the three directional variables for each group are displayed in Figure 17. Data in the left three columns are plotted on a logarithmic scale for clarity, and represent the relationships between raw performance scores and each of the three directional variables. Data in the right three columns represent the relationships between the ranked performance scores, expressed as percentiles, and each of the three directional variables. The strengths of modulation appear to be quite similar for all groups with HD and cerebellar subjects

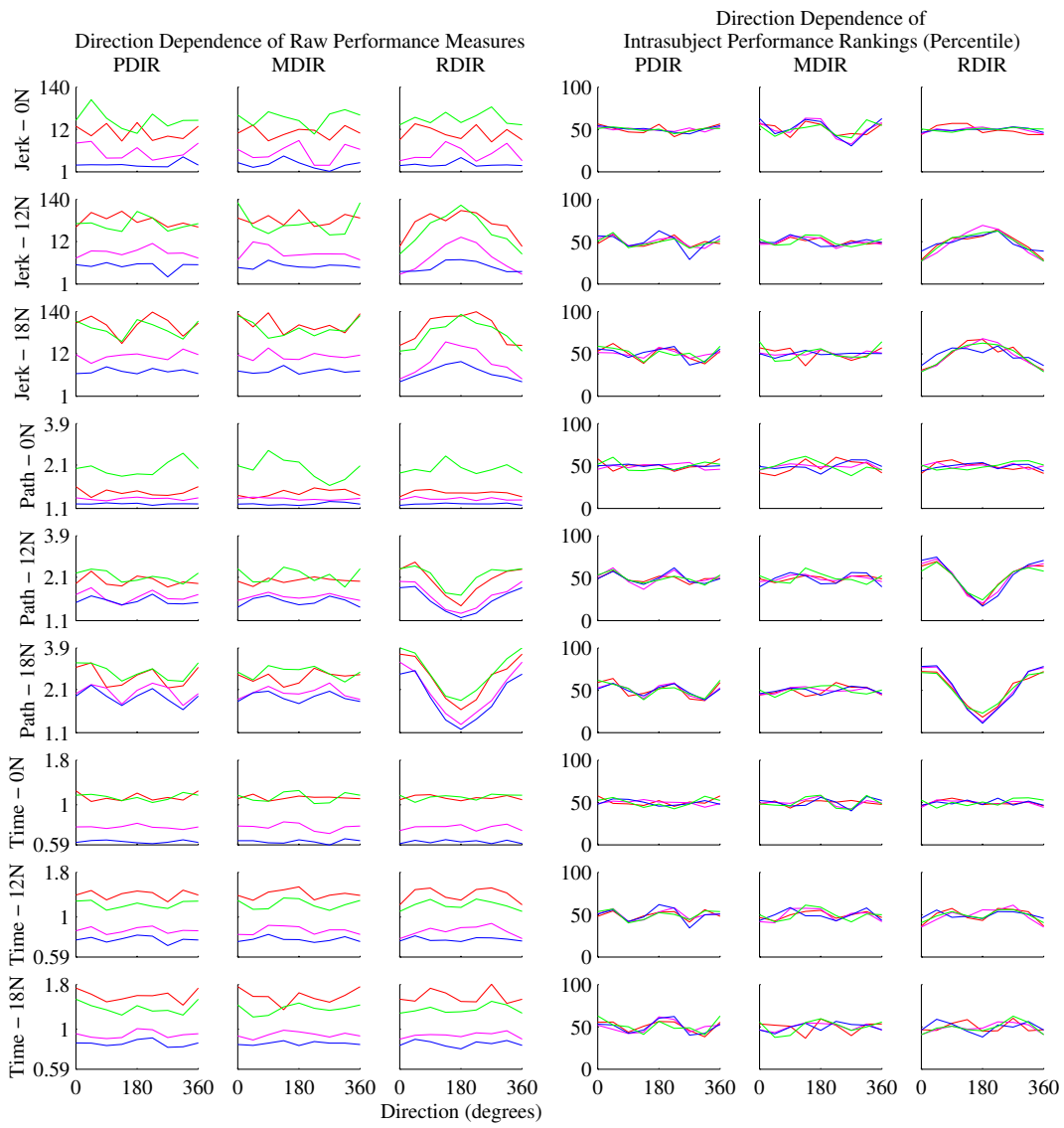

Figure 4.17: Dependence of Performance Measures on Perturbation Direction (PDIR), Movement Direction (MDIR), and Relative Perturbation Direction (RDIR). The **three leftmost columns** show the dependence of changes in the raw performance measures from baseline (unperturbed movements) on each directional parameter, while the **three rightmost columns** show this dependence for the performance measure rankings. The **six rows** represent combinations of three performance measures: post-perturbation jerk, post-perturbation path length, and movement time and the two largest perturbation magnitudes: 12 & 18N.

shifted upward from the controls fairly uniformly across directions for all performance measures and directional variables. This upward shift in all directions for all directional

variables indicates that HD subjects perform more poorly than controls in all directions of movement and perturbation.

The key difference between HD and cerebellar subjects is that HD subjects perform more poorly in perturbed than unperturbed movements in all directions; whereas cerebellar subjects consistently perform slightly better on some measures in some directions when movements are perturbed than they did for unperturbed movements. Figure 18 shows the relationship between perturbation induced changes in performance the directions of movement and perturbation. Note the performance change of cerebellar subjects for jerk at an RDIR of 0 or 45, path length at an RDIR of 135 or 180 degrees, and movement time at 0 degrees, all for both 12 and 18N perturbations. HD subjects appear to always be disturbed by the presence of perturbing forces, while cerebellar subjects are apparently undisturbed, and even aided in certain aspects of their performance, by these forces in some cases. The change in performance in HD subjects when perturbations are applied is also always greater than that of control subjects, indicating that HD subjects are more disturbed by perturbation in all directions of movement and perturbation than controls.

Examination of the dependence of change in jerk on RDIR (figure 18, third column), reveals that despite the fact that symptomatic HD subjects always display larger decrements in performance than controls, the performance change is consistently greater in some directions than others. RDIRs close to 0 degrees display much smaller changes in jerk than RDIRs close to 180 degrees for symptomatic HD subjects. Closer examination of the data, however, reveals that the difference between directions that symptomatic HD subjects display are not disproportionately greater than those displayed

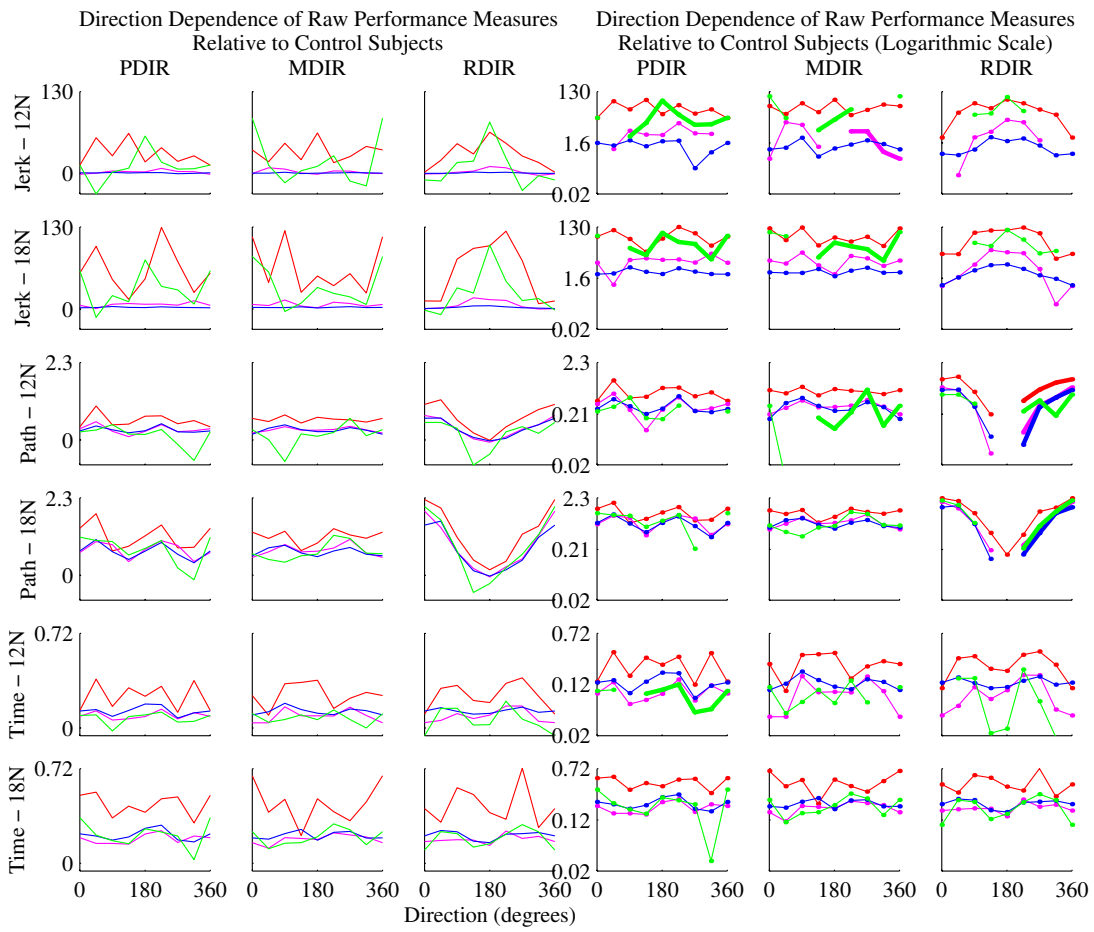

Figure 4.18: Direction Dependence of Perturbation Induced Changes in Performance Measures on Perturbation Direction (PDIR), Movement Direction (MDIR), and Relative Perturbation Direction (RDIR). The **three leftmost columns** show the dependence of changes in the raw performance measures from baseline (unperturbed movements) on each directional parameter, while the **three rightmost columns** show this same dependence plotted on a log scale. Missing data corresponds to improvements in performance when perturbations are applied (change ≤ 0). The **six rows** represent combinations of three performance measures: post-perturbation jerk, post-perturbation path length, and movement time and the two largest perturbation magnitudes: 12N and 18N.

by controls. The right panel of Figure 18 shows the direction dependence of perturbation-induced changes in performance plotted on a logarithmic scale. In these plots, a constant offset between two groups across directions, indicates a uniform multiplicative difference in performance for these different directions. The logarithmic offset between symptomatic HD subjects and controls does appear fairly uniform for these plots,

suggesting that HD subjects not only show signs of error feedback control dysfunction in all directions, but that the degree of dysfunction is fairly uniform.

In contrast, presymptomatic HD subjects appear to display greater perturbation-induced in jerk and movement time disturbance than controls more for backward directed (close to 180 degrees) than forward directed perturbations. This corresponds to the RDIRs in which controls are most jerky. If jerk is indeed the best indicator of perturbation-induced trouble with movement, then signs of Huntington's disease may first manifest by amplifying trouble in "difficult" relative perturbation directions, and later progress so that all directions are disturbed in a fairly uniform manner. Viewed in this way, the disparity in perturbation-induced jerk change that we observe early in the disease course may not be directly due to features of the disease pathology as much as it is a property of the difficulty variations within our task. Changes in "difficult" directions may be most easily seen, whereas changes in easy "directions" may not at first be detectable.

Quantifying the Degree and Consistency of Perturbation-Induced Performance Changes Across Directions.

How much of the trial-to-trial performance difference seen for perturbations of the same magnitude is dictated by the perturbation direction, movement direction, or combinations of these as opposed to random trial-to-trial variability? In order address this question, we used the fraction of the performance variability seen at one perturbation magnitude that was explained by performance at another perturbation magnitude. To make this comparison for the complete pattern of movement directions and perturbation direction, the correlation coefficient between these patterns of performance was used:

$$cc(p_{12},p_{18}) = \mathrm{sqrt}([p_{18}-\mathrm{mean}(p_{18})]\cdot[p_{12}-\mathrm{mean}(p_{12})] / \mathrm{sqrt}(\mathrm{var}(p_{18})*\mathrm{var}(p_{12})))$$

Where p_{12} and p_{18} are 64X1 vectors of the performance for a subject for all movements with 12 or 18N perturbations, mean and var represent the mean and variance of a vector's elements, sqrt is the square root operation, and · represents the vector dot product.

The correlation coefficient between two vectors is the square root of the fraction of the variance in either vector explained by the other. In order to make comparisons for subsets of the complete directional pattern (movement direction, perturbation direction, and relative perturbation direction), I used the square root of explained variance so that direct comparisons could be made across all types of patterns. Specifically, the average of the square root of the total variance at one perturbation magnitude explained by a collapsed pattern from the other was computed, and referred to as "consistent modulation." Simply correlating the collapsed patterns (MDIR, PDIR, and RDIR) seen in Figures 15-18, shows only the variability explained between those collapsed patterns while losing handle on the variability lost during the collapse. For example, if only a small fraction of the variability in jerk was explained by movement direction, but the shape of this pattern happened to be the same from one perturbation magnitude to another, a perfect correlation would be computed, despite movement direction not having a large influence on jerk.

The consistent modulation (cm) between 12 and 18N perturbations in movement direction can be computed as follows:

$$cm = cc(p_{12m},p_{18m}) * avg\{ sqrt(var(p_{12m})/var(p_{12})),sqrt(var(p_{18m})/var(p_{18})) \}$$

if we use the geometric mean for the average then:

$$cm = sqrt([p_{18m}-mean(p_{18m})]\cdot[p_{12m}-mean(p_{12m})] / sqrt(var(p_{18})*var(p_{12})))$$

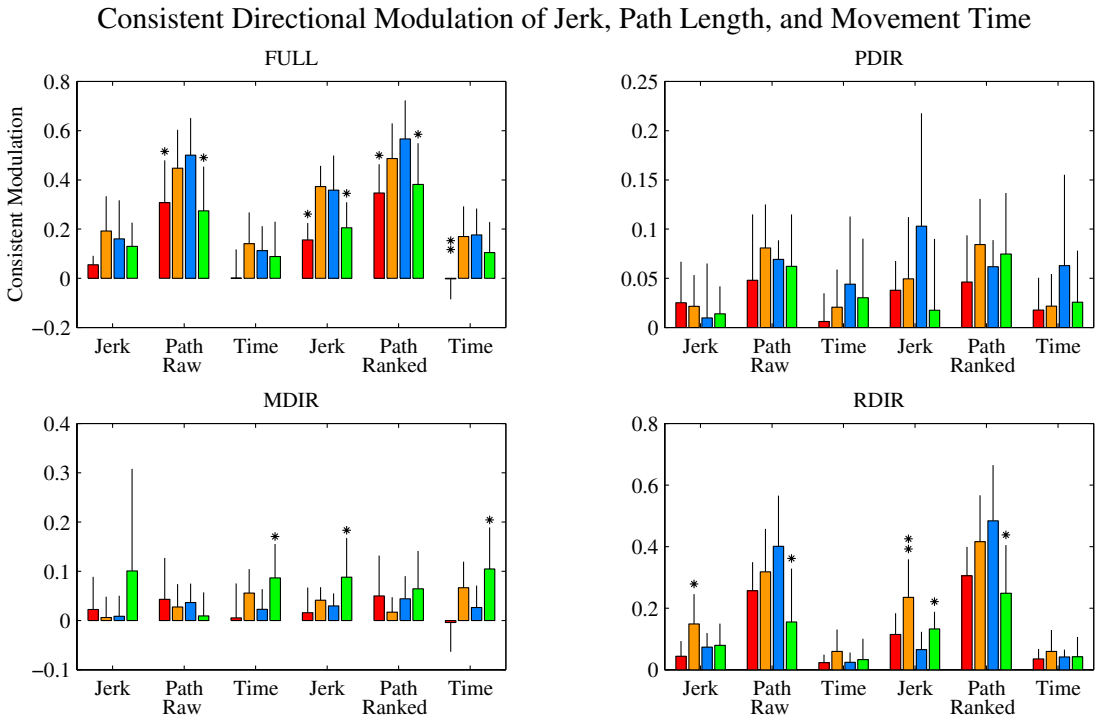

Figure 4.19: Analysis of the Degree of Directional Performance Modulation: Consistent Modulation of Jerk, Path Length, and Movement Time. Consistent modulation is displayed for raw and ranked scores for all performance measures. This shows the degree to which visually aided performance in response to unimodal-early perturbations depended on movement or perturbation direction. Red: symptomatic HD, orange: presymptomatic HD, blue: control, green: cerebellar subjects.

Note that this looks very much like the definition of the correlation coefficient between the vectors p_{12m} and p_{18m}, except that the covariance of these vectors is normalized by the variances of the full vectors p_{12} and p_{18}, instead of their own variances. p_{12m} and p_{18m} are products of collapsing p_{12} and p_{18} across perturbation directions then re-extruding them. These collapse-extrusion products are graphically represented in the MDIR, PDIR and RDIR columns of Figures 15 and 16.

Figure 19 displays the consistent modulation coefficients for raw and ranked scores on three performance measures: post-perturbation jerk, post-perturbation path length and movement time. Figure 20 combines the modulation of the three different performance measures into a single composite measure expressed in relation to the

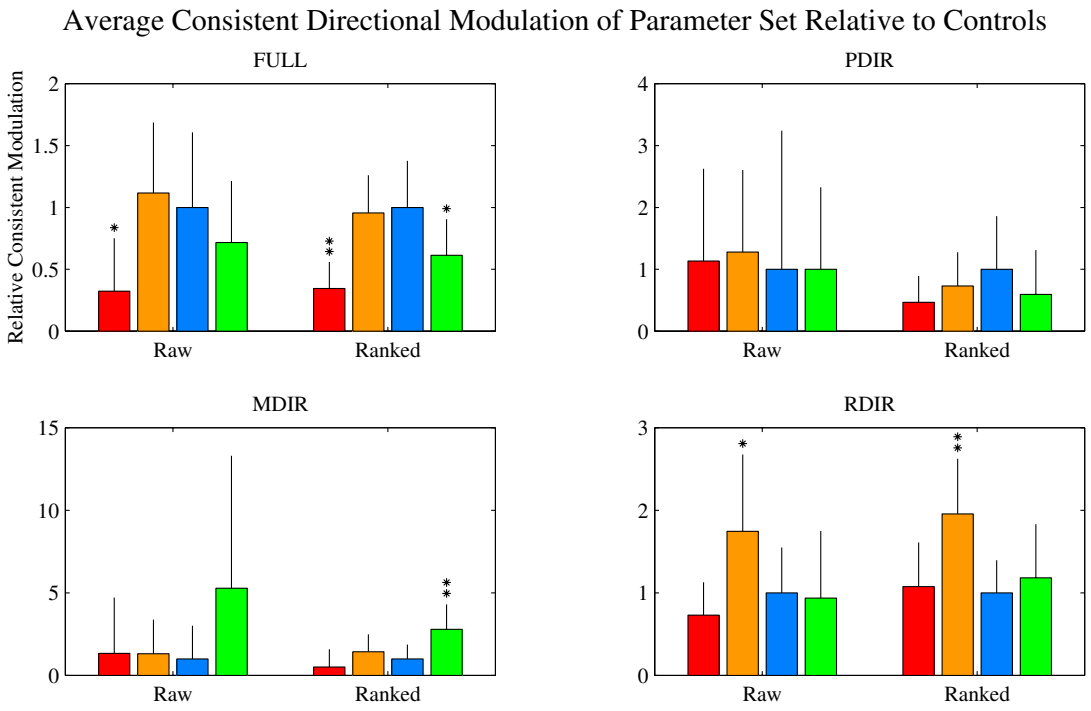

Figure 4.20: Composite of Consistent Directional Modulation Indices Across All Three Performance Measures. The consistent modulation indices for all performance measures relative to that of controls subjects were averaged for each directional measure to form a composite score for that measure for both raw and ranked performance scores. These measures are taken relative to control subjects so that the different performance measures have the same contribution to the composite regardless of the modulation strength .

control modulation level. Subjects with manifest HD generally display less consistent modulation than control subjects, indicating that random trial-to-trial performance variations account for a greater fraction of the variability in their performance than normal. We can also see that of the three directions of variability we used to collapse the two dimensional (perturbation direction, movement direction) data to a single dimension, RDIR preserved by far the most variance for all groups, except cerebellar subjects who displayed equal consistent modulation by RDIR and MDIR. Since the majority of the directional performance modulation for the HD and control groups was in the relative direction between movement and perturbation, there was less effect of the of the low-level substrates of motion, muscles and inertias, on perturbation response quality than the

relative geometry of the perturbation relative to motion, which is independent of these low-level factors.

Cerebellar subjects show significantly more consistent modulation than controls by movement direction. This suggests that much of their post-perturbation irregularity is not caused by the random perturbing force pulses, but by some dysfunction in compensating for the predictable direction dependent dynamics of movement. This agrees with the earlier findings that the degree of perturbation-induced irregularity (change in performance relative to unperturbed movements) was less than for HD subjects, and with the observation that the patterns of irregularity displayed in the hand paths of cerebellar subjects depended on the direction of movement (see Figure 6).

Summary

In this chapter we attempted to gain a better understanding the scope of the error feedback control dysfunction in HD. Generally, the results confirmed that the error feedback control dysfunction that we previously reported was specific to HD among the subject groups tested, and gave additional insight into the nature of this dysfunction. We varied the type and onset time of the external force pulses applied, and we found that the movements of subjects presymptomatic and symptomatic for HD were similarly disturbed by bimodal and unimodal force pulses, and by early-movement and late-movement perturbations.

HD gene positive individuals that we studied here were either asymptomatic (average time until predicted onset of 2.1 years), or only mildly affected (average QNE of

25). MRI analysis suggests that volumes of structures of the basal ganglia, particularly caudate and putamen, are abnormally small in gene positive individuals who are less than 10 years away from development of clinical symptoms[50] (Aylward et al. 1994) and may decline in size with proximity to the predicted onset of the disease[4] (Aylward et al. 1996). In asymptomatic gene carriers (AGCs), putamen volume appears to be the single measure that best differentiates gene positive from gene negative individuals (personal communication, J Brandt). In agreement with this, when the clinical symptoms are detected, the mildly affected individuals have significantly larger loss of volume in their putamen than in their caudate[51] (Harris et al. 1992). Examination of brain regions other than basal ganglia in mildly affected individuals (QNE < 41) has not found any significant differences in the volumes of the frontal, parietal, occipital, and temporal lobes, or the volumes of the cerebellum and the brainstem, despite having found clearly abnormal basal ganglia [52](Aylward et al. 1998). Taken together, it seems plausible that the HD genetic mutation in the individuals that we studied had resulted in atrophy of the basal ganglia, in particular the putamen.

What are the sensorimotor correlates to the early pathology of HD? Previous studies have noted that AGCs have slowed reactions to auditory or visual cues[8,76], and slowed speed of rapid alternating movements[53]. In addition, sensory evoked potentials (SEPs), as elicited through peripheral nerve stimulation, evoke abnormally small potentials in the cortex of some AGCs and this correlates with a reduced long-latency perturbation response in these subjects[24]. In the more advanced cases of the disease, abnormally small or absent long-latency responses to a perturbation are consistently observed[48]. Taken together with the imaging results, the disruption of basal ganglia

structures appears to be coincident with reduced somatosensory input to the cortex, and a diminished capacity for the cortex to respond to postural disturbances to the limb.

How might this affect control of voluntary movements in HD? In our earlier work[78], we noticed that reaching movements of HD subjects usually began quite normally, but diverged in jerkiness from movements of normal individuals about 300 msec after onset, resulting in difficulties in movement termination. While this was highly variable from trial to trial, we found that the amount of jerkiness later in the movement was strongly related to the occurrence of subtle self-generated errors earlier in the movement. Errors early in the movements of HD subjects were not substantially greater than those of normal individuals, but the response to early movement error was dramatically disturbed in HD. The sensitivity of late movement jerk to early movement error was significantly increased in both symptomatic and presymptomatic HD subjects compared to controls. In the context of the theory that the basal ganglia has a role in inhibitory control of motor actions, it seemed plausible that the motor reaction in HD was abnormally strong for the subtle errors.

To test this hypothesis, we imposed perturbations on the limb as reaching movements were performed. For unperturbed movements, our HD and CBL subjects had whole movement performance scores that were comparable to each other (and significantly worse than those of controls). However, when movements had errors imposed upon them, the response was quite different in the two groups. For example, in HDs unimodal force pulses early in their movements produced 250% increase in hand jerkiness relative to unperturbed trials. This was 5 times greater than normal and 3 times greater than CBL. When visual feedback was withheld, the relative increase in jerk for

18N perturbations was 800% in HDs. This again was 3 times the changes displayed in CBL.

This suggested that the motor disorder in HD was more sensitive to the presence of errors than the disorder in cerebellar dysfunction. When visual feedback was removed, HD subjects had unperturbed endpoint error distributions that were larger than control subjects. The spread of these distributions almost doubled in size when large perturbations were applied. In contrast, cerebellar subjects displayed unperturbed endpoint error distributions similar to HD subjects, but the sizes of these distributions changed by only a small amount when perturbation was applied. AGCs had unperturbed distributions similar to those of controls, but, like HD subjects, the spread of their distributions grew dramatically when perturbations were applied. Therefore, when visual feedback was withheld, the application of perturbations resulted in disproportionately larger increases in end-point error spread among AGCs and HD subjects than CBL or controls.

Was there a pattern in the way the HDs responded to the perturbations? In control and CBL subjects, perturbations induced an elongation of the endpoint error distributions only in the axis of the perturbation vector. This suggests that in these subjects, the response to a perturbation that displaced the intended movement was to supplement the ongoing motor commands by a force vector that roughly pushed the limb opposite to the direction of the perturbation. However, in the HD and AGC subjects, the perturbation-induced changes in the ongoing motor program were not limited to the direction that compensated the perturbation. Instead a spillover in perturbation response occurred such

that the supplementary motor commands, on average, produced errors as large orthogonal to as along the perturbation direction.

When we looked at the directional dependence of perturbation recovery performance, we found the dependence of performance on perturbation direction was small for the HD subjects as well as the other subject groups, suggesting that the error feedback control dysfunction in HD is not muscle or muscle group specific. If the disturbance was specific to a muscle then only the perturbation directions for which the muscle participated in the response would be disturbed, instead we find that the disturbance is nearly uniform across perturbation directions. When we looked at the dependence of perturbation recovery performance on all the different directions of movement and perturbation, we found that HD subjects did have strong directional dependences for some performance measures, but that these dependences were not as strong for symptomatic HD subjects as controls. Additionally, the patterns of directional performance modulation seen with HD subjects were not unique to these subjects, but rather matched the patterns of dependence seen in controls. The perturbation-induced decrements in performance displayed by symptomatic HD subjects were greater than normal in all directions, and expressed as a multiple of control performance decrements, the perturbation-induced decrements in the performance of symptomatic HD subjects were fairly uniform across directions, suggesting that the error feedback control dysfunction seen in HD is not direction specific but rather generalized across all movement directions and all perturbation directions.

One can imagine that the dysfunction in online feedback control in HD may be due to an inability to accurately estimate current error in limb trajectory from the delayed

sensory feedback, or an inability to respond to that error by selecting the appropriate compensatory motor command. Either or both of these account for the disturbance that we observed. Dysfunctional real-time action selection has been reported in visual reaction time experiments with HD subjects (Zee et al 1993) although presymptomatic subjects displayed only very small deficits[76]. Alternatively, dysfunctional sensory processing in HD may have contributed to the motor dysfunction that we observed. Abnormal cortical SEPs have been observed very early in the disease course[24,26] when damage tends to be restricted to the striatum. SEP abnormalities have also been correlated to decreased striatal metabolism[15]. Additionally, basal ganglia damage in rats is sufficient to induce SEP changes (Schwarz et al. 1992). Taken together, these pieces of evidence suggest that the problem of online error feedback control might have its origins in the interactions of the basal ganglia with somatosensory feedback, potentially resulting in an inaccurate estimation of the direction of error. If this were the case, then the reaction to a perturbation would of course be an inappropriate motor response.

The motor control system that we have observed in HD is capable of producing accurate commands to initiate a reaching movement, but appears impaired in modifying the descending commands to respond to ongoing sensory feedback as the movement progresses. Miall and colleagues have recently demonstrated through inactivation and recording studies at the thalamus that the basal ganglia may play a specific role in action selection when visual stimuli are not available and the selection is self generated[54,55]. In our task, even when visual feedback was removed the target of the movement was still displayed. Therefore, the dysfunction in error induced action selection that we observed in HD occurred for movements with externally specified goals that were visible

throughout. The movements in our task were only self-generated in the sense that subjects were instructed to begin their movements any time they chose after the target had appeared.

Neurons in the basal ganglia display both sensory and motor activity. It has been suggested that the primary role of the basal ganglia is to process and gate sensory information for motor systems[56,57]. The basal ganglia's potential role in modulating somatosensory feedback may take place directly at the level of thalamus, or indirectly via its output to regions of the motor and premotor cortex. Because basal ganglia efferents and somatosensory input project to different thalamic nuclei, the first alternative appears less likely. However, immediately before and during generation of voluntary arm movements, somatosensory signals are modulated so that, for example, an air-puff to the arm produces significantly reduced responses in cells of the somatosensory cortex than when the same air-puff is given at rest[58]. Cutaneous input to the foot during walking produce reduced responses in the thalamus and the somotosensory cortex with respect to rest[59]. Intriguingly, intracortical microstimulation of the motor cortex is sufficient to dramatically gate the normal response in the somatosensory cortex to the air-puff delivered to the arm[60]. This suggests that generation of motor commands to a limb may be coincident with modulation of sensitivity of the somatosensory regions to inputs received from afferents of that limb. A function of the basal ganglia may be to mediate this modulation so that sensory feedback associated with small errors in movement might stand out against the large amount of feedback that is associated with the movement itself. If this were the case, then a computational function of the basal ganglia would be in real-time prediction of sensory consequences of motor commands. Such a function is

central to the process of monitoring results of motor commands and correcting for potential errors[41,49].

Chapter 5 – Predictive Feedforward Procedural Learning: Subjects with HD Learn Viscous Curl Force-Fields but Subjects with Cerebellar Degeneration do not.

Introduction

Two different mechanisms can operate to make use of sensory information to correct motor errors. The first is online error correction, where errors are compensated "in flight", and the second is trial-to-trial learning, in which errors from one trial influence the motor output on subsequent trials. Both of these processes rely on the evaluation of sensory signals that can be used to determine error, and the subsequent processing of error information. If the processing of sensory information or error signals is generally disturbed, then both online error compensation and trial-to-trial learning should be impaired. In previous work we showed that online error correction was disturbed in Huntington's disease (HD), but largely intact in patients with cerebellar degeneration. Here we show that a double dissociation exists between these two mechanisms of error correction by studying motor learning on a task in which the dynamics of arm motion are systematically altered by application of a mechanical force field. This force field perturbs movement trajectories in a characteristic pattern, but healthy subjects can quickly learn to precisely compensate for and cancel these forces. Subjects with HD displayed unimpaired motor learning despite disturbed online error correction, while subjects with cerebellar degeneration showed greatly impaired motor learning but unimpaired online error correction. This dissociation suggests the existence of parallel neural pathways for processing error information as well as distinct but complementary roles for the basal ganglia and cerebellum in the control of movement.

To investigate error dependent learning we studied the task of making quick point-to-point reaching movements in a robotically applied force-field in subjects presymptomatic and symptomatic for HD and individuals with cerebellar lesions compared to controls. A force-field is a mechanical environment in which the applied force is a function of motion state. In general, the force could be any function of position, velocity, and acceleration, and it can simulate interaction with a physical object or system. For example, the motion of a point mass produces an acceleration dependent resistive force field, and viscous fluids produce velocity dependent resistive force-fields on objects moved within them. In our task, a velocity-dependent force-field perturbed movement in a consistent manner perpendicular to the motion direction over several blocks of trials producing hooking motions. Because the force-field produces predictable, stereotypic pattern of perturbations, it can be predictively compensated. In fact, with practice control subjects learn to compensate consistent force perturbations by forming an internal model such that the expected forces are cancelled and motion trajectories return to nearly their unperturbed states[21,61,62,63]. If the force field is suddenly removed after this learning has occurred, the resulting after-effect movements mirror the movements made upon initial exposure to the force-field because compensatory motor output equal and opposite to the expected force-field becomes unopposed. Learning during these experiments is believed to occur because the brain uses the errors experienced during a movement to adjust motor output on subsequent movements such that the error between the actual and desired trajectories of motion is reduced, perhaps by the adaptation of state dependent motor primitives[64].

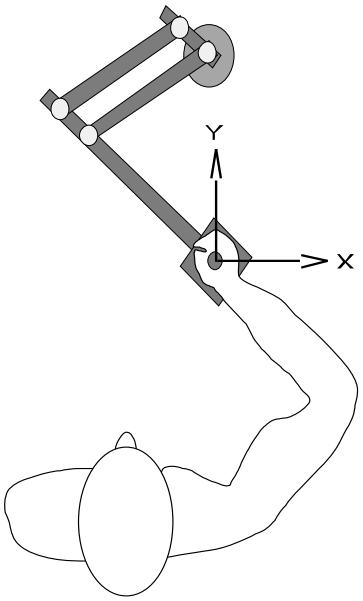

Figure 5.1: Diagram and photo of subject grasping robotic manipulandum.

Methods

Force-Field Description

The force-field that we applied to these movements was a viscous curl field: applied force was proportional to a 90 degree rotation of subject's hand velocity as shown in figure 2. The magnitude of the applied force was proportional to instantaneous hand speed, and the direction of applied force was perpendicular to the motion direction. The relationship between force (**F**) and velocity (**V**) is given by:

$$\mathbf{F} = B * \mathbf{V}$$

$B_1 = [0\ 13; -13\ 0]$ N/(m/s) $\qquad$ $B_2 = [0\ -13; 13\ 0]$ N/(m/s)

Where B is the viscosity matrix. Because B is chosen to be skew symmetric the force vector, **F**, is orthogonal to the velocity vector, **V**, and a curl field is produced. Note that

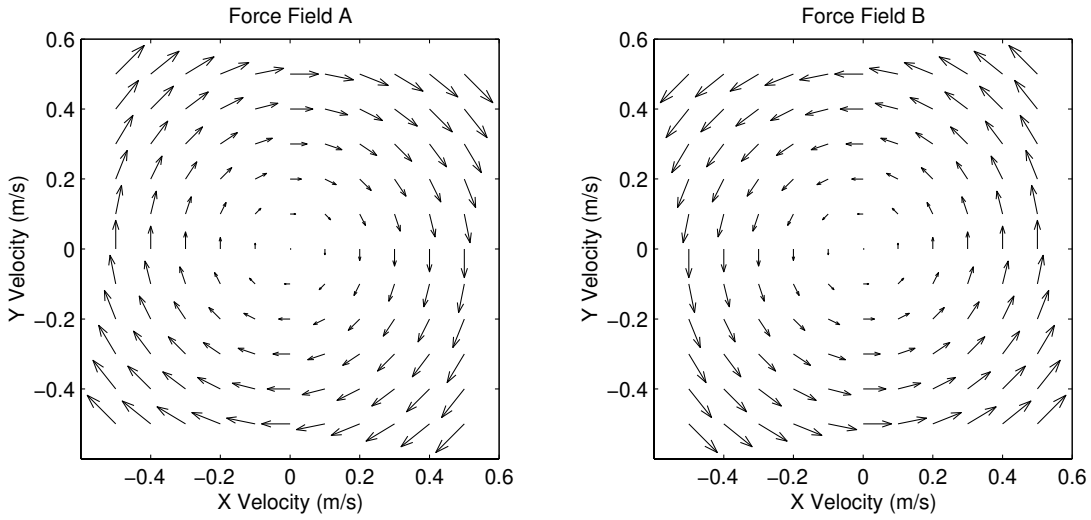

Figure 5.1: Illustration of Viscous Curl Force-Field. The arrows in each plot represent the force vectors applied as a function of X and Y velocity.

this force-field produces no force if there is no motion. This type of force field generally has the effect of perturbing trajectories laterally into a hooking motion.

Task

Subjects made quick reaching movements to targets spaced 10cm away while grasping a lightweight two-joint manipulandum. The 1cm square targets and a small cursor (4mm) indicating the subject's hand position were displayed on a vertically-oriented computer monitor in front of the subject. The robotic manipulandum was used to apply the force-field and measure the position and velocity during the task. Position and velocity data from the manipulandum were sampled at 100Hz and the computer monitor was refreshed 60 times per second.

The experiment was divided into short sets of 96 or 100 movements. Sets generally took 6-8 minutes to complete. The first four sets were performed in the null

field with the robot's motors effectively turned off. The next three to four sets were generally performed in force-field A, followed by 1 to 4 sets in force-field B, the opposite of A. In null field sets, all movements were made without external forces, but in force-field sets the force field was turned off occasionally for an entire movement. These movements were called after effects. They occurred at random about one in every six movements, and they showed how motor output was evolving during force-field exposure.

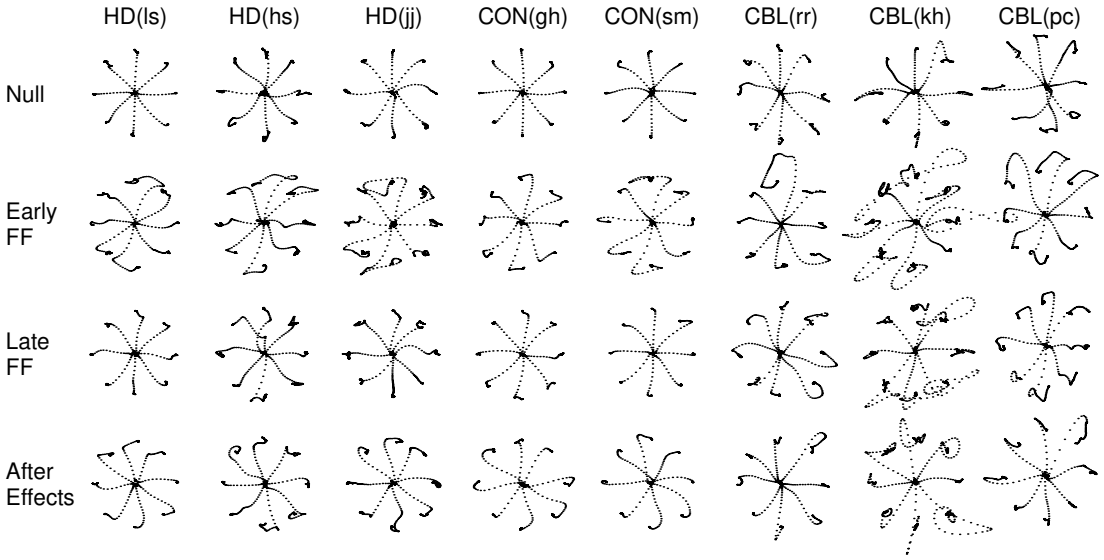

Figure 5.3: Hands During Force-Field Learning Task. Subjects groups: **HD** – symptomatic HD **CON** – controls, **CBL** – cerebellar dysfunction. Movement groupings: **Null** - Last movement in each direction before onset of force-field exposure. **Early FF** - First movement in each direction after onset of force-field exposure. **Late FF** - Last movement in each direction in third set after onset of force-field exposure. **After Effects** - Last after effect movement in each direction in third set after onset of force-field exposure.

Results

Typical Movement Trajectories

The hand paths of movement trajectories of several subjects in each group before and after force-field exposure are shown in Figure 3. Exposure to the force-field substantially perturbed the movements of all subjects as shown in the second row of Figure 3. Controls were able to learn to predictively cancel the force-field with practice. Exposure to the force-field substantially perturbed their movements (see Figure 3, 2nd row), but their movements late in the force-field are nearly straight (Figure 3, 3rd row) compared to initial exposure (Figure 3, 1st row), and the after effects they produce (Figure 3, 4th row) closely mirror the errors made on initial exposure to the force-field.

Subjects with Huntington's disease also appear to learn the force field well. HD subjects show some difficulty stopping their movements cleanly as discussed in chapter 2, but the initial aiming of their movements is quite similar to that of control subjects. Like controls, exposure to the force-field substantially perturbed their movements, but their movements late in the force-field are quite straight compared to initial exposure, and their after effect movements closely mirror the force-field induced errors made upon initial exposure.

Subjects with cerebellar dysfunction do not appear to learn the force-field well. Their unperturbed null movements appear more irregular than movements made by subjects in the other groups, but like HD and control subjects, their movement are perturbed substantially in the clockwise direction by the force-field. Unlike the other groups, however, cerebellar subjects did not move much straighter late in force-field exposure than upon initial exposure, and their after-effect movements do not show signs that these subjects learned to predictively cancel the force-field – the after effects did not have errors that mirrored the errors produced by the force-field upon initial exposure.

Time Course of Directional Errors

Figures 4 through 7 show the time course of learning during the force-field experiment for individual subjects in all groups. The average error in motion direction at a time point 300ms after movement onset is plotted as a learning metric. As the example hand path trajectories shown in Figure 3 suggested, the errors in motion direction for movements in Field A improve substantially with practice for control subjects. The errors in motion direction for after effect movements is opposite to that of the errors induced by

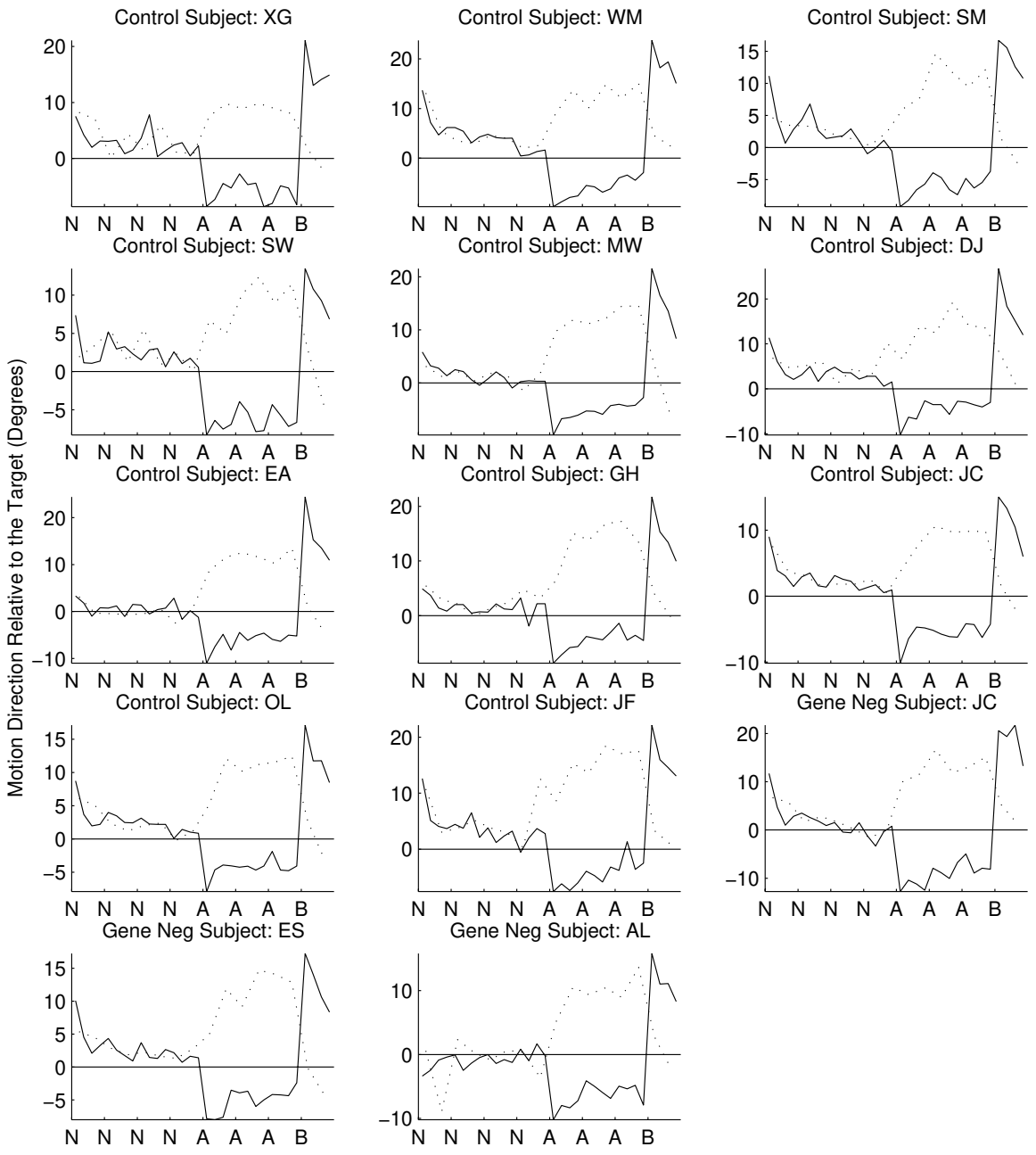

Figure 5.4: Time Course of Angular Aiming Errors During Force-Field Learning for Individual Control Subjects. Averages of angular aiming errors as displayed for fielded movements (solid lines) and after effect movements (dotted lines). Bins of 21 consecutive fielded movements and 8 consecutive after effect movements are used for averaging. In the null field sets, there are no fielded or after effect mvts, so the trajectories of the movement numbers which correspond to fielded or after effect movements in the force-field sets are used for comparison. The x-axis labels represent the type of force-field applied. N - Null Field, A - Field A (clockwise viscous curl) , B – Field B (counterclockwise viscous curl).

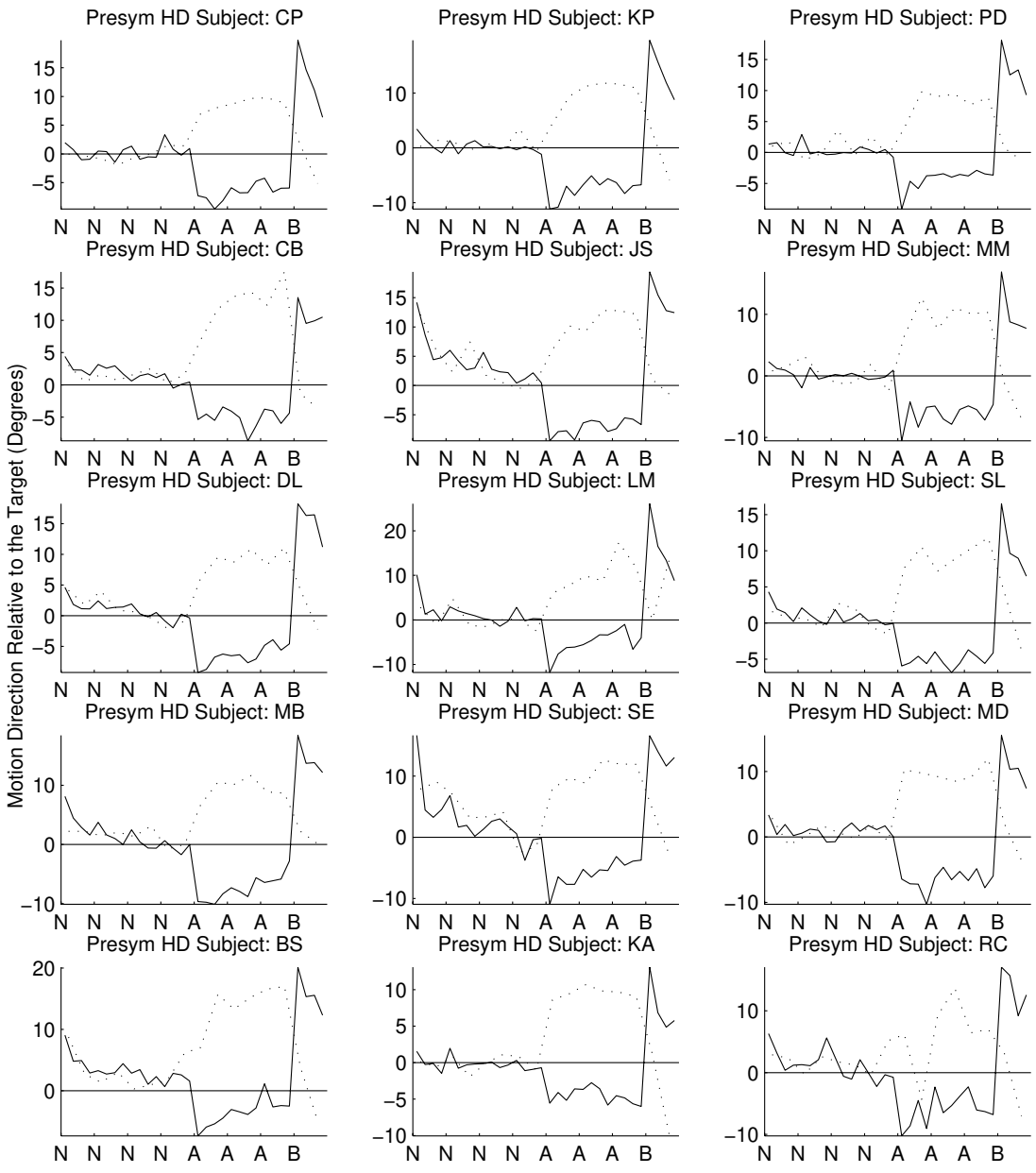

Figure 5.5: Time Course of Angular Aiming Errors During Force-Field Learning for Individual Presymptomatic HD Subjects. Averages of angular aiming errors as displayed for fielded movements (solid lines) and after effect movements (dotted lines). Bins of 21 consecutive fielded movements and 8 consecutive after effect movements are used for averaging. In the null field sets, there are no fielded or after effect movements so the trajectories of the movement numbers which correspond to fielded or after effect movements in the force-field sets are used for comparison. The x-axis labels represent the type of force-field applied. N - Null Field, A - Field A (clockwise viscous curl) , B – Field B (counterclockwise viscous curl).

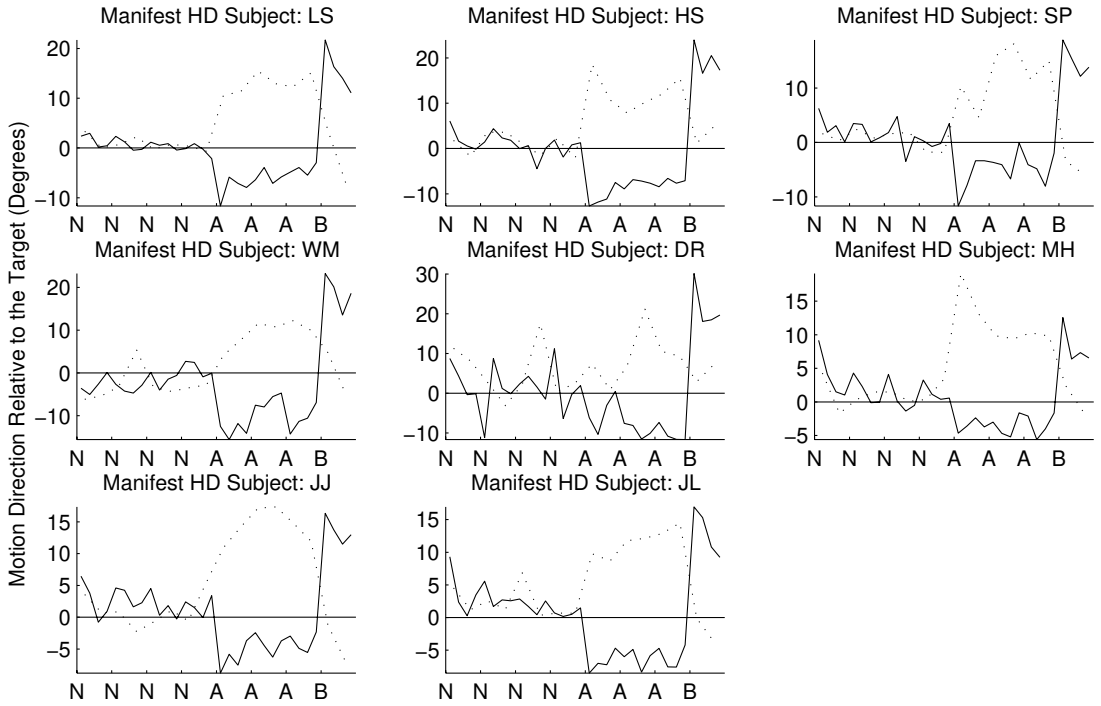

Figure 5.6: Time Course of Angular Aiming Errors During Force-Field Learning for Individual Subjects with Manifest HD. Averages of angular aiming errors as displayed for fielded movements (solid lines) and after effect movements (dotted lines). Bins of 21 consecutive fielded movements and 8 consecutive after effect movements are used for averaging. In the null field sets, there are no fielded or after effect movements so the trajectories of the movement numbers which correspond to fielded or after effect movements in the force-field sets are used for comparison. The x-axis labels represent the type of force-field applied. N - Null Field, A - Field A (clockwise viscous curl) , B – Field B (counterclockwise viscous curl).

The force-field, and the size of after effects increase with practice. By the third set in Field A, the magnitude of the error in motion direction for after effect movements is generally at least double or triple the error magnitude for fielded movements. The ratio between the size of aiming errors in after effect and fielded is a good indicator of the fraction of the force-field predictively learned. The larger this ratio the more complete the learning. For example, if the force-field was half learned, then the after-effect and fielded movements would be of the same magnitude, but opposite in direction. When the force-field is switched from Field A to Field B in the eighth set, extremely large aiming errors

are produced. Field B is opposite Field A, so switching suddenly between the two produces a force-field change of double the magnitude of either field. This large change in force-field produces large aiming errors for fielded movements, but these errors decline rapidly as control subjects learn the new field. Paralleling these changes in fielded movements, are large changes in after effects. When Field A is switched to Field B, the after effects change rapidly as they switch polarity and begin to become appropriate for Field B by displaying clockwise errors instead of counterclockwise errors.

Subjects presymptomatic and symptomatic for HD display very similar behavior to controls. The errors they display on fielded movements decrease with training, and they display large errors on after effects movements after force-field training, indicating that these subjects learn to predictively compensate for the force-field. Like control subjects, by the 2nd and 3rd sets of training in Field A, both groups of HD subjects produce after effect errors that are generally much larger in magnitude than errors in fielded movements. This indicates good learning of Field A. When the force-field is switched from A to B, signs of rapid learning can be seen in both the after effect and fielded movements, just as with the control subjects.

Subjects with cerebellar degeneration appear to display markedly impaired learning. Fielded movements do not appear to improve substantially with practice, and aiming errors on after effect movements, representative of force-field learning, are small, and do not change substantially from their pre-exposure (null field) levels. When the force-field is switched from A to B, subjects with cerebellar degeneration do not display the signs of the rapid learning apparent in both the after effect and fielded movements of control subjects and HD subjects. In fact, several of the cerebellar degeneration subjects

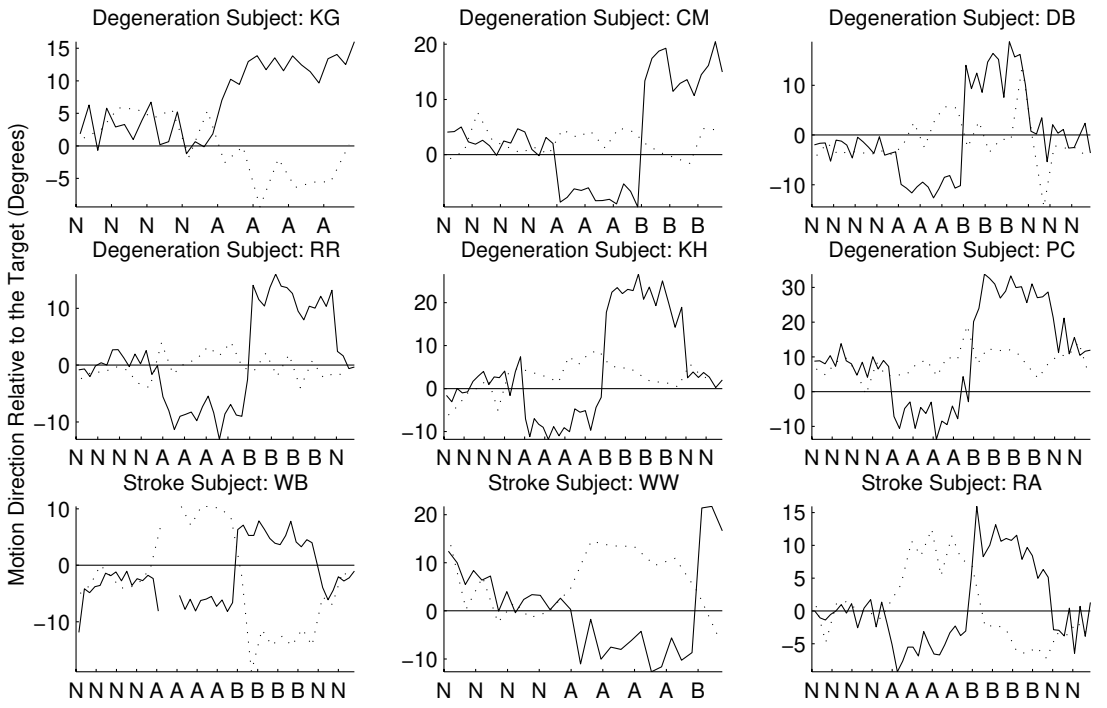

Figure 5.7: Time Course of Angular Aiming Errors During Force-Field Learning for Individual Subjects with Cerebellar dysfunction. Note that the top six suffered from global cerebellar degeneration while the bottom Averages of angular aiming errors as displayed for fielded movements (solid lines) and after effect movements (dotted lines). Bins of 21 consecutive fielded movements and 8 consecutive after effect movements are used for averaging. In the null field sets, there are no fielded or after effect movements so the trajectories of the movement numbers which correspond to fielded or after effect movements in the force-field sets are used for comparison. The x-axis labels represent the type of force-field applied. N - Null Field, A - Field A (clockwise viscous curl) , B – Field B (counterclockwise viscous curl).

(for example CM, RR, and PC) display no signs of predictive, feedforward force-field learning. The errors they display during fielded movements are large, and their after effects do not change from null field movements. In contrast, the three subjects who had experienced strokes in the cerebellum displayed signs of normal predictive force-field learning. After training in each force-field, aiming errors on after effects become large compared to errors on fielded movements, indicating much better predictive force-field learning than displayed by cerebellar degeneration subjects.

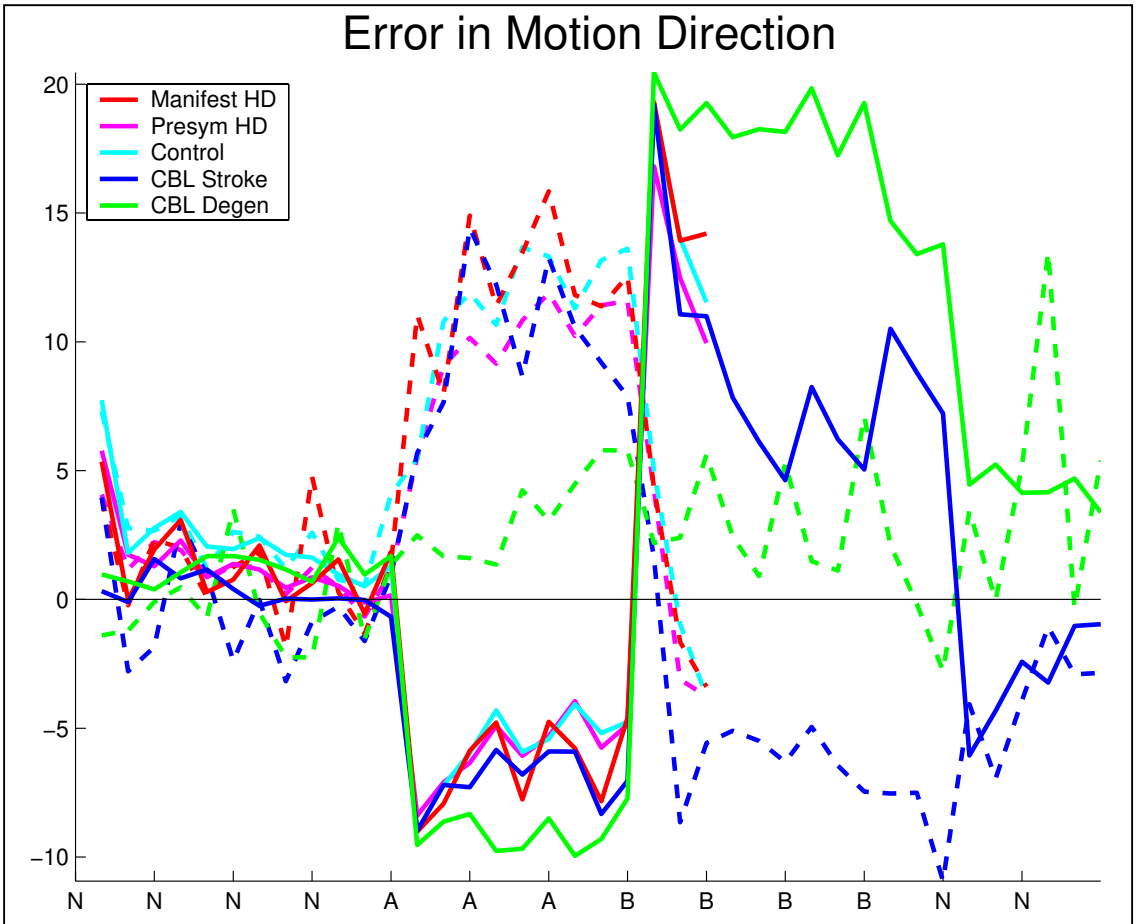

Figure 5.8: Time Course of Aiming Errors Compared Across Subject Groups. Aiming errors are represented by the angles between the net direction of movement during the first 300ms motion onset and the target direction for each trial. These errors are binned into 3 groups per set (there are about 28 fielded movements and 5 after effects per bin) and averaged across subjects in each group. Solid lines represent fielded movements and dashed lines represent after effect trials. In the null field sets, there were no true fielded movements or after effects, but the movement number corresponding to these during the force-field sets were designated as fielded or after effect trials for the sake of comparison.

The average time course of aiming errors during force-field learning for each subject group is shown in Figure 8. Note that cerebellar subjects were divided into stroke and degeneration groups. Comparison of the mean time course of learning between the different groups, bears out the trends seen with the individual subjects in each group. Subjects with manifest HD and asymptomatic gene positive subjects display quite normal learning of the force-field. Both groups learn the force-field well and display large after

effects, and the time course of both their fielded and after effect movements closely parallel normal behavior. Note that although aiming errors in the force field improve, they do not quite return to null field levels even for control subjects even though performance seems to asymptote, indicating that the adaptation is not complete. This could be because the learning processes that we observe on the time-scale of our task cannot only fully compensate for the force-field dynamics, or alternatively, because of the presence of occasional after-effect trials which make the force field environment somewhat non-stationary. The presence of after effects prevents full learning of the force-field, because each after effect movement causes some degree of local unlearning**Error! Bookmark not defined.**. However, fielded trials predominate over after effects in a 5:1 ratio so the "average" force-field is 5/6 of the imposed field, so a loose steady state is set in during normal learning that is biased toward force-field appropriate behavior. This is evidenced by the fact that aiming errors on fielded movements are substantially less than errors on after effect trials after force-field training.

In contrast to HD subject groups, subjects with cerebellar degeneration as a group display markedly worse force-field learning than controls. Their after effects are much smaller than the after effects displayed by normal and HD subjects, and their fielded movements improve to a smaller degree than the other groups. Quite oppositely, the small group of cerebellar stroke patients that we studied displayed substantially normal behavior in the time course of their aiming errors.

A more quantitative analysis of several properties of the time course of aiming errors during force-field learning is presented in Figure 9. Subjects with cerebellar degeneration display smaller after effects and larger errors for fielded movements late in

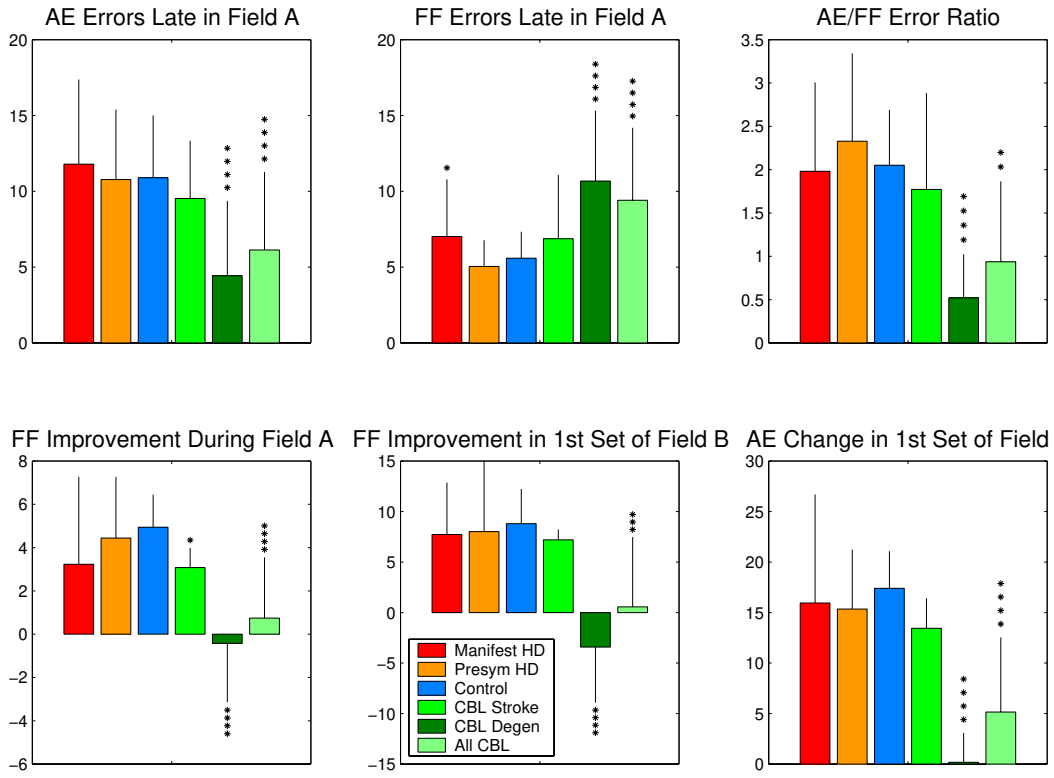

Figure 5.9: Quantitative Comparisons Force-Field Learning. All comparisons are based on aiming errors measured at 300ms after movement onset. The units for all plots, except AE/FF Ratio, which is dimensionless, are degrees. For clarity in presentation, the signs of errors for fielded movements have been changed for all groups. AE – after effect movements. FF – fielded movements. Of the nine subjects with cerebellar dysfunction, six had global degeneration and three had experienced strokes. Top left: Average errors for after effects in the third set of Field A. Top Center: Average errors for fielded movements in the third set of Field A. Top Right: Ratio between errors on AE and FF movements in the third set of Field A. Bottom Left: FF improvement from the first third of the first set to the last third of the third set in Field A. Bottom Center: FF improvement from the first third to the last third of the first set in Field B. Bottom Right: Change in AE movements from the first third to the last third of the first set in Field B. * p<0.05. ** p<0.01. *** p<0.001. **** p<0.0001.

Field A than controls ($p<0.0001$ in both cases). The AE/FF ratio, a metric of force-field learning, is also increased ($p<0.0001$). This ratio should be infinitely large for perfect force-field learning, and is 4 times greater on average for normal and HD subjects than subjects with cerebellar degeneration. Cerebellar degeneration subjects also fail to show improvement of fielded movements in Fields A or B, or change in after effects in field B.

These “improvements” are all significantly less than those of controls ($p<0.0001$ in all three cases).

Cerebellar stroke patients displayed much more normal performance than did the subjects with cerebellar degeneration. Force-field improvement during field A was the only performance measure on which they displayed significantly worse behavior than controls ($p<0.05$). Keep in mind however that the group of cerebellar stroke patients was by far the smallest subject group ($n=3$), so the statistical power of these comparisons and the confidence in population representative performance was smallest for this group. Presymptomatic HD subjects display performance that closely mirrors that of control subjects on all of these learning metrics. Subjects with manifest HD also display substantially normal behavior, but show a small increase in fielded movement aiming errors late in field A ($p<0.05$), despite normal after effects at this point.

Additional Characteristics of Motor Performance During Force-Field Learning

Several movement characteristics besides aiming errors can be used to assess motor performance during force-field learning. Figure 10 illustrates the time course of changes in movement time, path length, and movement regularity for fielded movements during force-field learning. These performance indices are plotted on logarithmic scales for clarity. The most striking feature of these plots is that cerebellar degeneration subjects fail to substantially improve their performance in any force-field, whereas the other groups show clear improvement in all fields for all performance measures studied. When a new force-field is introduced, performance suddenly plunges for fielded movements, then slowly improves as subjects learn the field.

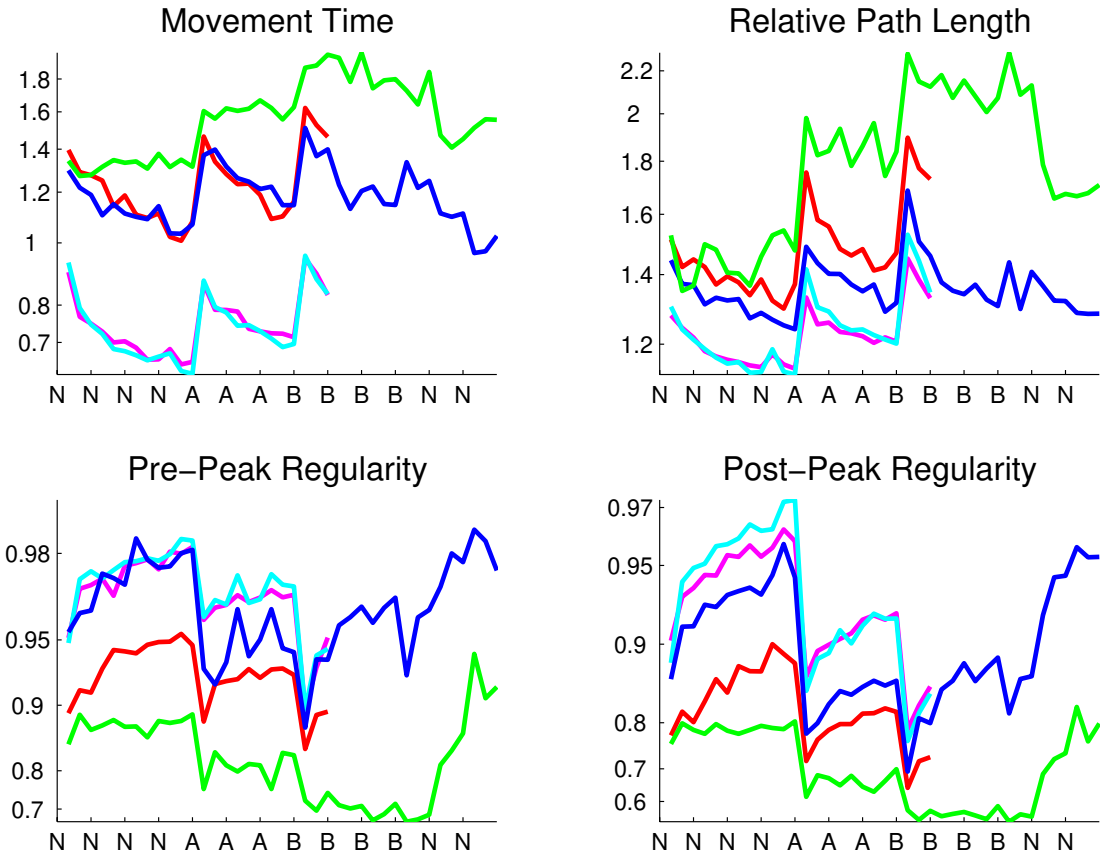

Figure 5.10: Time Course of Movement Characteristics During Force-Field Learning. These performance indices are plotted on logarithmic scales for clarity. Movement time is the time between initial velocity threshold crossing, and the final crossing before the velocity remained sub-threshold for 200ms. Subjects were rewarded on trial with movement times of 600 +/- 70ms. Relative path length is defined as the ratio between total path length and the net distance traveled for each trial. This ratio is minimal at unity for perfectly straight paths. Movement regularity was assessed by the correlation coefficient between the velocity profile of each trial and the trial in the fourth null set with highest average correlation to all the other movements in that set. Higher correlation between trials indicates greater similarity between the shapes of their velocity profiles. Perfect correlation yields a correlation coefficient of unity (one). Movements were split at the peak speed point and the regularity of the pre-peak and post-peak segments were assessed separately. See figure 8 for the subject group color codes.

Note that because of the log scaling, constant performance increments on each plot are multiplicative. So if two groups are offset from one another but display parallel learning curves, then they possess the same fractional improvement in their learning. Although subjects with manifest HD display impaired performance compared to controls

on all of these performance measures, the pattern of disturbance and learning/recovery appears quite normal. HD and control subjects display parallel learning curves in each panel, indicating quite similar fractional improvement on all four of these performance measures. This suggests that learning processes crucial for learning on our force-field task are substantially spared in HD. The capacity for adaptation that HD subjects display on this task contrasts remarkably with the striking learning deficits that cerebellar degeneration subjects exhibit, suggesting that the cerebellum is crucial for the trial-to-trial motor learning required to form a functional internal model of the force-field to correct force-field induced errors.

Both the cerebellum and striatum have been implicated as neural structures which contribute to motor learning. The learning deficits that we find in cerebellar subjects adds the learning of physical dynamics to the set of deficits in error-dependent motor learning that are associated with cerebellar damage. This set includes the learning of visuomotor remappings[65,66,67,68], adaptation of the vestibulo-ocular reflex[69], and classical conditioning[70,71]. Taken together, these findings suggest that the cerebellum is crucial for the modification of motor output to reduce consistently occurring errors.

It has also been suggested that habit formation and skill learning in general[72,73,74,75] or more specifically open-loop skill learning[37] is disturbed in HD and with striatal dysfunction. Our results suggest that these hypotheses are not correct. Because sensorimotor feedback delays exist[32,33], the first 200-300ms of movement is open-loop. Data taken from this open loop period in the force-field task (figures 2, 3 & 4c) show apparently normal learning by HD subjects indicating that skill learning in general and

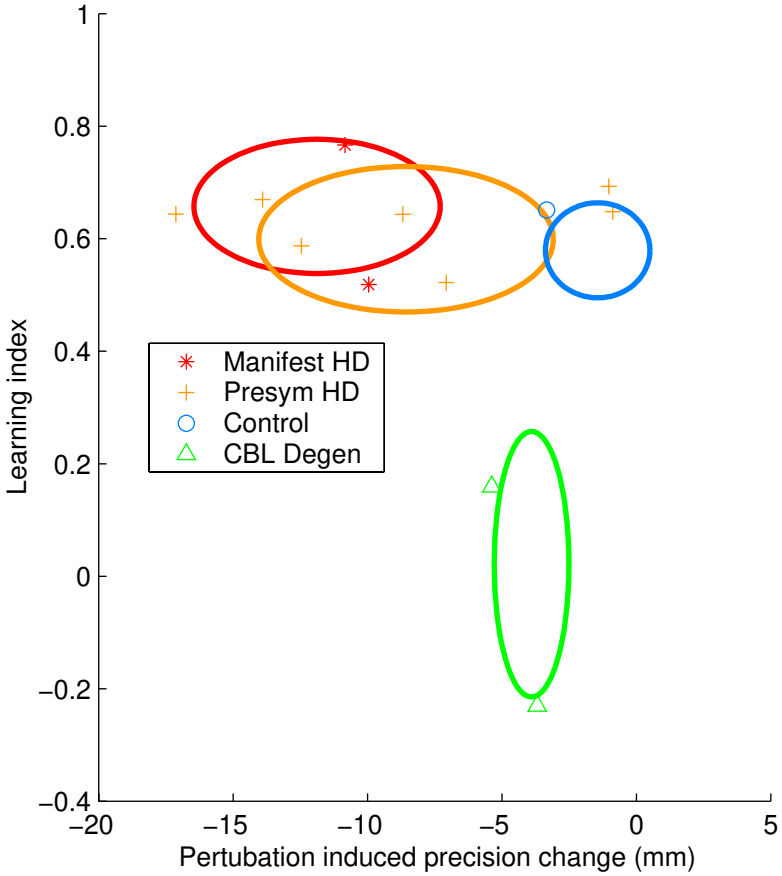

Figure 5.11 Comparison of error-dependent motor learning and online error correction. Measures of motor learning and online error correction are plotted against one another. Perturbation induced endpoint precision change, defined as negative the increase in endpoint variability when randomly occurring force pulse perturbations are applied during movement versus when these perturbations were withheld, is used as a measure of online error correction.. The learning index after the first set of trials in Field A is used as a measure of motor learning. The ellipses represent the pooled data for each subject group across both experiments. The ellipse's axes signify the mean ± standard deviation for that group's data. Only a few subjects participated in both experiments. Their results are plotted as symbols of the appropriate color. Note that normal subjects display good performance in both tasks, cerebellar degeneration patients show intact online error correction despite poor motor learning performance, while HD subjects show the opposite: normal motor learning ability but disturbed online error correction.

open-loop skill learning in particular can be well-preserved in both symptomatic and presymptomatic carriers of the HD gene.

Figure 11 presents a summary of the combined data from our studies of trial-to-trial and online[78] error correction. We created a learning index as a metric of force-field

learning to indicate the fraction of the force-field compensated at a given point in training. This index is 0 for null field appropriate movements and 1 for movements fully appropriate for the force-field (see Methods). The learning index after one set of force-field training is used here as a metric of trial-to-trial motor learning. The change in endpoint precision when unexpected perturbations are applied during movement without visual feedback is used as a performance measure for online error correction (see Chapter 4, figures 10-14). Control subjects display good performance on measures of both online and trial-to-trial error correction. In contrast, both groups of HD subjects display intact trial-to-trial learning but disturbed online error correction, while subjects with cerebellar degeneration display dysfunctional trial-to-trial learning but intact online error correction, suggesting a dissociation between these two types of sensory error processing.

Several lines of evidence point to disordered sensory feedback as a manifestation of Huntington's disease. Reaction times to both auditory and visual stimuli are slowed even early in the disease course[8,76]. The cortically-mediated[43,44,45] long-latency component of the stretch reflex responses is reduced or absent in HD patients[25,46,47], and electrical potentials evoked in somatosensory cortex by peripheral nerve stimulation are reduced throughout the course of HD[24,26]. Additionally, modulation of manual grip forces when grasping objects has also been found to be disturbed in HD[48,77]. Taken together with recent evidence that online error correction, also known as error feedback control, is disturbed long before clinical onset of HD, it would appear that a generalized dysfunction in the processing of sensory information occurs in HD[77].

The present study demonstrates that the processing of sensory information that subserves the modification of motor commands in order to reduce consistently occurring

motor errors from one trial to the next is substantially intact in HD. This suggests that the processing of sensory information is not generally disturbed in HD, but that the sensory processing deficits in HD may be limited to the online utilization of sensory information in movement. This would suggest the existence of two separate streams of sensory information: one stream for the online correction and modification of motor actions and another for use in shaping the plasticity of motor commands from one trial to the next. The first stream is susceptible to the pathology in HD but substantially spared by cerebellar damage while the second stream is spared in HD but disrupted by cerebellar damage.

Chapter 6 - Discussion

In this thesis we showed that motor signs of error feedback control dysfunction were prominent through a great deal of the course of Huntington's disease[78]. In making simple reaching movements, HD subjects displayed dysfunctional reactions to both self-generated errors and errors produced by external perturbations. Since the pathology of HD is believed to be restricted to the basal ganglia early in the disease course, our findings suggest that the basal ganglia take part in or have substantial influence on the pathways through which online error correcting responses are generated.

Remarkably, the increased end-movement jerk associated with error feedback control dysfunction in our task was elevated in subjects even more than 7-10 years from expected disease onset. In fact, a majority of the presymptomatic subjects we studied displayed end-movement jerk that was elevated above the normal range. This is striking, because in previous study, the existence of performance deficits on tests of behavioral function prior to the clinical onset of HD was controversial. Assessments of motor, cognitive, or psychiatric function in HD had revealed only subtle deficits in presymptomatic subject groups[6,7,8,76] (Siemers, 2k) if any[9,10,11]. Even when changes had been detected, they were not sufficiently specific to permit discrimination between mutation positive and mutation negative individuals, or even reliable identification of people with early stage manifest HD. In contrast, functional imaging of the basal ganglia reveals low glucose metabolism in about two thirds of asymptomatic at risk individuals[12,13,14,15] and basal ganglia volumes may be reduced years before clinical onset[4], suggesting that brain pathology may substantially lead manifestation of the

behavioral dysfunction previously studied. In contrast, the end-movement jerk measure we developed provides clear evidence of disturbed motor function very early in the pre-clinical course of HD, suggesting the existence of a direct behavioral correlate to the early brain pathology in HD.

Interestingly, despite the clear deficit in online error correction we demonstrate in HD, the trial to trial correction of error in feedforward motor learning appears quite normal late into the disease course, demonstrating that the sensory processing of error signals is not universally disturbed. Note that the term "error correction", that we have used extensively in this thesis, can be quite broad, and it is important to understand the differences between various types of error correction. Two distinctly different types of processes can operate to make use of sensory information to correct errors in discrete tasks such as point to point reaching. The first is online error correction, where errors are compensated “in flight”, and the second is trial-to-trial learning, in which errors from one trial influence the motor output on subsequent trials to prevent similar errors from occurring. In the second chapter of this thesis we analyzed online error correction, known to control systems engineers as error feedback control, and found this process markedly disturbed throughout the course of HD. This process makes nearly immediate use of real-time sensory information to compensate for errors in an ongoing movement. The sensorimotor processing, transmission, and actuating delays are large compared to the frequency components present in our movements[79]. For example, the arm movements in our task could be almost halfway over before compensatory motion could be generated from the first sensory information acquired after movement onset. Because of these long sensorimotor delays, a simple comparison of the sensory feedback with the desired

behavior and production of a proportional response would be intrinsically unstable, and could lead to wild oscillations in arm motion. Online error correction during movement may, therefore, present a formidable challenge to the central nervous system, and whatever ability we have to accomplish this process seems remarkable. Delay induced instabilities can be overcome in an error feedback control system by the inclusion of a predictive component known as a forward model of system dynamics. A forward model computes a prediction of current motion state based on the delayed sensory assessment of motion state and knowledge of how efferent motor commands should affect the physical dynamics of motion during the time period since the delayed sensory assessment has occurred. Neurons in the basal ganglia have been shown to predict reward[42] and predictive capacity may be a general feature of some basal ganglia structures. The main output of the basal ganglia modulates the action of the thalamus, which relays sensory information to the cortex. This information stream is likely to participate in error feedback control, thus the error correction process may be modulated by the basal ganglia, although the mechanism through which this occurs, including whether the predictive capacity of basal ganglia structures is involved, is not yet understood.

The use of error information in trial-to-trial motor learning is not addressed in our studies of error feedback control, but the work of Brainard, Solis, and Doupe mentioned by Dr. Lawrence strongly implicates the brain area analogous to the basal ganglia as crucial for this type of learning in the zebra finch songbird[80,81]. In recent years trial-to-trial procedural learning has received considerable attention. When consistent force[21,61,62,63] or visuo-spatial[63,31] perturbations are made during movements, healthy subjects learn to compensate for these perturbations such that, with practice, they

generally make movements that resemble their original unperturbed movements. If the perturbations are suddenly withdrawn, after-effect movements are produced with errors that mirror the original perturbation-induced errors. Learning during these experiments is believed to occur because the brain uses the errors experienced during a movement to adjust motor output on subsequent movements such that the error between the actual and desired trajectories of motion is reduced[64].

Although online error compensation appears substantially disturbed in HD, motor learning studies on HD patients have revealed that error signal dependent trial-to-trial learning is not uniformly disturbed. Individuals symptomatic for HD show intact learning on a mirror-tracing task[37], but impaired learning on rotary pursuit tasks[37,38]. Rotary pursuit involves long continuous movements, which are largely under closed-loop feedback control. Learning to perform this task requires the ability to modify parameters of an on-line feedback control system. In contrast, mirror tracing of polygons involves multiple short, discrete movements, which rely more heavily on open-loop feedforward control processes. Performing this task well requires trial-to-trial learning that modifies the commands generated for each movement segment. These segments are largely under feedforward control. Therefore, in HD, motor tasks that are largely under feedforward control (e.g., mirror tracing) appear to benefit from trial-to-trial pattern of errors, but tasks that largely stress online feedback control (e.g., rotary pursuit) show an abnormally low sensitivity to the trial-to-trial errors.

The results from the motor learning study in this thesis support this hypothesis. When we studied learning to make point-to-point reaching movements in a viscous curl force field, a task that strongly depends on feedforward predictive processes[21], we found

that neither presymptomatic nor symptomatic HD subjects were impaired. Both the rates of learning and the magnitude of the learning related effects on performance of this error-correcting task were quite normal even in subjects with manifest HD. In contrast, cerebellar patients were markedly impaired in learning this task as a group, and many showed no signs of learning. These results, taken together with the previously mentioned motor learning studies in HD patients, demonstrate that information from motor error signals can in some cases be used to promote normal learning in Huntington's disease while in other cases error signal dependent motor learning appears to be disturbed. This suggests that the type of the motor learning task, i.e., whether the task largely requires modification of feedforward predictive motor commands or instead mainly depends on the adaptation of on-line, feedback dependent motor responses, and not the general involvement of error signals or error correction may be the key factor predicting the task performance of HD subjects. To understand the role that the basal ganglia play in motor control and learning, more study is needed to clearly delineate what types of learning are impaired and intact in HD and other diseases of basal ganglia function. The performance of cerebellar patients on the force field learning task demonstrates that the cerebellum is involved in learning physical dynamics in addition to visuomotor transformations, and classically conditioned responses.

When movements were perturbed but visual feedback withheld, we found that the variability in the distributions of endpoint error was much more sensitive to perturbation for presymptomatic and symptomatic HD subjects than controls or subjects with cerebellar dysfunction. Interestingly, subjects with manifest HD showed abnormal increases in endpoint variability despite lack of significant changes in endpoint bias. The

spread of the endpoint error distributions increased significantly when perturbations were applied for even non-HD subjects. However when endpoint error distributions are aligned to perturbation direction, non-HD subjects only display increases in endpoint variability along the axis on which the perturbing force pulse was applied, whereas both HD subject groups display similarly large increases in spread along axes both in and orthogonal to the perturbation direction. This suggests a mismatch between the direction of perturbation and the direction of response leading to a spillover of feedback response onto the axis orthogonal to perturbation delivery. This spillover is very strong in HD subjects but appears absent in controls and subjects with cerebellar dysfunction. These data suggest that the error feedback control dysfunction in HD is not simply a the result of an overall net increase or decrease in feedback gain or even a mixture of these. Rather, the error feedback control dysfunction that we demonstrate is a more generalized disturbance in the error feedback control process. It is a disturbance that appears to depend on the overall magnitude of error but not its direction or which muscle groups are involved. This disturbance is capable of producing inappropriate responses in directions without large errors only when large errors do exist in other directions. The strong dependence of the extent of disturbance on error magnitude, implies that error magnitude is correctly computed in HD suggesting that a raw sensory processing deficit does not exist. If a raw sensory processing deficit did exist, motor error would not be correctly computed so strong modulation of error response by real error magnitude could not occur.

Lawrence draws interesting parallels between dysfunctional online error compensation in our motor task, and the exaggerated compensatory behavior

characteristic of obsessive compulsive disorder (OCD) (Lawrence, 2000). In OCD, errors (real or imagined, such as one's hands being dirty), draw an exaggerated response, such as compulsive washing. This is quite similar to the inappropriate, often exaggerated, responses that we found to motor errors in HD, whether these errors were extrinsically or self-generated. As Dr. Lawrence pointed out, basal ganglia dysfunction is believed to underlie OCD, and so patients with OCD may manifest some cognitive parallel of the error feedback control dysfunction in HD, hinting that the basal ganglia may play an important role in online error compensation for both lower level motor as well as higher level cognitive processes.

Obsessive compulsive behaviors occur both in Tourette patients and their family members[82], and there is likely a shared genetic basis between Gilles de la Tourette syndrome and some cases of obsessive compulsive behavior[83,84]. Tourette syndrome is characterized by the occurrence of verbal and other involuntary motor tics. The vocal tics are generally short comprehensible expressions which often include swear words. Swear words and other common complex vocal tic expressions[85] such as "shut up", "stop that", and "okay honey" can be classified as interjectional, responsive, or emotional speech[86,87,88] as opposed to propositional speech which makes up the majority of verbal discourse. This division of speech bears striking resemblance to the feedforward / feedback partitioning of motor control processes that we used to study the motor disorder in HD. Evidence that propositional and nonpropositional speech are generated differently in the brain, comes from studies with aphasic patients. These patients may lose the ability for propositional speech entirely, or this speech may be labored and misarticulated. Meanwhile, nonpropositional speech can be preserved, well articulated,

and situation-appropriate in these patients. The preserved utterances in aphasia often include swear words, "yes" / "no", and counting. Further evidence that the verbal tics may indeed be "feedback" as opposed to "feedforward" in nature, include findings that the premovement EEG potential seen in voluntary speech is absent during verbal tics[89], and the assertion that verbal tics occur more frequently at pauses in speech and at points of high indecision than at other times[90,91]. This closely parallels our findings in Huntington's disease that high end-movement jerkiness is more likely to occur during trials with larger initial errors in motion. The pathology of Tourette's syndrome is not yet understood, but it is believed to involve the basal ganglia[92,93], and neurotransmitters involved in basal ganglia function such as dopamine[94]. This suggests that Tourette syndrome, obsessive compulsive disorder, and Huntington's disease may all be alternate manifestations of dysfunctional error feedback compensatory processes caused by disease affecting basal ganglia function.

References

[1] The Huntington's Disease Collaborative Research Group. A novel gene containing a trinucleotide repeat that is expanded and unstable on Huntington's disease chromosomes *Cell* 72:6, 971-83 (1993).

[2] Folstein, S.E. *Huntington's Disease a Disorder of Families* (Johns Hopkins University Press, Baltimore, 1989).

[3] Aylward, E.H. et al. Longitudinal Change in Basal Ganglia Volume in Patients with Huntington's Disease. *Neurology* 48:2, 394-9 (1997).

[4] Aylward, E.H. et al. Basal Ganglia Volume and Proximity to Onset in Presymptomatic Huntington Disease. *Arch Neurol* 53:12, 1293-6 (1996).

[5] Brandt, J et al. Clinical correlates of dementia and disability in Huntington's disease. *J Clin Neuropsychol* 6:4, 401-12 (1984)

[6] Foroud, T. et al. Cognitive scores in carriers of Huntington's disease gene compared to noncarriers. *Ann Neurol* 37:5, 657-64 (1995).

[7] de Boo, G.M. et al. Early cognitive and motor symptoms in identified carriers of the gene for Huntington disease. *Arch Neurol* 54:11, 1353-7 (1997).

[8] Siemers, E. et al. Motor changes in presymptomatic Huntington disease gene carriers. *Arch Neurol* 53:6, 487-92 (1996),

[9] Rothlind, J.C., Brandt, J., Zee, D., Codori, A.M., & Folstein, S. Unimpaired verbal memory and oculomotor control in asymptomatic adults with the genetic marker for Huntington's disease [published erratum appears in Arch Neurol 1994 Mar;51(3):268] *Arch Neurol* 50:8, 799-802 (1993).

[10] Blackmore, L., Simpson, S.A., & Crawford, J.R. Cognitive performance in UK sample of presymptomatic people carrying the gene for Huntington's disease. *J Med Genet* 32:5, 358-62 (1995).

[11] Strauss, M.E. & Brandt, J. Are there neuropsychologic manifestations of the gene for Huntington's disease in asymptomatic, at-risk individuals? *Arch Neurol* 47:8, 905-8 (1990).

[12] Kuwert, T. et al. Striatal glucose consumption in chorea-free subjects at risk of Huntington's disease [see comments] *J Neurol* 241:1, 31-6 (1993).

[13] Hayden, M.R. et al. The Combined Use of Positron Emission Tomography and DNA Polymorphisms for Preclinical Detection of Huntington's Disease. *Neurology* 37:9, 1441-7 (1987).

[14] Mazziotta, J.C. et al. Reduced Cerebral Glucose Metabolism in Asymptomatic Subjects at Risk for Huntington's Disease. *N Engl J Med* 316:7, 357-62 (1987).

[15] Kuwert, T. et al. Comparison of Somatosensory Evoked Potentials with Striatal Glucose Consumption Measured by Positron Emission Tomography in the Early Diagnosis of Huntington's Disease. *Mov Disord* 8:1, 98-106 (1993).

[16] Schweighofer, N, Arbib, MA, & Kawato, M Role of the cerebellum in reaching movements in humans. I. Distributed inverse dynamics control. *Eur J Neurosci* 10:1, 86-94 (1998 Jan),

[17] Doyon, J et al. Role of the striatum, cerebellum, and frontal lobes in the learning of a visuomotor sequence. *Brain Cogn* 34:2, 218-45 (1997 Jul),

[18] Topka, H, Massaquoi, SG, Benda, N, & Hallett, M Motor skill learning in patients with cerebellar degeneration. *J Neurol Sci* 158:2, 164-72 (1998 Jun 30),

[19] Martin, TA, Keating, JG, Goodkin, HP, Bastian, AJ, & Thach, WT Throwing while looking through prisms. I. Focal olivocerebellar lesions impair adaptation. *Brain* 119 (Pt 4) (1996).

[20] Weiner, MJ, Hallett, M, & Funkenstein, HH Adaptation to lateral displacement of vision in patients with lesions of the central nervous system. *Neurology* 33:6, 766-72 (1983).

[21] Shadmehr, R. & Mussa-Ivaldi, F.A. Adaptive representation of dynamics during learning of a motor task. *J Neurosci* 14:5 Pt 2, 3208-24 (1994).

[22] Shidara, M., Kawano, K., Gomi, H., & Kawato, M. Inverse-dynamics model eye movement control by Purkinje cells in the cerebellum. *Nature* 365:6441, 50-2 (1993).

[23] Gomi, H. & Kawato M. Equilibrium-point control hypothesis examined by measured arm stiffness during multijoint movement. *Science* 272:5258, 117-20 (1996).

[24] Meyer, B.U. et al. Motor Responses Evoked by Magnetic Brain Stimulation in Huntington's Disease. *Electroencephalogr Clin Neurophysiol* 85:3, 197-208 (1992).

[25] Noth, J., Podoll, K., & Friedemann, H.H. Long-Loop Reflexes in Small Hand Muscles Studied in Normal Subjects and in Patients with Huntington's Disease. *Brain* 108 (Pt 1) (1985).

[26] Topper, R., Schwarz, M., Podoll, K., Domges, F., & Noth, J. Absence of Frontal Somatosensory Evoked Potentials in Huntington's Disease. *Brain* 116 (Pt 1) (1993).

[27] Noth, J., Engel, L., Friedemann, H.H., & Lange, H.W. Evoked Potentials in Patients with Huntington's Disease and Their Offspring. I. Somatosensory Evoked Potentials. *Electroencephalogr Clin Neurophysiol* 59:2, 134-41 (1984).

[28] Shadmehr, R. & Brashers-Krug, T. Functional stages in the formation of human long-term motor memory. *J Neurosci* 17:1, 409-19 (1997).

[29] Flash, T. & Hogan, N. The coordination of arm movements: an experimentally confirmed mathematical model. *J Neurosci* 5:7, 1688-703 (1985).

[30] Harris, C.M. & Wolpert, D.M. Signal-dependent noise determines motor planning. *Nature* 394:6695, 780-4 (1998).

[31] Wolpert, D.M., Ghahramani, Z., & Jordan, M.I. Are arm trajectories planned in kinematic or dynamic coordinates? An adaptation study. *Exp Brain Res* 103:3, 460-70 (1995).

[32] Miall, R.C., Weir, D.J., & Stein, J.F. Manual tracking of visual targets by trained monkeys. *Behav Brain Res* 20:2, 185-201 (1986).

[33] Cordo, P.J. Mechanisms controlling accurate changes in elbow torque in humans. *J Neurosci* 7:2, 432-42 (1987).

[34] Cordo, P.J. Kinesthetic control of a multijoint movement sequence. *J Neurophysiol* 63:1, 161-72 (1990).

[35] Atkeson, C.G. & Hollerbach, J.M. Kinematic Features of Unrestrained Vertical Arm Movements. *J Neurosci* 5:9, 2318-30 (1985).

[36] Gordon, J., Ghilardi, M.F., & Ghez, C. Impairments of reaching movements in patients without proprioception. I. Spatial errors. *J Neurophysiol* 73:1, 347-60 (1995).

[37] Gabrieli, J.D., Stebbins, G.T., Singh, J. Willingham, D.B., & Goetz, C.G., Intact Mirror-Tracing and Impaired Rotary-Pursuit Skill Learning in Patients with Huntington's Disease: Evidence for Dissociable Memory Systems in Skill Learning. *Neuropsychology* 11:2, 272-81 (1997).

[38] Heindel, W.C., Butters, N., & Salmon, D.P. Impaired Learning of a Motor Skill in Patients with Huntington's Disease. *Behav Neurosci* 102:1, 141-7 (1988).

[39] Hogan, N. Mechanical imepedance of single- and multi-articular systems. In: Winters, J.M., Woo S.L.Y. (Eds.), *Multiple Muscle Systems* 149-64 (Springer, New York, 1990).

[40] Miall, R.C., Wolpert, D.M. Forward models for physiologic motor control. *Neural Networks* 9:8, 1265-1279 (1996).

[41] Bhushan, N. & Shadmehr, R. Computational nature of human adaptive control during learning of reaching movements in force fields. *Biol Cybern* 81:1, 39-60 (1999).

[42] Schultz, W., Dayan, P., & Montague, P.R. A neural substrate of prediction and reward. *Science* 275:5306, 1593-9 (1997).

[43] Marsden CD, Merton PA, Morton HB, Adam J (1978) The effects of lesions of the central nervous system on long-latency stretch reflexes in the human thumb. In: Cerebral motor control in man: long loop mechanisms, Desmedt JE (ed.). Karger:Basel Switzerland. pp. 334-341.

[44] Rothwell JC (1990) Long latency reflexes of human arm muscles in health and disease. In: New Trends and Advanced Techniques in Clinical Neurophysiology, Rossini PM, Mauguiere F (eds.). Elsevier, pp. 251-263.

[45] Petersen N, Christensen LOD, Morita H, Sinkaer T, Nielsen J (1998) Evidence that a transcortical pathway contributes to stretch reflexes in the tibialis anterior muscle in man. J Physiol 512:267-276.

[46] Thompson PD, Berardelli A, Rothwell JC, Day BL, Dick JP, Benecke R, Marsden CD (1988) The coexistence of bradykinesia and chorea in Huntington's disease and its implications for theories of basal ganglia control of movement. Brain 111:223-44.

[47] Thilmann AF, Schwarz M, Topper R, Fellows SJ, Noth J (1991) Different mechanisms underlie the long-latency stretch reflex response of active human muscle at different joints. J Physiol 444:631-643.

[48] Fellows S, Schwarz M, Schaffrath C, Domges F, Noth J (1997) Disturbances of precision grip in Huntington's disease. Neurosci Lett 226:103-106.

[49] Gordon J, Ghez C (1987) Trajectory control in targeted force impulses. III. Compensatory adjustments for initial errors. Exp Brain Res 67:253-269.

[50] Alyward EH, Brandt J, Codori AM, Mangus RS, Barta PE, Harris GJ (1994) Reduced basal ganglia volume associated with the gene for Huntington's disease in asymptomatic at-risk persons. Neurology 44:823-28.

[51] Harris GJ, Aylward EH, Peyser CE, Pearlson GD, Brandt J, Roberts-Twillie JV, Barta PE, Folstein SE (1996) Single photon emission computed tomographic blood flow and magnetic resonance volume imaging of basal ganglia in Huntington's disease. Arch Neurology 53:316-324.

[52] Aylward EH, Anderson NB, Bylsma FW, Wagster MV, Barta PE, Sherr M, Feeney J, Davis A, Rosenblatt A, Pearlson GD, Ross CA (1998) Frontal lobe volume in patients with Huntington's disease. Neurology 50:252-258.

[53] Kirkwood SC, Siemers E, Stout JC, Hodes ME, Conneally PM, Christian JC, Foroud T (1999) Longitudinal cognitive and motor changes among presymptomatic Huntington disease gene carriers. Arch Neurolog 56:563-568.

[54] van Donkelaar P, Stein JF, Passingham RE, Miall RC (1999) Neuronal activity in the primate motor thalamus during visually triggered and internally generated limb movements. J Neurophysiol 82:934-945.

[55] van Donkelaar P, Stein JF, Passingham RE, Miall RC (2000) Temporary inactivation in the primate motor thalamus during visually triggered and internally generated limb movements. J Neurophysiol 83:2780-2790.

[56] Lidsky TI, Manetto C, Schneider JS (1985) A consideration of sensory factors involved in motor functions of the basal ganglia. Brain Res 356:133-46.

[57] Schneider JS, Levine MS, Hull CD, Buchwald NA (1985) Development of somatosensory responsiveness in the basal ganglia of awake cats. J Neurophysiol 54:143-54

[58] Jiang W, Chapman CE, Lamarre Y (1991) Modulation of the cutaneous responsiveness of neurones in the primary somatosensory cortex during conditioned arm movements in the monkey. Exp Brain Res 84**:**342-354.

[59] Shin HC, Chapin JK (1990) Movement induced modulation of afferent transmission to single neurons in the ventroposterior thalamus and somatosensory cortex in rat. Exp Brain Res 81:515-522.

[60] Jiang W, Chapman CE, Lamarre Y (1990) Modulation of somatosensory evoked responses in the primary somatosensory cortex produced by intracortical microstimulation of the motor cortex in the monkey. Exp Brain Res 80**:**333-44.

[61] Conditt MA, Gandolfo F, Mussa-Ivaldi FA. (1997) The motor system does not learn the dynamics of the arm by rote memorization of past experience.*J Neurophysiol*. 78, 554-560.

[62] Lackner JR, Dizio P. (1994) Rapid adaptation to Coriolis force perturbations of arm trajectory. *J Neurophysiol* 72, 299-313

[63] Krakauer JW, Ghilardi MF, Ghez C. (1999) Independent learning of internal models for kinematic and dynamic control of reaching. *Nat Neurosci* 2:11,1026-31

[64] Thoroughman K.A., Shadmehr R. Learning of action through adaptive combination of motor primitives. *Nature* 407, 742-747 (2000).

[65] Thach WT et al. Throwing while looking through prisms. I. Focal olivocerebellar lesions impair adaptation (1996).

[66] Miall et al. Visuomotor adaptation during inactivation of the dentate nucleus

[67] Sanes JN, Dimitrov B & Hallett M. Motor learning in patients with cerebellar dysfuncion. Brain 113,103-120 (1990).

[68] Hallett (1983)

[69] Lisberger S, VOR and CBL: (Science 1996)

[70] Chen L, Bao S, Lockard JM, Kim JK, Thompson RF. Impaired classical eyeblink conditioning in cerebellar-lesioned and Purkinje cell degeneration (pcd) mutant mice. J Neurosci.16(8):2829-38(1996)

[71] Thompson RF, Kim JJ. Memory systems in the brain and localization of a memory. Proc Natl Acad Sci 93(24), 13438-44 (1996)

[72] Mishkin M., Malamut B., Bachevalier J. Memories and habits: Two neural systems, in Neurobiology of Learning and Memory (lynch G, MgGaugh JL, Weinberger NM eds) pp65-77. Guilford Press, NY (1984).

[73] Mishkin M., Appenzeller T. The Anatomy of Memory. Sci Am 256, 80-89 (1987)

[74] Bachevalier J. Ontogenetic development of habit and memory formation in primates. Ann NY Acad Sci 608, 457-484 (1990).

[75] Paulsen, J.S. et al Prism adaptation in Alzheimers and Huntington's didease. Neuropsychology 7,73-81 (1993).

[76] Kirkwood SC, Siemers E, Bond C, Conneally PM, Christian JC, Foroud T (2000) Confirmation of subtle motor changes among presymptomatic carriers of the Huntington disease gene Arch Neurol 57:1040-1044.

[77] Schwarz M., Fellows S.J., Schaffrath C., Noth J. Deficits in sensorimotor control duing precise hand movements in Huntington's disease. Clinical Neurophys 112, 95-106 (2001).

[78] Smith, M.A. et al. (2000) Motor disorder in Huntington's disease begins as a dysfunction in error feedback control. *Nature* 403, 544-549

[79] Grill S.E. et al. (1997) Timing of onset of afferent responses and of use of kinesthetic information for control of movement in normal and cerebellar-impaired subjects. *Exp Brain Res* 113, 33-47

[80] Brainard, M.S. and Doupe, A.J. (2000) Interruption of a basal ganglia-forebrain circuit prevents plasticity of learned vocalizations. *Nature* 404, 762-766

[81] Solis, M. and Doupe A.J. (2000) Compromised neural selectivity for song in birds with impaired sensorimotor learning. *Neuron* 25, 109-121

[82] Robertson, M.M. (2000) Tourette syndrome, associated conditions and the complexities of treatment. *Brain* 123, 425-462

[83] Pauls, D.L., Leckman, J.F. (1986) The inheritance of Gilles de la Tourette syndrome. *N Engl J Med* 315, 993-997

[84] Pauls, D.L. et al. (1986) Gilles de la Tourette syndrome and obsessive-compulsive disorder: evidence supporting a genetic relationship. *Arch Gen Psychiatry* 43, 1180-1182

[85] Leckman J.F. et al. (1999) Tics and Tic Disorders. in: *Tourette's Syndrome – Tics Obsessions and Compulsions: Developmental Psychopathological and Clinal Care* (Leckman J.F. and Cohen D.J., eds) pp23-42, John Wiley & Sons

[86] Jackson, J.H. (1878) On affections of speech from disease of the brain. *Brain* 1,304-330

[87] Critchley, M. (1970) *Aphasiology and Other Aspects of Language*, Edward Arnold

[88] Lum, C.C. and Ellis A.W. (1994) Is "Nonpropositional" speech preserved in aphasia? *Brain and Language* 46, 368-391

[89] Obeso, J.A. et al. (1982) The neurophysiology of Tourette Syndrome. in: *Advances in Neurology, Gilles de la Tourette syndrome*, Vol. 35 (Friedhoff J.H. and Chase T.N., eds.), pp 105-114, Raven Press

[90] Frank, S.M. (1978) Psycholinguistic indings in Gilles de la Tourette syndrome, *J. Hum. Commun. Disord* 11, 349-363

[91] Martindale, C. (1977) Syntactic and semantic correlates of verbal tics in Gilles de la Tourette syndrome: a quantitative case study, *Brain and Language* 4, 231-247

[92] Peterson, B. et al. (1993) Reduced basal ganglia volumes in Tourette's syndrome using three dimensional reconstruction techniques for magnetic resonance images. *Neurology* 43, 941-949

[93] Van Lancker D. and Cummings J.L. (1999) Expletives: neurolinguistic and neurobehavioral perspectives on swearing. *Brain Res Rev* 31,83-104.

[94] Baker H.S. (1997) Neurobiology of Tourette syndrome. *Neurol Clin* 15, 357-379